UNIVERSITÀ DEGLI STUDI DI TRIESTE

XXXVII ciclo del Dottorato di Ricerca in

Ingegneria Industriale e dell'Informazione

Prodigys Technology srl

Redefining the Hardware and Computational Algorithms for Bilirubin and Hematocrit Assessment in a Point-of-Care Device for Developing Countries

Settore scientifico-disciplinare:

ING-INF/06 Bioingegneria Elettronica ed Informatica

Dottorando
Lorenzo Zucchini

Coordinatore
Prof. Fulvio Babich

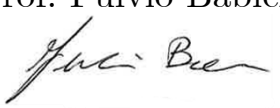

Supervisore di tesi
Prof. Agostino Accardo

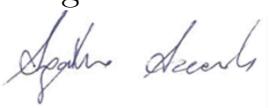

Anno Accademico 2023/2024

University of Trieste

XXXVII cycle of PhD in Industrial and Information Engineering

Funded by Prodigys Technology srl

Thesis title: Redefining the Hardware and Computational Algorithms for Bilirubin and Hematocrit Assessment in a Point-of-Care Device for Developing Countries

Scientific Disciplinary Sector: ING-INF/06 Electronic and Informatics Bioengineering

PhD student: Lorenzo Zucchini

Programme coordinator: Prof. Fulvio Babich

Supervisor: Prof. Agostino Accardo

Academic year: 2023/2024

Abstract

Neonatal Hyperbilirubinemia (NH) affects over half of newborns globally, with severe cases risking neurological damage or death. While developed countries benefit from guidelines and accessible healthcare to mitigate these risks, limited resources in low- and middle-income countries (LMICs) increase vulnerability. Although laboratory-grade instruments offer high accuracy, their cost and complexity make them impractical for low-resource settings, and simpler methods often lack necessary precision. Direct spectrophotometry offers a promising alternative for portable, point-of-care (POC) devices, though hemoglobin interference in neonatal samples remains a challenge.

Hematocrit (HCT) is also essential for assessing neonatal health and guiding NH treatment, especially phototherapy. Traditional HCT measurement relies on costly equipment or manual methods prone to error. This thesis explores an approach to estimate HCT using the same small sample employed for bilirubin measurement on a simplified photometric device.

Additionally, this work addresses regulatory and structural barriers in LMICs, where inadequate infrastructure, fragmented health systems, and limited regulatory oversight restrict the diffusion of even essential diagnostics.

The studies presented here demonstrate that portable, direct spectrophotometry-based devices can achieve accuracy and reliability without the use of expensive electronic, optical, or chemical components, preserving simplicity and cost-effectiveness. A hemoglobin interference compensation algorithm utilizing two wavelengths has been designed, optimized, and successfully tested across a range of bilirubin and hemoglobin concentrations.

In addition, an algorithm for estimating hematocrit based on plasma penetration velocity through a nitrocellulose membrane was developed and tested across various hematocrit levels, confirming its potential for neonatal screening. This novel algorithm can operate alongside bilirubin measurement on the same reflectance photometer and sample, reducing sample volume and turnaround time while providing clinicians with valuable information.

Finally, the challenges of diagnostic diffusion and use in resource-limited settings were analyzed, exploring the roles of manufacturers, the World Health Organization, and National Regulatory Agencies in supporting the supply of devices in these regions. This work highlighted two promising frameworks—the A.S.S.U.R.E.D. criteria and the Pre-Qualification of in vitro devices combined with the Collaborative Registration Procedure—offering a review of current advancements and future prospects aimed at aligning manufacturers' economic interests with improved health outcomes in developing countries.

Sommario

L'iperbilirubinemia neonatale (NH) colpisce oltre la metà dei neonati a livello globale, con casi gravi che rischiano danni neurologici o morte. Mentre i paesi sviluppati beneficiano di linee guida e accesso alle cure che consentono di mitigare questi rischi, le risorse limitate dei paesi a basso e medio reddito (LMIC) aumentano la vulnerabilità dei pazienti agli effetti neurotossici della bilirubina. Sebbene gli strumenti di laboratorio offrano un'elevata precisione, il loro costo e complessità li rendono impraticabili nei contesti a basse risorse e i metodi più semplici spesso non offrono prestazioni analitiche adeguate. La spettrofotometria diretta, in particolare di riflettanza, offre una promettente alternativa per dispositivi portatili e point-of-care (POC), sebbene l'interferenza dell'emoglobina nei campioni neonatali resti una sfida.

L'ematocrito (HCT) è anch'esso essenziale per valutare le condizioni cliniche e orientare il trattamento della NH, in particolare durante la fototerapia. La misurazione tradizionale dell'HCT si basa su apparecchiature costose o metodi manuali soggetti a errori. Questa tesi esplora un approccio per stimare l'HCT utilizzando lo stesso ridotto campione ematico impiegato per la misurazione della bilirubina su spettrofotometro di riflettanza.

Inoltre, questo lavoro affronta le barriere regolatorie e infrastrutturali LMIC, dove l'inadeguatezza delle strutture, i sistemi sanitari frammentati e una limitata supervisione regolatoria impediscono la diffusione dei diagnostici, anche essenziali.

Gli studi presentati dimostrano che dispositivi portatili basati sulla spettrofotometria di riflettanza possono ottenere accuratezza e affidabilità senza l'uso di componenti elettronici, ottici o chimici costosi, preservandone semplicità ed economicità. È stato progettato, ottimizzato e testato con successo un algoritmo di compensazione dell'interferenza dell'emoglobina utilizzando due lunghezze d'onda, applicato su diverse concentrazioni di bilirubina ed emoglobina.

Inoltre, è stato sviluppato e testato un algoritmo per stimare l'ematocrito basato sulla velocità di penetrazione del plasma attraverso una membrana di nitrocellulosa, confermandone il potenziale per lo screening neonatale. Questo innovativo algoritmo può operare parallelamente alla misurazione della bilirubina sullo stesso campione, riducendone il volume richiesto e i tempi di risposta, fornendo al contempo informazioni preziose per i clinici.

Infine, sono state analizzate le barriere che impediscono la diffusione e l'uso dei diagnostici nei contesti a risorse limitate, esplorando i ruoli dei produttori, dell'Organizzazione Mondiale della Sanità e delle Agenzie Regolatorie Nazionali nel supportare la fornitura di dispositivi in queste regioni. Questo lavoro ha messo in evidenza due strumenti promettenti: i criteri A.S.S.U.R.E.D. e la Pre-Qualificazione dei dispositivi in vitro combinata con la Procedura di Registrazione Collaborativa,

offrendo una rassegna dei progressi attuali e delle prospettive future con l'obiettivo di allineare gli interessi economici dei produttori con il miglioramento dei risultati sanitari nei paesi in via di sviluppo.

Contents

List of Figures

List of Tables

List of Abbreviations

ABE	Acute Bilirubin Encephalopathy
ANDI	African Network for Drugs and diagnostics Innovation
ARSO	African organization for Standardization
AU	African Union
CB	Conjugated Bilirubin
CBE	Chronic Bilirubin Encephalopathy
CRP	Collaborative Registration Procedure
DMSO	Dimethyl Sulfoxide
EDTA	Ethylenediaminetetraacetic acid
EOI	Expression of Interest
FDA	Food and Drug Administration
G6PD	Glucose-6-Phosphate Dehydrogenase
GHTF	Global Harmonization Task Force
GNI	Gross National Income
HCT	Hematocrit
HIV	Human Immunodeficiency Virus
HPLC	High Performance Liquid Chromatography
IVD	In-vitro Diagnostics
IVDR	In-vitro Diagnostics Regulation
LFA	Lateral Flow Assay
LMIC	Low-to-Middle Income Country
MDR	Medical Device Regulation
NGO	Non-Governmental Organization
NH	Neonatal Hyperbilirubinemia
NJ	Neonatal Jaundice
NRA	National Regulatory Agency
PAD	Paper-based Analytical Device
RMSE	Root Mean Square Error
TSB	Total Serum Bilirubin
UCB	Unconjugated Bilirubin
UN	United Nations
UNECA	United Nations Economic Commission for Africa
UNICEF	United Nations International Children's Emergency Fund
WHO	World Health Organization
WHO-PQ	World Health Organization Pre-Qualification

Chapter 1. INTRODUCTION

1.1. Preface

Over half of newborns worldwide experience an increase in bilirubin concentration in their blood during the first days of life due to the breakdown of erythrocytes [1–3]. While this is usually a physiological condition, a significant number of newborns develop Neonatal Hyperbilirubinemia (NH), a pathological form that can rapidly escalate to severe, permanent neurological impairments and, in worst cases, death [1,3,4]. Such outcomes are preventable and can be avoided through the implementation of screening procedures for all newborns, or at least for those presenting certain risk factors, along with timely and accurate diagnosis [1,2,5,6].

Developed countries have established national guidelines for managing NH and generally have well distributed technologies and facilities across their territories, resulting in a significant reduction of negative outcomes [7–10]. In contrast, developing and low-income countries still bear the burden of this condition due to less structured health systems, limited financial resources, and insufficient knowledge [5,11–13]. For these areas, it is crucial to measure bilirubin concentration in a fast, reliable, and cost-effective manner. In fact, while laboratory-grade instruments are typically accurate, they are not always economically feasible and require trained staff and proper management. On the opposite side, qualitative methods, whether instrument-based or instrument-free (as hyperbilirubinemia can be visibly evident by the yellowing of the newborn's skin), are inexpensive but highly inaccurate [7,14,15].

Several methods are commonly available in routine practice to measure bilirubin concentration in blood. Among them, direct spectrophotometry has been used for decades for bilirubin and other examinations, and it holds significant potential for

resource-limited environments [16–18]. These settings require solutions that are simple, sufficiently accurate, and point-of-care (POC) compatible [19] — characteristics that can be achieved with a dedicated design utilizing this method. In this PhD thesis, such challenges are addressed starting with a simple, portable reflectance photometer designed for total serum bilirubin (TSB) measurement and by proposing and validating enhancements under three main aspects, namely hemoglobin interference compensation, hematocrit (HCT) estimation contemporary to bilirubin measurement, and temperature influence characterization.

While, at the technological level, addressing neonatal hyperbilirubinemia involves developing such instrumentation, at a higher health system level, the regulation, diffusion, and management of diagnostic devices remain under-addressed and slow to improve [20–22]. Global organizations, primarily the World Health Organization (WHO), have proposed guidelines and regulatory frameworks to increase the penetration of diagnostics in low-income countries and address their specific clinical needs [23,24]. To enhance the adoption of diagnostic systems in low-income countries, both technological and regulatory considerations must be addressed from the design phase. Starting from these considerations, this PhD thesis proposes strategies for achieving successful diffusion, considering perspectives from manufacturers, and health systems alike.

1.2. Thesis objectives

This thesis studies and proposes enhancements for a portable, economical, POC device for bilirubin measurement, with the aim of making its use possible in resource-limited settings. It also proposes solutions to access the potentially vast markets of such countries from a regulatory and policy perspective, with the ultimate goal of reducing the burden of NH.

This PhD thesis is divided into three parts. The first part, presented in Chapter 2, explores the measurement of TSB using direct spectrophotometry, with a particular focus on compensating for hemoglobin interference. The second part, detailed in Chapter 3, involves the design and characterization of a novel method for estimating neonatal HCT from a small blood sample, using a simple photometer similar to that used for bilirubin measurement. The final part, discussed in Chapter 4, proposes conceptual and operational tools, guidelines, and frameworks to enhance the diffusion of diagnostic devices, including bilirubinometers, in developing and low-income countries.

1.2.1. Measurement of total serum bilirubin in the newborn by reflectance photometry

Bilirubin measurement in newborns presents several challenges that encompass technological, demographic, and management aspects.

From a technological perspective, the methodology and instruments used for measurement must be sufficiently accurate to have diagnostic validity and robust enough to maintain this accuracy in the presence of interfering substances or external factors that may degrade performance and clinical reliability. Demographically, NH is a global phenomenon affecting newborns of all ethnicities, nationalities, and social backgrounds. It is essential to develop a solution that provides consistent performance for any newborn, regardless of their environment. From a management perspective, diagnosing NH typically requires more than one measurement: national guidelines recommend periodic monitoring of bilirubin levels to establish a temporal trend and predict necessary treatments [7,9]. Clinicians and nurses must often reach the patient to perform these measurements, especially since the patient may be in rural areas or outside the reach of standard laboratories.

Measuring bilirubin directly in blood rather than through the skin minimizes the influence of the patient's demographic characteristics, particularly skin tone and

composition [9,15,25–27]. Utilizing a direct spectrophotometry-based instrument allows for a reduction in the required blood volume compared to other established techniques [17,28,29]. Additionally, in general, measuring reflectance instead of transmitted light simplifies the system, enabling the development of compact, portable, and cost-effective instruments [30,31]. However, this simplification may compromise the robustness of the method, as it is sensitive to interference from other analytes, primarily hemoglobin [17,18,28]. The design of an efficient compensation algorithm could significantly enhance the clinical reliability and accuracy of the instrumentation without increasing costs and complexity.

Finally, given that portability is a desirable feature, it is important to evaluate the robustness of this method against varying environmental conditions such as temperature, lighting, and relative humidity. This evaluation will help in designing and implementing an algorithm to compensate for these influences. The data and results obtained from this aspect will be beneficial for further studies and improvements of the instrument.

1.2.2. Hematocrit estimation in the newborn from a blood microcapsule

HCT is an important health indicator in both adults and newborns [32,33]. In newborns, HCT values outside the normal reference ranges can indicate severe pathological conditions [33,34]. For patients with NH, HCT is crucial as it is both a risk factor in diagnosis and a parameter to consider during treatment, particularly with phototherapy [8,35].

HCT can be measured using either automated or manual, visual methods in both developed and developing countries [36–38]. The possibility of obtaining an automated, quantitative estimation of HCT from the same small blood sample used for bilirubin measurement is described in this thesis and it is believed to be a promising advancement. Although not reaching a sufficient accuracy to be used as

a standalone diagnostic method yet, the benefit of this method in clinical practice could come from the capability of obtaining a screening-level information in parallel with bilirubin measurement [8]. Hence, this integration would allow for two independent examinations from one drop of blood without increasing turnaround time and investigation-related costs.

1.2.3. Strategies for the diffusion of diagnostic devices in developing countries

Health systems in developing and LMICs differ significantly from those in developed and wealthier nations. These countries often lack sufficient infrastructure, facilities, technology, and trained staff, leading to a higher burden of diseases, including NH [5,22,39–41].

One of the most prominent reasons for this disparity is the shortage of unified and comprehensive regulatory frameworks, as well as solid and autonomous NRAs [20,42]. This lack creates difficulties for manufacturers attempting to enter these markets, as they are often discouraged by unstandardized certification processes and the associated costs and time requirements [43].

To increase the diffusion of diagnostic devices, it is crucial to consider both technological and regulatory aspects from the very beginning of development. Manufacturers can follow technocentric guidelines such as the WHO's A.S.S.U.R.E.D. (subsequently updated to R.E.A.S.S.U.R.E.D.), which outlines the features and constraints to consider when developing a device for resource-limited settings [19,44,45]. Additionally, the WHO is working with NRAs in developing countries to establish a more efficient and straightforward market authorization process for diagnostics, known as Prequalification [46,47]. This initiative promises to enhance diffusion, benefiting both manufacturers and, most importantly, patients.

To achieve a comprehensive understanding of this topic, literature and documentation from various sources were reviewed, and the collected data led to an analysis of the current state of the art.

1.3. Impact of the research and significance

The significance of this research lies in its potential to enhance neonatal care and diagnostics in both developed and developing regions. The novel algorithm for hemoglobin compensation proposed by this thesis improves the accuracy of bilirubin measurements at the point of care, outside advanced laboratories, and hospitals, ensuring that neonates receive timely and appropriate care where most needed. Due to the portable nature of such instrument, it is essential to guarantee their robustness and reproducibility in diverse environments. The studies performed on the temperature influence on reflectance photometers for bilirubin measurement represent a significant advancement in understanding this instrumentation. Furthermore, introducing a novel approach for neonatal HCT screening based on penetration velocity in lateral flow test strips addresses the critical need for quick, reliable, and minimally invasive testing methods.

This research also explores the broader implications for in vitro diagnostics (IVDs) in LMICs. By analyzing the criteria for WHO-Prequalification and the A.S.S.U.R.E.D. framework, this work aims to provide valuable insights into the diffusion of IVDs in resource-limited settings. The findings could guide policymakers and healthcare providers in adopting cost-effective and reliable diagnostics, while also assisting manufacturers in designing profitable diagnostics tailored to specific constraints. Ultimately, this could enhance healthcare accessibility and quality in underserved regions. Overall, this thesis contributes to the field of biomedical and clinical engineering by offering innovative solutions to critical challenges in neonatal diagnostics and by promoting the dissemination of essential diagnostic technologies.

Chapter 2. MEASUREMENT OF TOTAL SERUM BILIRUBIN IN THE NEWBORN BY REFLECTANCE PHOTOMETRY

2.1. Introduction

Neonatal Hyperbilirubinemia, also known as Neonatal Jaundice (NJ), is a common clinical condition affecting more than half of newborns worldwide [1]. It is caused by an excessive amount of bilirubin in their blood. Due to the neurotoxic effects of bilirubin, its concentration needs to be closely monitored during the first days of life to initiate necessary treatments and prevent potentially severe and permanent damage [9,48,49]. Various measurement methods, both invasive and non-invasive, have been developed for this purpose. These range from small, portable, non-invasive transcutaneous bilirubinometers to complex blood-based laboratory equipment [18,29]. Despite the variety of instruments available, there is a pressing need in clinical practice for simple, portable, cost-effective, yet accurate and reliable measurement devices [1,6,18,29]. This need is crucial in both developed and developing countries to ensure the effective management of NJ, although the majority of the burden falls on the latter, where health facilities and technologies are often inadequate and widely dispersed [40,50].

Direct spectroscopy, particularly reflectance photometry, represents a highly promising method to meet clinical needs. Its adaptability to compact, low-cost, portable systems makes it a viable candidate for the challenges of NJ management. However, ensuring accuracy and robustness must not be compromised by the necessity for simplification [45]. A major limitation and research question for this solution is the interference from other analytes present in the sample, notably hemoglobin. The following sections introduce the design of a simple reflectance

photometer and report on investigations into hemoglobin interference, as well as a study on the temperature influence on this system.

2.2. Bilirubin and neonatal jaundice

2.2.1. Bilirubin metabolism in neonates

Bilirubin is formed from the breakdown of heme, a component of hemoglobin in red blood cells and other heme-containing proteins such as myoglobin and cytochromes (Figure 1) [4,51,52].

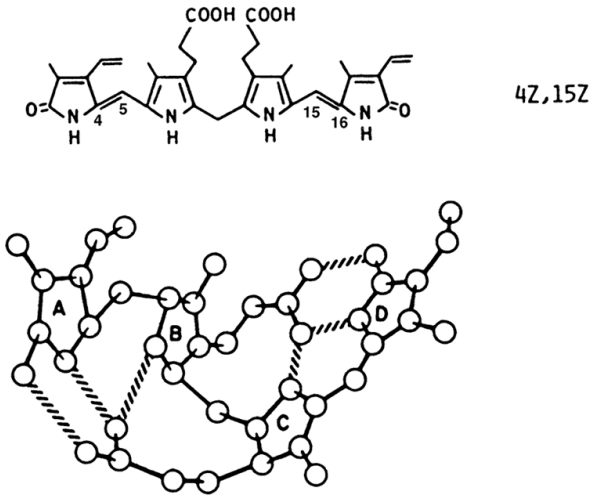

Figure 1. Chemical structure of the naturally occurring unconjugated bilirubin. Adapted from [4].

This process begins with the enzymatic action of heme oxygenase, which cleaves the heme ring at the α carbon bridge, producing biliverdin, carbon monoxide, and iron. Biliverdin is then reduced to bilirubin by the enzyme biliverdin reductase (Figure 2) [4,51,52].

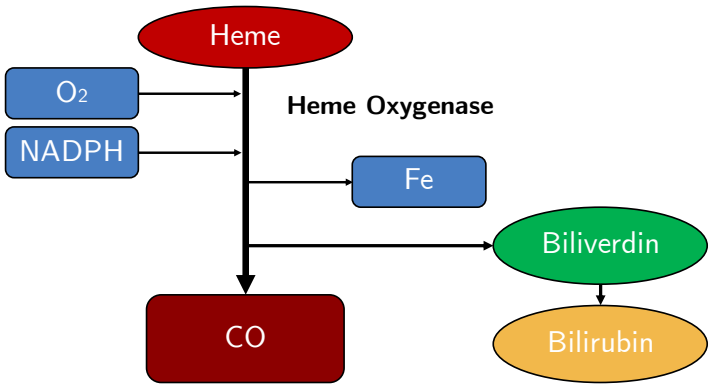

Figure 2. Schematic representation of the heme catabolic pathway.

In adults, about 250-300 mg of bilirubin is produced daily, with a higher amount in neonates due to increased red blood cell turnover [53,54]. Once formed, unconjugated bilirubin (UCB) is hydrophobic and insoluble in water, necessitating its binding to plasma albumin for transport in the blood [4,51,52]. UCB is taken up by hepatocytes through both passive diffusion and mediated by organic anion transporter proteins. Within hepatocytes, UCB binds to intracellular proteins such as glutathione-S-transferase A (ligandin) and fatty acid-binding proteins, maintaining low levels of free, toxic bilirubin [4,51]. The conjugation of bilirubin occurs in the liver's microsomes, where UCB is converted into water-soluble conjugated bilirubin (CB) by the enzyme UDP-glucuronosyltransferase (UGT), encoded by the UGT1A1 gene. This reaction attaches glucuronic acid to bilirubin, making it more hydrophilic and less likely to bind to albumin or other intracellular proteins. CB is then excreted into the bile and passes into the intestine [4,51,52]. In the intestine, bilirubin undergoes further breakdown by bacterial enzymes into urobilinogen. Some of this urobilinogen is reabsorbed into the bloodstream and taken up by the liver again, a process known as enterohepatic circulation, while the rest is excreted in feces. The initial formation of bilirubin in the spleen and its subsequent processing in the liver is a continuous cycle, critical for the body's management of heme and its byproducts [4,51,52].

In neonates, UCB levels in plasma can rise due to a combination of factors such as a larger hemoglobin mass compared to adults, lower albumin concentration in plasma, a reduced conjugation rate due to immature UGT enzyme, an underdeveloped biliary secretory apparatus, and the absence of bacterial flora [4,52]. Non-protein-bound bilirubin (also known as free UCB) can diffuse across the blood-brain barrier and enter astrocytes and neurons, where it exhibits neurotoxic effects. Furthermore, some speculate that an already damaged brain may bind bilirubin to such an extent that it is unable to clear bilirubin rapidly, causing even further damage [4].

2.2.2. Neonatal jaundice

The condition in which UCB levels increase beyond normal values is commonly referred to as unconjugated hyperbilirubinemia, or NJ [51,52]. In neonates, NJ is a ubiquitous and frequently benign condition attributable to a metabolic imbalance favoring bilirubin production over hepatic-enteric bilirubin clearance [4]. It affects about 60% of full-term and 80% of pre-term newborns [55–57]. Translating these percentages to absolute numbers, this means that 84-112 million babies develop this condition yearly in their first two weeks of life [1]. Since one in ten newborns are likely to develop a clinically significant form of NJ, the need for proper monitoring is substantial. Data from the Global Burden of Disease study in 2016 showed that NJ accounted for 1309.3 deaths per 100,000 live births and ranked seventh globally among all causes of neonatal death in the early-neonatal period, which is the first six days of life [58,59].

The complexity of managing NJ also stems from the diverse array of risk factors contributing to its clinically significant forms, some of which are listed in Table 1 [3,60].

Genetic	Maternal	Perinatal	Neonatal
Gilbert's syndrome	Race or ethnic group	Mode of delivery	Male sex
G6PD deficiency	Primiparity	Birth trauma or asphyxia	Prematurity or low birthweight
Bilirubin UGT polymorphism	Diabetes	Delayed cord clamping	Hypothyroidism
Erythrocyte structural defects	Rhesus incompatibility	Congenital infections	Polycythemia
	ABO incompatibility	Sepsis	Breast milk jaundice
	Exclusive breastfeeding		Chronic hemolysis

Table 1. Common risk factors for significant and severe NJ.

The correct management of NJ, as outlined in major clinical guidelines, focuses on avoiding mortality and neurotoxicity by preventing serum bilirubin from reaching potentially neurotoxic concentrations. NJ management can be logically subdivided into three phases: "primary prevention," "early detection, diagnosis, and monitoring," and "treatment" [1].

Primary prevention involves promptly recognizing and controlling neonates at risk of severe NJ. NJ, in both its physiological and clinical forms, is characterized by the yellowish discoloration of the skin, sclera, and mucous membranes [60]. Despite the universal understanding of its inaccuracy, particularly with darker skin tones, visual assessment remains a common practice for diagnosing NJ [13,14,61–63]. Additionally, since the physiological serum bilirubin peak occurs between the third and fifth day, most neonates would have been discharged from the hospital in both developed and developing countries by this time [62,64,65]. Furthermore, births in poorer areas frequently occur outside hospitals, often in homes, making home births the most common situation [66]. Therefore, a crucial step in effective prevention is educating mothers on the difficulty of distinguishing innocuous jaundice from significant hyperbilirubinemia [67]. In developed countries, NJ is among the most, if not the single most, frequent reason for hospital readmission after birth. In a large retrospective study of over 33,000 live births in the USA, NJ

was identified as the leading cause of rehospitalization, accounting for 34.3% of all cases [68]. Another study in the United Kingdom found that NJ was responsible for 22.3% of all readmissions from home during the period from 2011 to 2013 [69]. In conclusion, major established guidelines, such as those from the AAP [13] or NICE [7], strongly recommend implementing pre-discharge screening for all newborns, particularly those with one or more risk factors for developing significant hyperbilirubinemia. Additionally, timely follow-up examinations in the days following discharge are crucial [70,71]. These follow-ups can and should be conducted in primary or secondary healthcare settings by community and district nurses in high-income countries, or by community and voluntary health workers in lower-income countries. The use of a portable, POC device capable of measuring TSB offers a dual benefit: reducing costs and stress for families who can receive care at home or in a nearby healthcare facility, and alleviating costs and workload for central facilities, such as hospitals, which are currently required to readmit newborns just a few days after discharge.

2.2.3. Neurotoxicity of bilirubin, acute encephalopathy, and kernicterus

High levels of UCB can lead to the deposition of bilirubin in the brain of the neonate, where it exerts its neurotoxic effects. The associated condition is referred to as Acute Bilirubin Encephalopathy (ABE), and manifests within the first 14 days of life [6]. The early signs of ABE are non-specific and can be easily overlooked especially if the newborn is discharged and the mother is not educated to look for specific behaviors and traits [5,6]. The mechanisms underlying such conditions are complex and outside the scope of this Thesis, as well as not being fully understood yet, however TSB levels are strictly correlated with the risk of developing ABE [49]; there is no universally accepted and shared definition of “safe” or “dangerous” concentrations, however, in Table 2 a general definition is proposed [6].

TSB Concentration [mg/dl]	Definition	Notes
≥12	Significant	Requires treatment with phototherapy
≥20	Severe	Can require exchange transfusion; can lead to early signs of mild ABE
≥25	Extreme	Requires exchange transfusion; can lead to signs of mild to moderate ABE
≥30	Hazardous	Requires exchange transfusion; can lead to signs of moderate to severe ABE

Table 2. A possible categorization of NH levels based on UCB concentration in plasma. Adapted from [6].

Early ABE signs include lethargy, poor feeding and irritability, high-pitched cry, oculogyric movements, as well as changes in muscle tone and vomiting [6,72]. A prolonged exposition to high bilirubin concentrations, mostly caused by delayed diagnosis and/or incorrect treatment, causes these damages to further exasperate and become permanent: Kernicterus, or Chronic Bilirubin Encephalopathy (CBE), presents with athetoid cerebral palsy, dystonia, upward gaze and sensorineural hearing impairment [49,60,73]. Survivors of this condition are likely to develop heavy developmental delays and cognitive impairments, while in other cases the illness ends with death due to respiratory failure, progressive coma and intractable seizure [41,74].

The real extent of the burden of bilirubin encephalopathy and kernicterus is unsure yet and, despite the availability of past and more recent literature, incidence and prevalence figures need to be carefully interpreted, especially those regarding LMICs [2,50]. A systematic review estimated that 18% of the 134 million liveborn babies in 2010 developed clinically significant NJ in 2010, while 481,000 of them developed extreme hyperbilirubinemia. This led to 114,000 deaths and more than 63,000 survivors with moderate to severe kernicterus [41]. True population-based data, however, are difficult to find and national- or local-level studies are not easily generalizable, in addition to being often not carefully designed. Another study

reported impressive differences of severe NJ incidence rates between high income countries and LMICs: 667.8 and 251.3 cases per 10,000 live births in Africa and Southeast Asia, respectively, versus 4.4 and 3.7 in Americas and Europe, respectively [50]. Figures 3 and 4 show neonatal deaths attributable to kernicterus and rates of kernicterus with respect to geographic distribution, respectively [41].

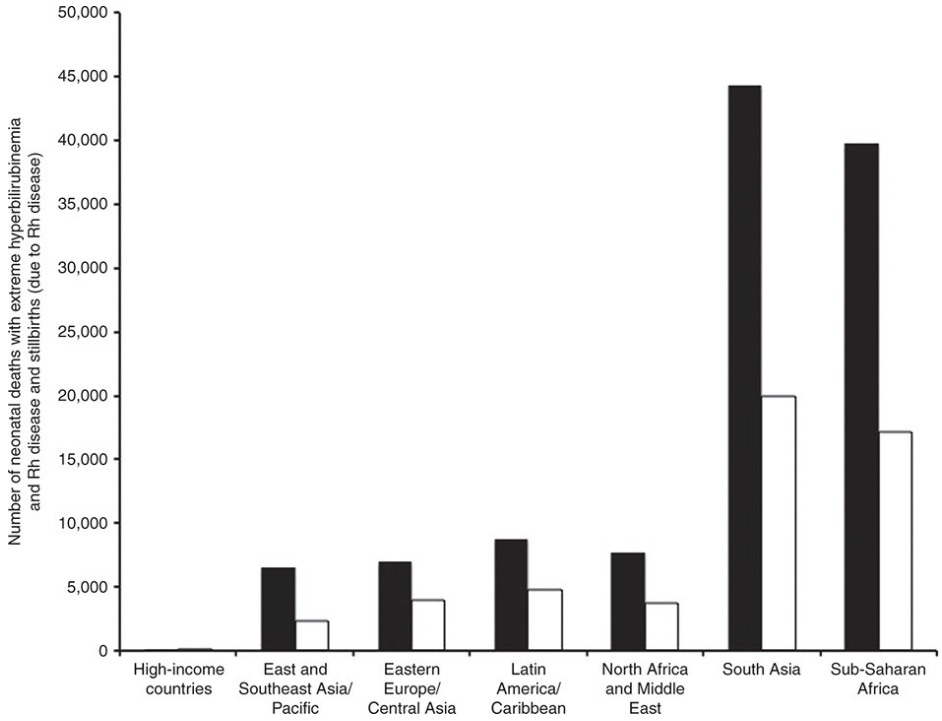

Figure 3. Number of stillbirths due to Rh disease (white bars) and neonatal deaths per 100,000 live births due to kernicterus (black bars) for all live births in 2010. Adapted from [41].

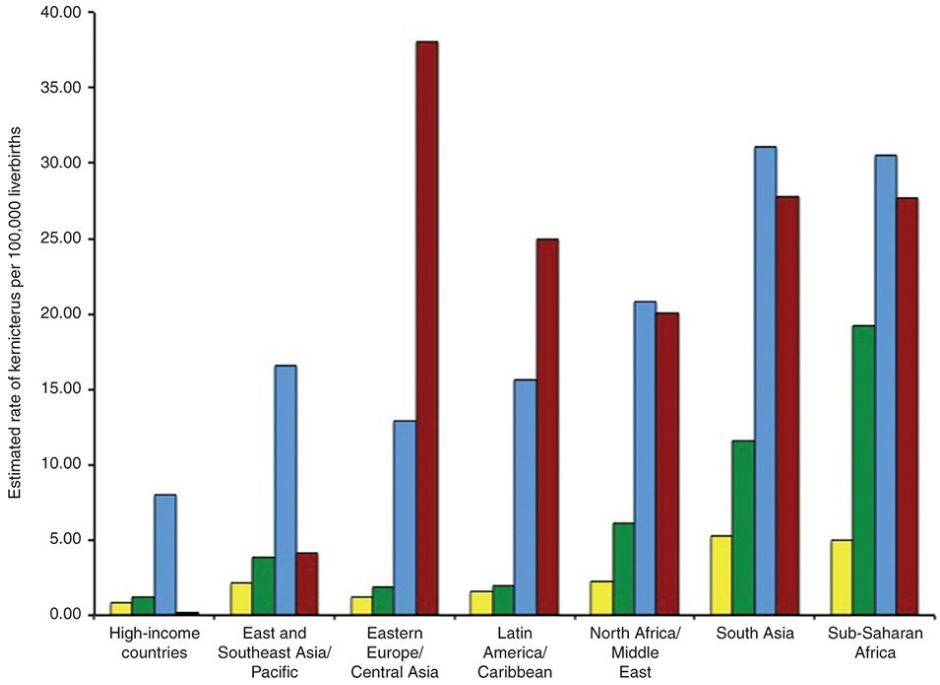

Figure 4. Estimated rates of kernicterus per 100,000 live births, due to prematurity (yellow bars), G6PD deficiency (green bars), hemolytic and idiopathic (blue bars), and RH disease (red bars). Adapted from [41].

2.3. Conventional laboratory methods for bilirubin measurement

Having acknowledged, although summarily, the mechanisms and critical aspects of NJ from clinical and management perspectives, the most interesting facet for this thesis is the incomparable utility of assessing the risk of severe NJ before and shortly after discharge, while the newborn can still receive medical attention. There is a strong need for easy-to-use, cost-effective, POC devices for measuring total serum bilirubin at the bedside or at home by a trained staff member [75]. Avoiding hospital readmission is crucial both in wealthier and poorer countries, and accurate POC measurement is the solution to this dual problem—clinical first and economical second.

To date, bilirubin can be measured using substantially different approaches and methodologies of diverse natures. Generally, bilirubin measurement techniques fall

under three categories: optical, chemical, and electrical [18]. The last two categories fall outside the scope of this thesis and will not be considered.

Since its proposal and evolution in the late 1980s and early 1990s, High Performance Liquid Chromatography (HPLC) has been considered the gold standard for bilirubin measurement, whether as TSB or its fractions, including UCB [18,72,76–78]. HPLC is used to separate, identify, and quantify specific components in a mixture or solvent. At its simplest, it consists of a cylindrical tube containing different adsorbing materials, called the solid phase, through which the sample, called the liquid phase, is forced to flow by high-pressure pumps [79,80]. Due to the specific interaction between a substance and an adsorbing material, each substance migrates at a different rate, achieving separation with great sensitivity and, most importantly, specificity. A specific detector is positioned at the tube's output, measuring the quantity of each substance and retrieving other structural or chemical information [79–81]. A schematic representation of this method is presented in Figure 5, and an example of a commercial HPLC system is presented in Figure 6.

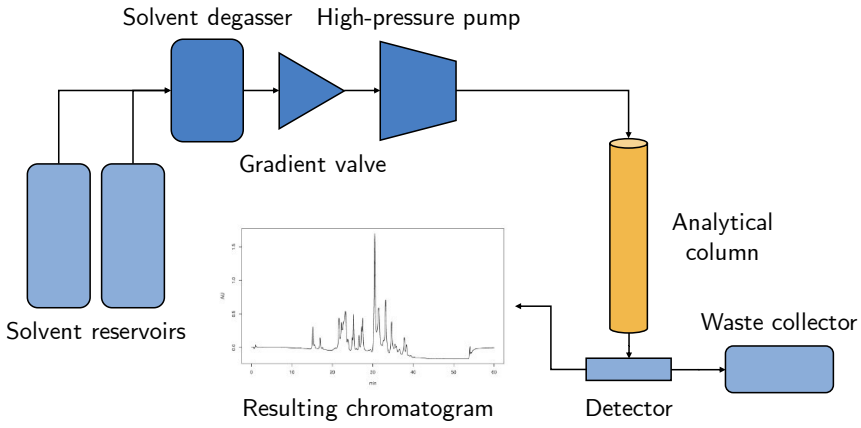

Figure 5. A simplified, schematic representation of the major components of a HPLC system.

Figure 6. An example of a commercial HPLC System.

This method presents outstanding precision and specificity, as well as being enough sensible to allow measurements of remarkably low concentrations of analytes. Despite having such good performance, HPLC is labor and time-consuming as well as being costly due to the presence of reagents, filters and other consumables involved in the measurement process. Another non negligible downside is the requirement of a specialized, well-trained operator in order to correctly prepare and manipulate the sample [18]. For these reasons, this method is only used for research purposes or, in rare cases, in high-level central analysis laboratories [28].

The two most commonly used methods in clinical practice are Diazo and Vanadate Oxidase [77]. Both were proposed in the first decades of the nineteenth century and have been subsequently upgraded and modified over the years. As of 2008, over 60% of laboratories in the UK used Diazo, and 26% used Vanadate Oxidase [72].

With the Diazo method, first introduced by van den Bergh, bilirubin is quantified through a reaction with diazotized sulfanilic acid, forming two isomeric azo pigments with absorption maxima at 530 nm [77,82]. CB reacts directly with the diazo

reagent, hence referred to as "direct bilirubin," due to its greater solubility in serum. Conversely, UCB requires an accelerator for its solubilization, thus named "indirect bilirubin". Malloy and Evelyn suggested using methanol as an accelerator and adding alkaline tartrate at the end of the reaction to shift the absorption maxima from 530 to 600 nm [83]. Subsequently, Jendrassik-Grof replaced methanol with caffeine and sodium benzoate [84]. These variants brought several improvements, including reducing interference caused by hemoglobin and high concentrations of proteins and insensitivity to pH changes [77]. Today, further modified formulations are in current use, to some extent depending on the instrument manufacturer. However, literature reports under- or overestimation errors due to hemoglobin spectral interference, which can lead to unacceptable results [85–87].

Vanadate Oxidase, on the other hand, is based on the use of vanadic acid as an oxidizing agent to convert bilirubin into biliverdin [88,89]. This method is typically simpler and faster than Diazo and more robust toward interfering analytes, primarily hemoglobin and triglycerides [88,89]. A recent retrospective analysis demonstrated a major decrease in test cancellations due to hemolysis in the sample when using Vanadate Oxidase compared to conventional Diazo (0.6% versus 30.6%, respectively) [88]. Despite being a more robust method, Vanadate Oxidase is typically more costly and requires more human intervention and operations [89].

Overall, these methods are routinely used at global scale for the measurement of TSB and its conjugated and unconjugated forms. The instrumentation implementing such methods, however, is bulky and expensive, and requires the presence of trained laboratory technicians to work properly. Moreover, constrained settings or rural areas can hardly afford the technological, infrastructural, and operational requirements necessary for the correct management of such machinery [29].

Direct spectrophotometry emerges as a third option alongside the two aforementioned methods. This alternative approach has seen multi-decadal development, leading to the proposal of several research-level and commercial instruments [16,28,29,90,91]. Unlike the Diazo and Vanadate Oxidase methods, direct spectrophotometry does not require any dilution of the sample or the use of reagents or other chemical substances for measurement a priori [28,29,92]. This fundamental characteristic allows the method to be adapted to simplified and more cost-effective devices, making it particularly well-suited for the development of POC instruments. Such devices are capable of meeting the stringent requirements of under-resourced areas, including LMICs. It is also true, however, that this method often requires centrifugation of the sample before performing the analysis, bringing the necessity of a trained operator and an adequate centrifuge [17,93]. Additionally, due to the absence of reagents, this method is only applicable to blood samples from neonates less than two to three weeks old [94]. After this period, interfering pigments such as lipochromes, carotenoids, and proteins begin to form, rendering the method inapplicable or, at least, significantly less reliable [95]. Blood gas analyzers can measure TSB using direct spectrophotometry without requiring prior centrifugation of the sample [29,96]. Typically, whole, unprocessed blood is delivered to the instrument, where it is internally and automatically hemolyzed [96,97]. Multi-wavelength spectrophotometry is then employed to calculate bilirubin concentration, effectively subtracting the influence of other analytes. Over the past two decades, these instruments have become widely adopted due to their short turnaround time, automated operation, minimal sample requirements, and lower costs compared to traditional laboratory equipment [98]. Additionally, their compact size makes them suitable for POC use in neonatal intensive care units, wards or lower-level healthcare facilities [98]. However, despite these advantages, concerns remain regarding the accuracy of blood gas analyzers [99–102]. Moreover, these instruments must be carefully calibrated for neonatal use, as neonatal samples

contain fetal hemoglobin, which differs from pediatric and adult samples and must be accounted for when calibrating the bilirubin concentration algorithm [99,103].

2.4. Reflectance photometry

2.4.1. Theoretical notes

Reflectance photometry is a specific application of the broader direct spectrophotometry method. In essence, direct spectrophotometry measures the concentration of one or more substances in a liquid solution by determining the intensity of transmitted light relative to the incident light, at a specific wavelength. This method relies on the well-known Lambert-Beer law, reported below in Equation 1. This is the principle used in virtually all direct spectrophotometry-based instruments, like blood gas analyzers and bench-top bilirubinometers.

$$A_\lambda = \log\left(\frac{I_0}{\mathrm{I}}\right) = \epsilon_\lambda c l \qquad \text{Eq. 1}$$

Equation 1. The Lamber-Beer Law for transmission spectroscopy for a specific wavelength λ, where A is the absorbance, I_0 is the intensity of incident light, I is the intensity of transmitted light, ε is the molar absorptivity, c is the concentration of absorbing species in the sample, and l is the path length through the sample.

This method requires that both the sample and its container, typically referred to as a cuvette, be transparent or semi-transparent at the wavelengths used for the analysis, and that the scattering behavior of both the solution and the cuvette be negligible compared to the transmitted light. In contrast, reflectance photometry measures the ratio between incident and reflected light intensities from a sample characterized by an opaque, highly scattering nature. Diffuse reflectance measurements are governed by the Kubelka-Munk function, shown in Equation 2, which describes the relationship between diffuse reflectance and the material's absorption and scattering properties.

$$F(R) = \frac{(1-R)^2}{2R} = \frac{K}{S} \qquad \text{Eq. 2}$$

Equation 2. The Kubelka-Munk function describing the absorption and scattering of an opaque, scattering material at a certain wavelength. F(R) is the Kubelka-Munk function, R is the diffuse reflectance, K is the absorption coefficient of the material, and S is the scattering coefficient.

Figure 7 provides simplified, conceptual schemas of basic elements composing traditional transmittance spectrometers and diffuse reflectance spectrometers.

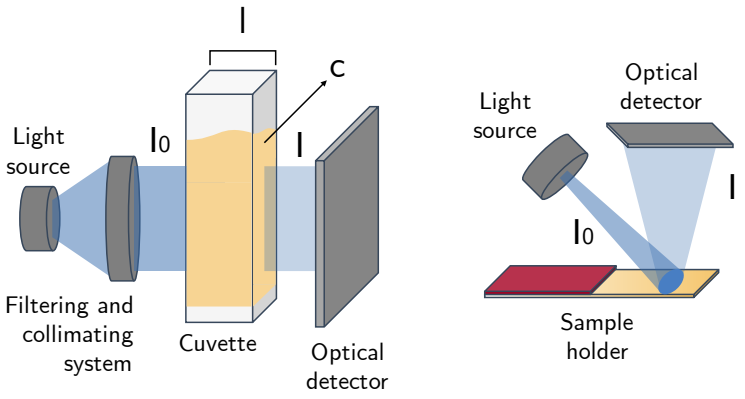

Figure 7. On the left the basic setup and elements of a transmittance spectrometer. A light source (e.g., a halogen lamp, a xenon lamp, or an LED) emits a wavelengths spectrum which is subsequently filtered and collimated by optical filters and lenses; the incident light irradiates the sample contained in a cuvette characterized by a certain optical path length, then the transmitted light intensity is collected by an optical detector. On the right side, the basic setup of a diffuse reflectance spectrometer. The sample is positioned on a sample holder (i.e., a nitrocellulose membrane in this case); a fraction of the incident light is absorbed by the sample, while the remaining is scattered in all directions and reflected in a specular manner.

The Kubelka-Munk theory assumes a homogeneous scattering and absorbing medium, along with diffuse illumination and collection [104–106]. The reflectance photometer used in the studies presented in this thesis requires the sample—whether whole blood, plasma, or external quality control serum—to be applied to a disposable, paper-based lateral flow assay, which is detailed later in this section. This component is designed to collect a specific volume of sample sufficient to fully saturate the membrane. Therefore, an additional assumption must be made regarding the homogeneity of the sample once it saturates the membrane: that the

bilirubin concentration, the primary absorbing analyte, is uniformly distributed across the region of the membrane illuminated by the system. Conversely, if the membrane is oversaturated—such as when an excessive sample volume is applied—its reflectance and scattering properties change significantly due to the formation of a liquid layer. This layer ideally reduces the scattering of reflected light and increases specular reflection. Figure 8 illustrates the scattering and specular reflection phenomena.

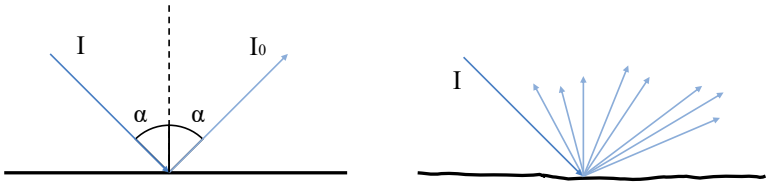

Figure 8. On the left, an ideal smooth reflective surface irradiated with a certain angle of incidence α reflects the individual ray of light with the same angle of reflection. On the right, a rough surface reflects each ray of light with a certain angle depending on the specific point of incidence.

The lateral-flow paper-based assay, referred to as the 'strip', consists of a fiberglass filter and a nitrocellulose membrane enclosed in a plastic cassette, as shown in Figure 9. Both the filter and the membrane are adhesively coupled to a plastic backing card which functions as a structural support element for the assay as well as making the assay optically opaque. The membrane has a thickness of 0.3 mm, a length of 11 mm, and a width of 4 mm, for a total volume of 13.2 µL. The sample is applied to the filter through a well, designed to hold 35 µL of fluid. From there, erythrocyte-free serum flows toward the membrane via capillary action until the membrane is fully saturated. The filtration grade of the filter was selected to ensure proper saturation across a wide range of HCT levels, up to 70%, to accommodate the higher HCT values typical in neonatal blood compared to adult blood [34]. No reagents, either in dry or wet form, are involved in the measurement, and no test lines are present. From an optical standpoint, this absence significantly

simplifies the process. If reagents or other substances were present on the membrane, ensuring their homogeneous distribution would be essential for accurately measuring diffuse reflectance.

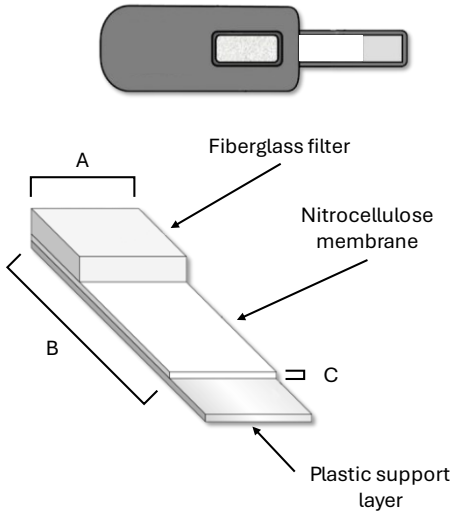

Figure 9. A schema of the strip components. A, B, and C are the width, length, and thickness of the membrane, respectively. (A=4 mm, B=11 mm, C=0.3 mm).

The intensity of scattered light depends on the solid angle relative to the membrane surface. In other words, the angular distribution of reflectance is not uniform, making the results of a reflectance measurement sensitive to the position and surface area of the sensor [106]. Factors like luminous intensity and luminance also need to be considered. However, these concerns are mitigated because the optical system is geometrically fixed, with the relative positions of the light source, strip, and detector being constant and unchanging. Additionally, the optical characteristics of the surrounding environment—specifically, the dark optical chamber described later—can be disregarded, as it is not illuminated by the light source and has no impact on the reflectance signal detected by the sensor.

There are three potential issues related to the Kubelka-Munk theory in this application: i) non-homogeneity of the nitrocellulose membrane, ii) non-homogeneity of plasma saturation, and iii) over-saturation of the membrane.

The first issue, membrane non-homogeneity, is the most challenging to address and requires a procedural solution. Ensuring that quality materials are used is critical, and nitrocellulose membrane providers guarantee physical and chemical uniformity through quality control systems and the release of a Certificate of Quality for each batch and lot produced, confirming that all specified requirements are met.

The second issue, non-homogeneous plasma saturation, also requires a procedural approach but falls under the responsibility of the user, such as the nurse or medical staff. Non-homogeneous plasma distribution can result from a defective membrane or filter, or from an insufficient plasma volume passing through the membrane. The latter may occur due to an inadequate whole blood sample volume (less than 35 µL) or a high HCT level, leaving too little plasma to fully saturate the membrane. In these cases, visual inspection of the strip by the operator is crucial to detect incomplete saturation. If testing a sample with measurable bilirubin, unsaturated areas on the membrane can increase reflectance, causing an underestimation of bilirubin concentration. This error is indistinguishable from a well-saturated membrane with a lower bilirubin concentration sample. Figure 10 shows an example of an incomplete and a complete saturation of a strip.

Figure 10. On the left, an example of a non-complete saturation of a test strip. A white jagged zone is clearly visible on the membrane region farthest from the filter. On the right, a complete, normally saturated membrane. Bilirubin-spiked plasma was used for this test, TSB concentration was around 16 mg/dl.

The third issue, over-saturation of the membrane, can be addressed by the instrument using an appropriate software algorithm. The reflectance photometer used in the studies reported in this thesis is equipped with two discrete LED light sources: one for bilirubin concentration measurement and the other for strip detection and other procedural functions (discussed in detail later in this section). Specifically, the second LED, which emits light at 570 nm in the standard version of the photometer, monitors the filling process of the membrane after blood sample application. Since bilirubin absorbs negligibly at this wavelength, the sample can be safely irradiated before bilirubin measurement without causing photooxidation. The algorithm is designed to periodically irradiate the membrane at 570 nm and take corresponding reflectance measurements. Initially, the reflectance remains constant and at its maximum as long as the membrane area being irradiated is still dry. As the plasma saturates the membrane, the reflectance decreases proportionally, reaching its lowest point once saturation is complete. If the plasma volume is correct, this condition remains stable, allowing bilirubin concentration measurement to proceed. However, if too much plasma is applied, a layer of pure plasma forms over the membrane, altering its optical properties by creating a shiny, smooth surface. This leads to a detectable increase in reflectance, indicating over-filling. In such cases, the bilirubin concentration is measured based on the previous stable reflectance values. Figure 11 shows the typical temporal trend of measured reflectance highlighting the corresponding physical events.

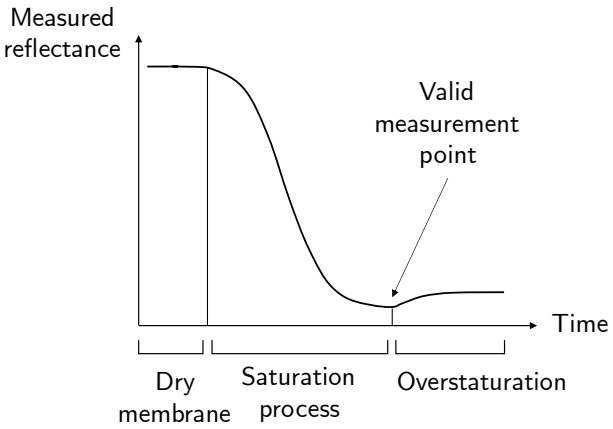

Figure 11. A typical reflectance temporal trend with the description of each phase.

2.4.2. Description of the reflectance photometer

The studies presented in this thesis utilize a two-wavelength reflectance photometer, with its software and hardware modified during the experiments conducted and described in Chapters 2 and 3. Figure 12 reports the core components of the optical system.

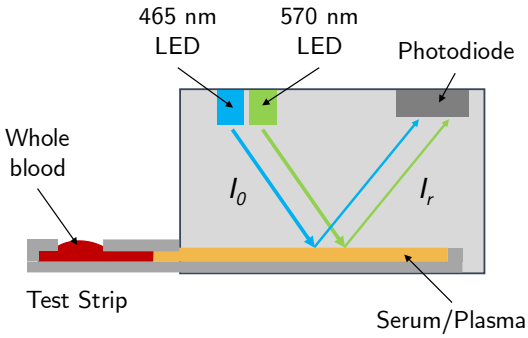

Figure 12. A schema of the components enclosed in the optical chamber, the core elements of the reflectance photometer (not in scale).

An optical chamber encloses all components responsible for illumination and signal detection, along with the portion of the strip that is irradiated during testing. The insertion of the strip, combined with the internal geometry of the chamber, creates a physical barrier that blocks any extraneous light from the external environment. An early study on the optical chamber was conducted to assess the

impact of ambient lighting on the signal collected by the photodiode. Reflectance measurements were taken without a test strip, leaving the optical chamber partially open, under varying illuminance conditions ranging from complete darkness to direct sunlight. The variation in the reflectance signal between the darkest and brightest conditions was less than 0.1% of the instrument's measuring range. Given that the insertion of the strip provides additional light blockage, it is safe to conclude that external lighting does not affect the measurement. This feature is especially important for the instrument's portability, ensuring robustness against environmental variables, lighting included [19].

The light source is composed of two, separate LEDs. The characteristics of the two LEDs are reported in Figure 13 and 14.

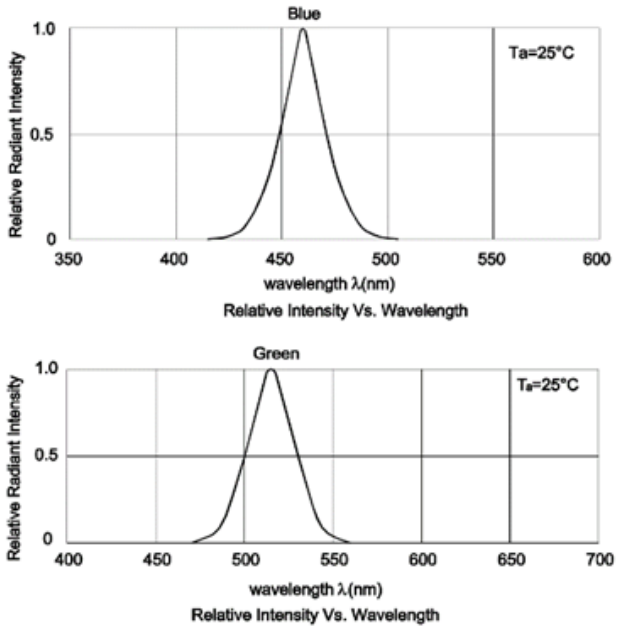

Figure 13. The emission spectra of the two LEDs.

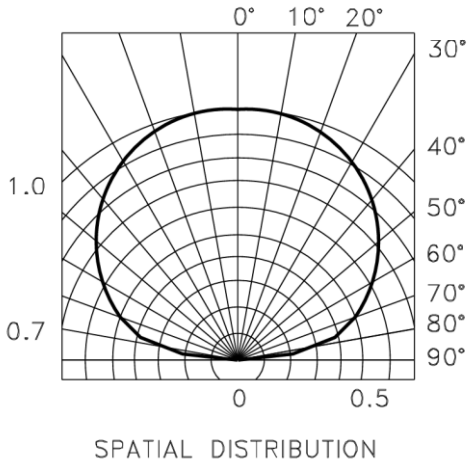

Figure 14. The spatial distribution of emitted light, identical for the two LEDs.

Two key factors guided the selection of the LEDs: i) the dominant wavelength, and ii) the lens geometry over the semiconductor element. The wavelength for the measuring LED was selected based on bilirubin's absorption spectrum, with 465 nm blue light chosen for its proximity to bilirubin's peak absorption point [91,107]. The opposite consideration applied to the auxiliary LED, which was used to monitor the saturation process. It was essential that this LED had no significant effect on the sample analytes, particularly bilirubin. Consequently, 570 nm was chosen, as bilirubin absorption is theoretically negligible at this wavelength (Figure 15). Additionally, this wavelength was intended to detect the presence of hemoglobin in the sample, indicating some degree of hemolysis.

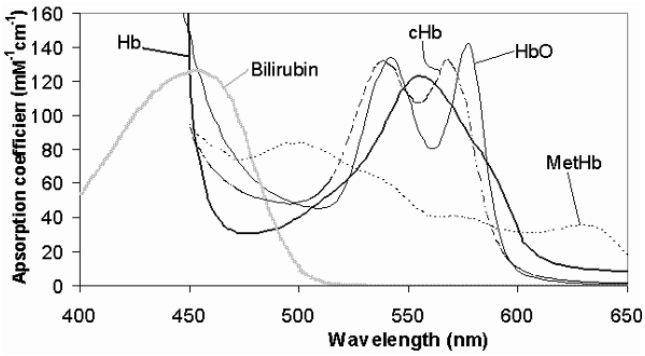

Figure 15. The absorption spectra for bilirubin and hemoglobin in its various forms. Adapted from [108].

This feature is crucial for ensuring the reliability of the system's results, even though the instrument, in its basic configuration, lacked the capability to quantify hemoglobin or compensate for its impact on bilirubin measurements. A preliminary analysis demonstrated that hemolysis significantly influenced results before becoming visibly detectable by an operator inspecting the strip post-test. While excessive erythrocytes on the membrane or massive hemolysis are clearly visible, leading to the test being discarded, a small presence of hemoglobin could go undetected, potentially resulting in misleading results and overtreatment. For this reason, a hemoglobin detection function was developed and implemented, enhancing the system's reliability and specificity in line with the WHO's A.S.S.U.R.E.D. guidelines [45]. Figure 16 shows examples of erythrocyte leakage, visible hemolysis, non-visible hemolysis, and a standard, non-hemolyzed sample.

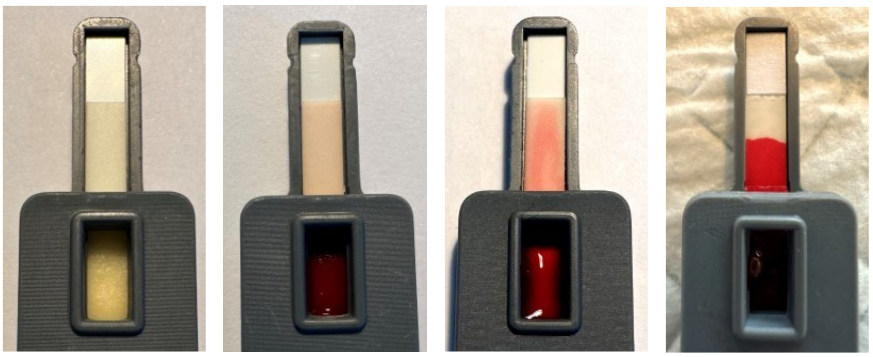

Figure 16. From left to right: a reference, non-hemolyzed strip loaded with bilirubin-spiked serum simulating the expected result of a successful separation; a slightly hemolyzed whole blood sample, which would be challenging to recognize by an operator inspecting the strip after a measurement; a visibly, massively hemolyzed sample; a non-hemolyzed sample with incorrect plasma separation resulting in clearly visible erythrocyte presence in the membrane.

The second factor considered was the geometry of the lenses for the two LEDs. Flat, water-clear lenses were selected to maximize sample irradiation while ensuring uniform light distribution. As shown in Figure 14, the spatial distribution of relative luminous intensity remains constant and above 95% up to approximately 25° from the optical centerline. This solid angle was considered adequate to uniformly

irradiate the membrane surface, avoiding excessive light concentration in any specific area.

Another critical aspect, as in any transmittance or diffuse reflectance system, is the measurement of blank reflectance. For this specific application, this step serves multiple purposes: ensuring the LEDs' performance remains consistent over time, detecting LED malfunctions, and measuring the blank strip's reflectance. By design, once the system detects strip insertion, it measures the blank reflectance at both wavelengths. If the reflectance value falls below a predetermined threshold, a fault in either the LEDs or the strip is suspected and reported. Measuring the blank reflectance of the irradiated strip section also ensures proper compensation for inter-assay variations by normalizing the reflectance results to the blank value before calculating concentrations. This procedure, being fully automated and rapid, offers a notable advantage over other instruments, even those at the laboratory level, where light source inspections are often manual and conducted daily.

The last component of interest for this thesis is the detector, which is a commercial high sensitivity ambient light sensor (i.e., a photodiode). The fundamental characteristics of this component are reported in Figures 17 and 18.

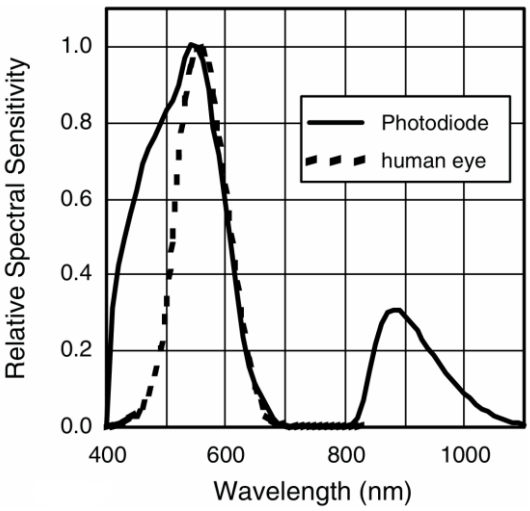

Figure 17. The relationship between relative spectral sensitivity and wavelength of the photodiode used for collecting the reflectance signal.

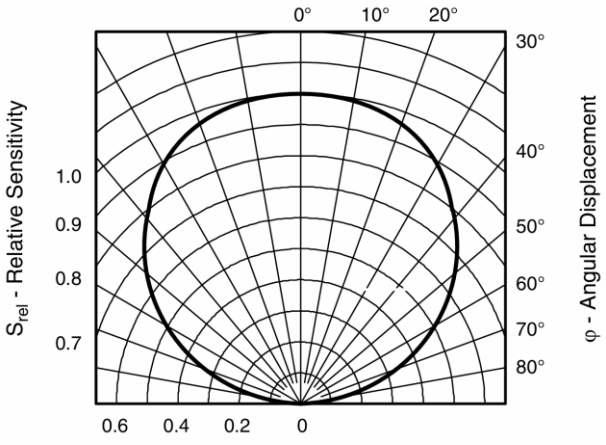

Figure 18. The relationship between relative sensitivity and angular displacement of the photodiode.

Regarding the relative sensitivity as a function of angular displacement, shown in Figure 17, the same principles applied to the LEDs hold true: sensitivity remains constant and maximal between 0° and 10°, and above 95% up to approximately 25°, which is sufficient for detecting the diffused reflectance signal from the membrane. However, the relative spectral sensitivity at the measurement wavelength of 465 nm is around 0.7, which represents one of the non-idealities of the system. For this reason, identifying a similar, low-cost, commercial sensor with higher sensitivity at 465 nm would be beneficial for future enhancements.

This section has outlined the essential components of the reflectance photometer, forming the basis for the research studies detailed later in this thesis. The following sections will cover the published research efforts aimed at improving the instrument's performance, specificity, and robustness.

2.5. Design of an algorithm for hemoglobin compensation [109]

2.5.1. Introduction

Bilirubin is the major product of erythrocytes breakdown; under normal conditions UCB is released in plasma where bounds to albumin, until it is excreted in bile as conjugate bilirubin [1,52]. In neonates, due to several factors, UCB can form in higher concentrations: more than half of newborns experience a temporary and controlled increase of UCB known as hyperbilirubinemia during their first days of life, which is a physiological condition [2,60]. However, roughly one in ten newborns develops clinically significative hyperbilirubinemia: due to the neurotoxicity of bilirubin, this condition can be severe and lead to kernicterus or death [1,2,60]. In these cases, frequent monitoring of serum bilirubin is needed to establish a proper treatment and reduce chances of neurological damage [15,110]. Several guidelines for the management of neonatal hyperbilirubinemia were established [7,8,10]; however, in LMICs, the lack of infrastructures, technologies, and accessibility hinder their effective use [6,48,111]. Direct spectrophotometry for the measurement of bilirubin has been in use for decades and several variants, both for laboratory and POC applications, have been proposed [16,18,28,84,91,112].

The main limitation of this method is the interference from other pigments, mainly hemoglobin, which can be present in plasma samples due to hemolysis or bad blood samples handling or collection. Interferent analytes compensation is normally accomplished through the use of reagents [84] or the use of lamps combined with optical filtering systems capable of generating up to 512 different wavelengths [113]. These aspects increase complexity, dimensions, cost and reduce usability of direct photometry-based devices limiting their applicability in low-resource settings such as LMICs [29]. The aim of this work is to propose and test a novel algorithm

for hemoglobin interference compensation on a simple, portable, inexpensive two-wavelengths reflectance photometer for the measurement of TSB applicable to LMIC scenarios.

2.5.2. Materials and Methods

2.5.2.1. *The measuring setup*

A two-wavelengths reflectance photometer was used for the measurement of bilirubin and hemoglobin samples (Figure 19). Two discrete LEDs irradiated the sample at 465nm and 570 nm, respectively (KPHHS-1005QBC-D-V and KPT-1608CGCK, Kingbright, Taiwan); a photodiode (TEMD6200FX01, Vishay, USA) was used to measure reflected light intensity at each wavelength; these components, as well as the sample, were enclosed in a dark chamber blocking any external light. Other electronic components necessary for the acquisition and digitalization of the signal were also included. The 35 µL plasma samples were positioned on lateral flow test strips, composed of a fiberglass filter coupled with a nitrocellulose membrane laid on a plastic support; since no light was transmitted through the sample, the fraction of light not absorbed by the sample was reflected towards the photodiode. In this way, the photometer acquired the intensity of reflected light.

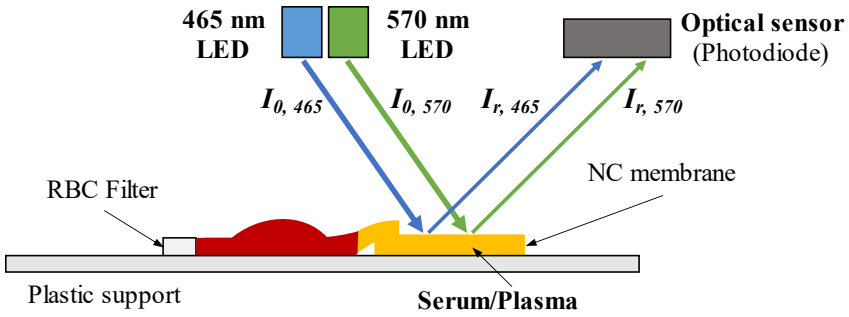

Figure 19. A drawing of the discrete LED light sources, the irradiated sample, and the photodiode placement. All these elements were enclosed in the darkened optical chamber and controlled by other electronics.

2.5.2.2. *Test samples*

A panel containing two different levels of bilirubin concentration and five different levels of hemoglobin was prepared. Commercial purified bilirubin (Bilirubin powder ≥ 98% – Code B4126, Sigma Aldrich) was dissolved in DMSO to obtain a mother bilirubin solution. Meanwhile, 10 mL of blood was drowned from one adult volunteer in a tube containing K3 EDTA anticoagulant and, after centrifugation, two aliquots of plasma were transferred to separated test tubes. The bilirubin mother solution was added in different proportions to each of the test tubes to obtain 5.0 mg/dL and 15.0 mg/dL bilirubin concentrations, respectively. To obtain a mother hemoglobin solution the same blood sample was lysed and centrifuged again to separate lysed cells fragments; the high hemoglobin concentration plasma was collected and used to prepare five levels of hemoglobin concentration for each one of the test tubes. The final concentration of hemoglobin for each sample was verified using conventional methods. The final panel of samples is shown in Table 3; each sample was tested in replicates of three.

Sample	Expected Bilirubin [mg/dL]	Hemoglobin [g/dL]
B_1_H_1	5.0	0.21, 0.23, 0.21
B_1_H_2		0.32, 0.30, 0.30
B_1_H_3		0.46, 0.46, 0.48
B_1_H_4		0.62, 0.57, 0.59
B_1_H_5		0.68, 0.68, 0.71
B_2_H_1	15.0	0.16, 0.16, 0.16
B_2_H_2		0.27, 0.30, 0.27
B_2_H_3		0.39, 0.39, 0.39
B_2_H_4		0.50, 0.52, 0.50
B_2_H_5		0.64, 0.64, 0.68

Table 3, The panel of samples for this experiment. Three samples were prepared for each of the two different bilirubin levels in combination with five different hemoglobin concentrations.

2.5.2.3. *Hemoglobin interference compensation algorithm*

The reflectance photometer device response to different bilirubin concentrations was characterized by testing non-hemolyzed samples with different bilirubin concentration in a sufficiently wide range for this experiment: specifically, the 465 nm wavelength was used as it is relatively close to the bilirubin absorption peak. A function was used to approximate the relation between 465 nm reflectance and bilirubin concentration. This reflectance-bilirubin calibration curve was used to estimate bilirubin concentration.

At 465 nm both bilirubin and hemoglobin show significative absorption, while at 570 nm only hemoglobin shows significative absorption and bilirubin response is close to zero. For this reason, a given hemoglobin concentration causes a specific decrease in reflectance at each wavelength (ΔR_{570} and ΔR_{465}, respectively) with respect to a non-hemolyzed sample. To subtract the influence of hemoglobin from reflectance at 465 nm, thus, to measure bilirubin without hemoglobin interference, a relation between ΔR_{570} and ΔR_{465} had to be defined.

Reflectance data for non-hemolyzed samples (B_1_H_1 and B_2_H_1 in Table 3) was defined as reference for 570 and 465 nm wavelengths and indicated as $R_{570, ref}$ and $R_{465, ref}$, respectively. For each of the other tests, ΔR_{570} and ΔR_{465} were calculated as reported in Equation 3 and Equation 4, where $R_{570, [Hb]}$ and $R_{465, [Hb]}$ are the reflectance values for a certain hemoglobin concentration at each wavelength.

$$\Delta R_{570} = R_{570,ref} - R_{570,[Hb]} \qquad \text{Eq. 3}$$

$$\Delta R_{465} = R_{465,ref} - R_{465,[Hb]} \qquad \text{Eq. 4}$$

Equations 3 and 4. The equations used to calculate the differences between reference values and reflectance values for a certain hemoglobin concentration at both wavelengths.

Subsequently, ΔR_{570} and ΔR_{465} were correlated using a linear function. In such way, a certain difference between $R_{570,\,[Hb]}$ and $R_{570,\,ref}$ could have been associated with a difference between $R_{465,\,[Hb]}$ and $R_{465,\,ref}$, calculating the difference in reflectance at 465 nm caused by hemoglobin. The ΔR_{465} itself was then added to the resulting reflectance and bilirubin concentration was calculated.

2.5.3. Results

Reflectance at 465 nm was highly correlated with hemoglobin, leading to major overestimation errors at both levels (Table 4).

A significative correlation was found between ΔR_{465} and ΔR_{570} ($r = 0.85$, $p < 0.02$); a linear equation was used to approximate this relation (Figure 20).

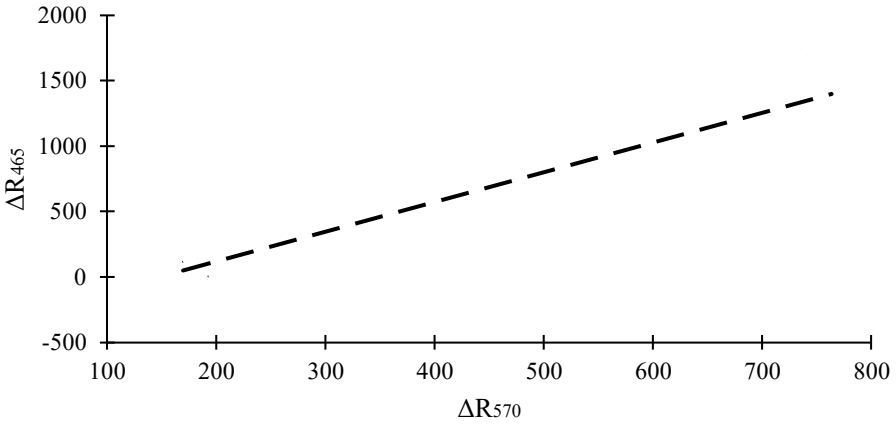

Figure 20. The linear equation used to approximate the relation between ΔR_{465} and ΔR_{570} (dashed line). The upper and lower dotted lines represent the interpolation of lower and higher bilirubin level samples, respectively.

In Table 4 compensated bilirubin data is reported before and after the application of the proposed algorithm. Without any compensation the relative errors were higher than 20% for almost every hemoglobin concentration apart from the non-hemolyzed samples, and as high as 94% in the worst case. The algorithm effectively reduced relative errors and resulted in a 15.4% error in the worst case.

		No compensation		After compensation	
Sample	Expected [mg/dL]	Measured [mg/dL]	ε%	Measured [mg/dL]	ε%
B_1_H_1	5.0	5.3	3.3	5.0	3.4
B_1_H_2		6.4	28.7	5.4	4.6
B_1_H_3		7.7	54.7	5.7	9.4
B_1_H_4		8.4	68.0	5.5	6.1
B_1_H_5		9.7	94.0	5.7	11.0
B_2_H_1	15.0	15.9	1.8	14.6	4.6
B_2_H_2		17.0	13.3	14.1	7.6
B_2_H_3		18.3	22.0	13.4	12.3
B_2_H_4		19.9	32.7	12.9	15.4
B_2_H_5		22.8	52.2	13.1	13.9

Table 4. Results of the bilirubin measures without compensation and with compensation algorithm. Relative percentage errors are reported ($\varepsilon_{\%}$).

The discrepancy highlighted in Figure 20 between the two tested bilirubin levels suggests that bilirubin absorption at 570 nm is not negligible, resulting in an increased dispersion of data points; to confirm this aspect, all reflectance data at 570 nm from each bilirubin level was averaged, and a slight correlation was observed ($r = 0.38$).

2.5.4. Discussion

In this study, a method for hemoglobin influence compensation on bilirubin measurement was proposed and tested on a simple two-wavelengths reflectance spectrometer; the instrument used two discrete LEDs emitting light at 465 nm and 570 nm, respectively, and a photodiode measuring reflected light intensity. The sample size was 35 µL.

The testing of a panel containing two levels of bilirubin and five hemoglobin concentrations resulted in extensive overestimation errors using 465 nm light without any compensation, since the absorption spectra of bilirubin and hemoglobin overlap significantly at such wavelength. The choice of adding a 570 nm light was based on the hypothesis that at this wavelength bilirubin shows negligible

absorption, thus reflectance signal is only attributable to hemoglobin concentration. The results indicated a relation, albeit limited, between reflectance at 570 nm and bilirubin concentration: this resulted in different data distributions for the two levels, hence a not negligible deviation from the ideal case of having a calibration law depending only on hemoglobin concentration. Although this limitation, the algorithm led to a significant reduction of overestimation errors at both levels of bilirubin: the use of a linear law allowed a reduction of the relative errors from 94% to 15.4% in the worst case.

In a previous work, a simple two-wavelengths spectrophotometer with hemoglobin compensation capabilities was proposed [91]: the authors reported a coefficient of determination r^2 of 0.89 on bilirubin determination in serum, however no data was reported concerning hemoglobin influence. In another study, a three-wavelengths handheld reader was used to test plasma samples with bilirubin concentrations ranging from 0.0 to 36.3 mg/dL [63]: the authors speculated that measured spectra showed little to no change in absorption due to hemoglobin, although no data regarding hemoglobin concentrations was disclosed. Lastly, a wearable device for real-time detection of jaundice capable of measuring bilirubin, SpO_2, and heart rate was recently proposed [114], resulting in good agreement with commercial transcutaneous bilirubinometers.

Future effort will be aimed at optimizing the wavelength used for hemoglobin detection, thus at finding a wavelength for which bilirubin absorption is negligible and hemoglobin absorption is adequate for this application. In addition, a larger panel of bilirubin and hemoglobin concentrations will be needed to confirm the applicability of this approach to the screening for NH in low-resource settings.

2.6. Identification of the optimal wavelength for the compensation performance [115]

2.6.1. Introduction

Bilirubin is the ultimate breakdown product of erythrocytes, it is released in plasma as UCB where, due to its poor solubility in water, bounds to albumin until its excreted in bile [1,52]. An excessive amount of UCB, known as hyperbilirubinemia, is frequently caused by an enhanced production of bilirubin due to hemolysis; on the other hand, UCB accumulates in blood if conjugation with albumin occurs at lower rates, or certain physical or pathological conditions are present [52,60,116]. Sixty to eighty percent of neonates experience temporary and controlled hyperbilirubinemia during the first days of life, which typically does not require medical treatment. However, approximately one in ten newborns develops pathological hyperbilirubinemia, which can potentially lead to severe neurological damage, kernicterus, or death [2,49,52,60,73,116]. Regardless of the type of hyperbilirubinemia, it is essential to conduct precise and timely bilirubin concentration measurements in the first days of life, ideally following international guidelines, to maximize outcomes and minimize the need for late interventions [7,8,15]. Several methods for TSB measurement in whole blood or plasma were developed, with direct spectrophotometry being one of the most extensively used both for laboratory and POC applications [16,18]. Direct spectrophotometry-based devices can be designed to meet the specific requirements of LMICs where the burden of NH is particularly high due to economical, infrastructural and accessibility limitations [2,6,111]. Various examples of small, portable, economical and easy-to-use devices are reported in recent literature [91,117–119]. One of the major limitations of direct spectrophotometry is interference from other pigments, primarily hemoglobin, which can be present in plasma samples due to hemolysis. Hemolysis can occur in vivo due to enzyme deficiencies, infections, or other

pathological conditions, or in vitro due to mechanical damage of the sample, careless collection, or the modality and equipment used for collection [120]. The latter is especially relevant for neonates: being less invasive and painful, blood collection is most frequently executed by capillary heel-stick, which is associated with higher levels of hemolysis [121,122]. In LMICs, where there is a shortage of skilled professionals and defined protocols for sample collection and manipulation, the probability of in vitro hemolysis is further increased. A recent study reported that sample hemolysis was most common in the departments of Pediatrics (16.2%) and Neonatology (11.3%) [123]. Given these conditions and the likelihood of hemolysis due to hyperbilirubinemia itself, it is clear that direct spectrophotometry-based devices need to incorporate an algorithm to compensate for the influence of hemoglobin on bilirubin measurement. Interferent analytes compensation, including hemoglobin, in direct spectrophotometry-based devices is commonly obtained using reagents or lamps combined with optical filtering systems capable of selectively generating up to 512 wavelengths [84,91,124]. These solutions are normally achievable for laboratory applications, where dimensions and complexity are not strict requirements, besides raising purchase and operating costs. However, LMICs, and low-resource settings in general, present characteristic limitations that make typical instrumentation too complex, too expensive, or unsuitable. This necessitates the design of devices following specific requirements [19,44]. An earlier study [109], conducted on a limited panel of bilirubin and hemoglobin concentrations, showcased the feasibility of a straightforward compensation method relying solely on two wavelengths, specifically 470 and 570 nm. This algorithm effectively reduced overestimation errors on visibly hemolyzed plasma samples. However, the 570 nm wavelength exhibited a slight dependency on bilirubin concentration, limiting the algorithm's ability to compensate optimally for hemoglobin and thereby constraining its error reduction capabilities. The aim of this study is to assess the performance of additional wavelengths—575, 590, and 605 nm—in addition to the

570 nm wavelength for compensating hemoglobin interference in bilirubin measurement. This will be achieved using a simple, low-cost two-wavelength reflectance photometer.

2.6.2. Materials and Methods

2.6.2.1. *The measuring setup*

A two-wavelengths reflectance photometer was used for this experiment; two discrete commercial LEDs irradiated the sample, and a commercial photodiode was used to measure reflected light intensity at each wavelength. The sample, the LEDs and the photodiode were enclosed in a dark chamber blocking any external light. Other electronic components necessary for the acquisition and digitalization of the signal were also included. The 30 µL plasma samples were positioned on lateral flow test strips, composed of a fiberglass filter coupled with a nitrocellulose membrane laid on a plastic support; since no light was transmitted through the sample, the fraction of light not absorbed by the sample was reflected towards the photodiode. In this way, the photometer acquired the intensity of reflected light (Figure 21). The first LED emitted light at 465 nm, a wavelength at which bilirubin exhibits peak absorption [91]. This LED was used to measure the concentration of bilirubin in the samples during the experiments, following a preliminary calibration of the system. The second LED, the primary focus of the investigation, was replaced for each of the four experiments and emitted light at 570, 575, 590, and 605 nm, respectively.

These wavelengths were elected based on the commercial availability of LEDs and in consideration of the absorption spectra of hemoglobin and bilirubin: at all the aforementioned wavelengths the first exhibits significant absorption, whereas the latter exhibits negligible absorption. The device was programmed to detect the filling progress of the lateral flow test strip and to execute two consecutive readings as soon as complete saturation was detected. This process allowed for four

measurements to be taken for each test, with two being conducted at each of the wavelengths used.

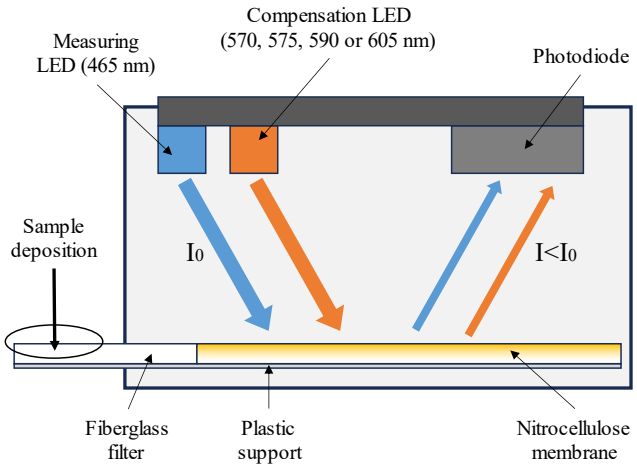

Figure 21. A schematic representation of the reflectance photometer used for the experiment. The second LED indicated here as "compensation LED" was replaced for each wavelength tested.

2.6.2.2. *Test samples*

Two independent investigations were conducted, one focusing on varying concentrations of bilirubin and the other on varying concentrations of hemoglobin. As a result, two panels of plasma samples were prepared. Two commercial quality controls were used for the first panel (Verichem Laboratories Inc., USA, Bilirubin standard kit, list No. 9450, lot No. A432006, expiration date 2024-07-30 and Bilirubin standard Level F, list No. 9436, lot No. E432801, expiration date 2024-09-30). Due to the light sensitivity of bilirubin, samples belonging to this panel were stored away from light and tested within an hour from the preparation. For the second panel, whole blood was drawn from one healthy adult volunteer into a tube containing K3 ethylenediaminetetraacetic acid (EDTA) and centrifuged to obtain plasma separation. An aliquot of separated plasma was then transferred to a separate test tube. The same blood sample was lysed and centrifuged again to separate the lysed cell fragments. Hemolyzed plasma was then transferred to different test tubes to create five different concentrations of hemoglobin. In

conclusion, the first panel consisted of six non-hemolyzed plasma aliquots with six different bilirubin concentrations, while the second panel consisted of five different plasma aliquots, each showing a different hemoglobin concentration and a unique, negligible bilirubin concentration. Bilirubin and hemoglobin concentrations were then verified using standard methods. The resulting levels for the bilirubin and hemoglobin panels are reported in Table 5.

Panel type	Level					
	1	2	3	4	5	6
Bilirubin [mg/dL]	0.5	5.5	10.5	15.5	20.5	30
Hemoglobin [g/dL]	0.41	0.62	0.82	1.05	1.21	-

Table 5. The two plasma samples test panels used in the experiment.

2.6.2.3. *Wavelengths testing protocol*

The same protocol was used for each tested wavelength. Five independent measurements were executed for each level of the two panels. For each measurement, a new lateral flow test strip was inserted into the reader, and blank reflectance, as well as the temperature of the system, were recorded. Correct saturation of the nitrocellulose membrane and the absence of any abnormal condition were verified after each measurement. If necessary, the measurement was repeated. After the test execution phase, raw reflectance data for each measurement were normalized by blank reflectance to remove variations dependent on the optical characteristics of the individual lateral flow test strips.

The presence of outlier data was verified, and corresponding data points were excluded. For each of the wavelengths, results were deemed acceptable if data analysis: i) excluded any or negligible dependence between bilirubin concentration and normalized reflectance across the bilirubin panel, and ii) showed a significant relationship between hemoglobin concentration and normalized reflectance across

the hemoglobin panel, with sufficient sensitivity and monotonic trend. In both cases, statistical significance tests were performed to support the results.

2.6.3. Results

A total of 55 test were conducted, hence 110 single measurements from the two panels were available for the analysis. Data from the bilirubin panel were used to assess the system's performance and verify the concentration of bilirubin across different levels. A strong correlation and statistical significance were demonstrated by interpolating reflectance at 465 nm against bilirubin concentration using an exponential law ($R^2 = 0.998$, p-value < 0.001). Figure 22 illustrates the normalized reflectance results for the bilirubin and hemoglobin panels, respectively, for each of the four tested wavelengths. For the bilirubin panel, a linear equation was used to approximate the relationships, while for the hemoglobin panel, a quadratic law was used. The Kruskal-Wallis test was conducted on the results of both panels to assess the statistical significance. Table 6 reports regression data and statistical results for the bilirubin panel, while Table 7 reports the same for the hemoglobin panel.

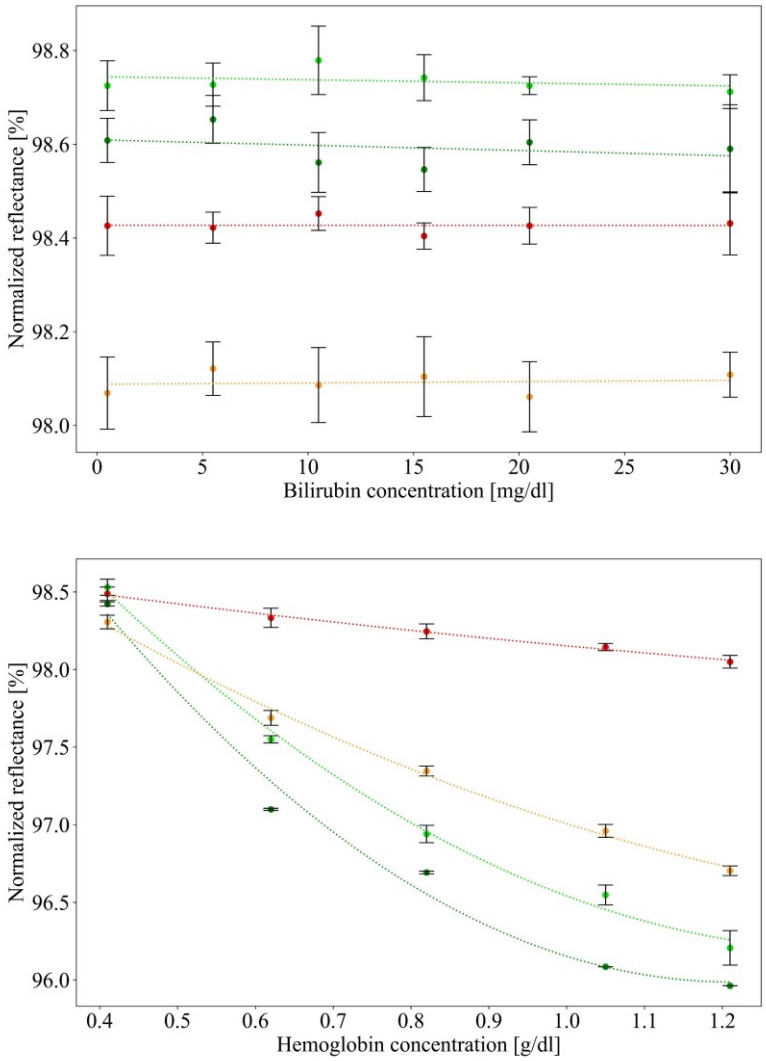

Figure 22. On the top normalized reflectance is plotted against bilirubin concentration for each of the wavelengths tested; on the bottom normalized reflectance is plotted against hemoglobin concentration for each of the wavelengths tested. In both pictures data points represent the average of single measurements for each level, while error bars represent the standard deviation. Red points indicate the 605 nm wavelenght, while amber points the 590 nm one, light green points the 575 nm one, and dark green points the 570 nm one.

Wavelength	Linear regression		Kruskal-Wallis test	
	m	R^2	$\chi 2$	p-value
570	-0.0011	0.103	8.91	0.11
575	-0.0006	0.089	5.38	0.37
590	0.0002	0.016	6.91	0.23
605	0,00002	<0.001	5.93	0.31

Table 6. Bilirubin panel results.

Wavelength	Quadratic regression	Kruskal-Wallis test	
	R^2	$\chi 2$	p-value
570	0.986	8.83	0.06
575	0.995	47.06	<0.001
590	0.996	47.06	<0.001
605	0.993	45.75	<0.001

Table 7. Hemoglobin panel results.

2.6.4. Discussion

In this study, the performance of four different wavelengths was investigated by assessing their independence from bilirubin concentration as well as their sensitivity to hemoglobin. Direct spectrophotometry is an established method for measuring TSB and has been studied and developed for decades. However, the availability of such instrumentation in LMICs is not guaranteed due to various restrictions and limitations. Reference [117] demonstrated the technical feasibility of a simple, portable device based on two discrete light sources, while [109] proposed a novel algorithm for compensating for the influence of hemoglobin on TSB measurement using the same simple reflectance photometer. However, the accuracy of the algorithm was reduced by the non-negligible influence of bilirubin itself on the auxiliary wavelength, which was 570 nm. The present study confirmed this aspect: among the tested wavelengths, the 570 nm one showed the largest dependence on bilirubin concentration with a slope of -0.001 and the "highest" coefficient of determination of 0.1. Regarding the other wavelengths, the least dependent on bilirubin concentration was the 605 nm with a slope of 0,00002 and a coefficient of determination lower than 0.001, followed by the 590 nm wavelength with a slope of 0.0002 and a coefficient of determination of 0.015. The Kruskal-Wallis test results confirmed the absence of significative differences among groups. On the other hand, hemoglobin sensitivity results were significant for both 575, 590 and 605 nm — with 590 nm retrieving the highest coefficient of determination of 0.996 — although the 605 nm wavelength showed a relatively limited variation between the minimum and

the maximum hemoglobin concentrations tested. Summing up, the 605 nm wavelength was the less dependent on bilirubin concentration although showing a limited sensitivity on hemoglobin; the 590 nm was the second-best wavelength in terms of bilirubin independence and showed sufficient dynamics in terms of hemoglobin concentration; the 575 nm wavelength behaved similarly to the 570 nm one in terms of bilirubin independence, which makes it less preferable despite showing a good sensitivity to hemoglobin.

2.7. Application of the optimized compensation algorithm [125]

2.7.1. Introduction

Bilirubin is the final breakdown product of erythrocyte metabolism, released into plasma as UCB, which binds to albumin and is excreted in bile [1,52]. Hyperbilirubinemia, marked by elevated UCB, often results from hemolysis or impaired conjugation with albumin. When hyperbilirubinemia occurs in a neonatal patient, it is referred to as NH. While 60–80% of newborns experience temporary physiological NH within the first days of life, usually without needing treatment [2,12,60], about one in ten newborns develop pathological NH, which poses a risk of severe neurological damage, kernicterus, or death [2,12,59,60]. LMICs bear the greatest burden of NH [3,11,41,50,126,127], with most cases of permanent neurological damage or death from kernicterus occurring in these regions. Despite NH being a well-known issue, reliable data on its incidence and consequences are scarce and difficult to generalize. Two recent meta-analyses addressed the challenge of analyzing avail-able data, revealing that severe NH is 11 times more common in poorer countries compared to wealthier ones. In 2010, stillbirths due to kernicterus were 119 per 100,000 in low-income countries compared to just 1 per 100,000 in high-income countries [41,50]. Both studies agreed that the real burden of NH is

likely underestimated, especially in LMICs, where data quality and key clinical or demographic details are often lacking. This disparity reflects a multifaceted issue, including inadequate infrastructure, inefficient technologies, poor maternal education, and limited healthcare accessibility [6,11,40,111,128]. A timely and quantitative bilirubin assessment in the early days of life is crucial [10,15,110]. Consequently, major clinical guidelines for NH diagnosis and treatment emphasize the need for precise and prompt bilirubin screening, with diagnostic evaluations based on TSB levels in the blood [7,8,12,48,129,130]. While non-invasive methods like transcutaneous bilirubinometers can estimate bilirubin concentration for screening purposes [131,132], diagnosis and subsequent clinical decisions must rely on quantitative, invasive, and blood-based measurements.

Direct spectrophotometry is a valuable method for measuring TSB and is an established technique for both laboratory and POC or field instrumentation [16,18,28,84,91,112]. The recent literature reports various examples of small, portable, economical, and easy-to-use devices that address the specific needs and constraints of LMICs. However, a major limitation of direct spectrophotometry is interference from other pigments in the sample, with hemoglobin being among the most common [25,94,120,122,133]. Hemoglobin may be present in plasma as a result of hemolysis, which can occur in vivo as a result of enzyme deficiencies, infections, or other pathological conditions [134,135]. Alternatively, hemolysis may occur in vitro due to mechanical damage, improper collection techniques, or issues with the equipment used for collection [136–138]. This issue is particularly critical in neonatal care. Capillary heel stick blood collection, favored for being less invasive and painful, is widely utilized; however, it is strongly associated with higher levels of hemolysis [122,123,137]. In LMICs, where there is a shortage of skilled professionals and well-defined protocols for sample collection and handling, the likelihood of in vitro hemolysis is further exacerbated.

Laboratory-grade instruments utilizing direct spectrophotometry compensate for interfering analytes by employing reagents or irradiating the sample with multiple wavelengths, up to 512 [84,91,113,124]. While these techniques provide more robust and accurate results, they also introduce greater complexity and increase the size and cost of the instrumentation, as well as the expense of individual measurements. Furthermore, these techniques restrict their application in well-equipped facilities, limiting their accessibility in resource-constrained settings. This contrasts with the recent literature focusing on the spread of diagnostic devices and technologies in limited resource settings [19,44,45]. The WHO's A.S.S.U.R.E.D. criteria outline fundamental design principles that diagnostic devices should meet to be effective in harsh and under-resourced environments, namely that devices be affordable, sensitive, specific, user-friendly, rapid and robust, equipment-free, and deliverable.

In summary, addressing the challenges of LMICs requires that measurement devices remain simple and economical while maintaining sufficient accuracy for reliable diagnostics with the capability to deliver results quickly and close to the patient. In this work, we present a method for compensating for hemoglobin interference in the measurement of TSB using a simple reflectance photometer. This instrument operates with two wavelengths—465 nm and 590 nm—where the former is employed to measure bilirubin concentration, while the latter is used to determine hemoglobin levels. The photometer requires only 30 µL of plasma to perform a measurement, and no reagents are necessary. A panel of plasma samples was prepared to encompass a wide range of bilirubin concentrations from 4.96 to 28.00 mg/dL. Additionally, these bilirubin samples were divided into groups with varying degrees of hemolysis, ranging from 0.06 to 0.99 g/dL. To demonstrate the performance and applicability of the proposed method, results are presented both before and after hemoglobin compensation, and their implications are discussed.

2.7.2. Materials and Methods

2.7.2.1. *The measuring setup*

A two-wavelength reflectance photometer was employed to measure bilirubin and hemoglobin in the samples (Figure 23). The device used two distinct commercial LEDs to illuminate the sample at wavelengths of 465 nm and 590 nm, respectively (KPHHS-1005QBC-D-V and KA-1608SYSK, Kingbright, Taiwan). Reflected light intensity at each wavelength was detected by a photodiode (TEMD6200FX01, Vishay Intertechnology, Inc., Malvern, Pennsylvania, USA). The entire setup, including the sample, was housed within a dark chamber to prevent interference from external light and limit sample degradation. Essential electronic components for signal acquisition and digitalization were also incorporated. The angle of incidence of light on the sample significantly influenced the measurement results and system accuracy. This parameter was carefully considered in selecting the LED lens geometry, with flat transparent lenses chosen for their uniform light spatial distribution at relatively wide angles. Furthermore, the optical chamber's geometry, including the arrangement and angle of the LED light sources in relation to the membrane surface, was fixed and kept constant throughout all tests. As a result, the influence of the incident angle could be disregarded. The 30 µL plasma samples were applied to disposable lateral flow test strips, which consisted of a fiberglass filter and a nitrocellulose membrane mounted on a plastic support. The fiber-glass filter served to block and retain any red blood cell or fragment that might be present in the sample, thereby preventing their entry into the nitrocellulose membrane. As no light passed through the plastic support, the unabsorbed light was reflected in multiple directions within the optical chamber, enabling the photodiode to measure the reflected intensity.

For each test, a new lateral flow test strip was inserted into the optical chamber and its blank reflectance was measured. Then, the plasma sample was deposited on

the filter. The system was designed to detect the filling process of the membrane and perform the measurement once complete saturation was perceived. The membrane filling detection process was carried out using the compensation wavelength of 590 nm. This ensured that the measurement wavelength of 465 nm was only used for the actual bilirubin measurement, preventing the sample from being exposed to light near its absorption peak, thereby avoiding degradation. The reflectance intensities at both wavelengths, and thus the result of a single test, were normalized to the blank value to compensate for any differences between test strips. As a result of this normalization process, the reflectance values were expressed as unitless numbers. The photometer performed two consecutive measurements for each test, which were then averaged. At the end of each test, the lateral flow test strip was examined to detect any abnormal conditions or an incomplete saturation of the membrane; if such issues were observed, the test was repeated.

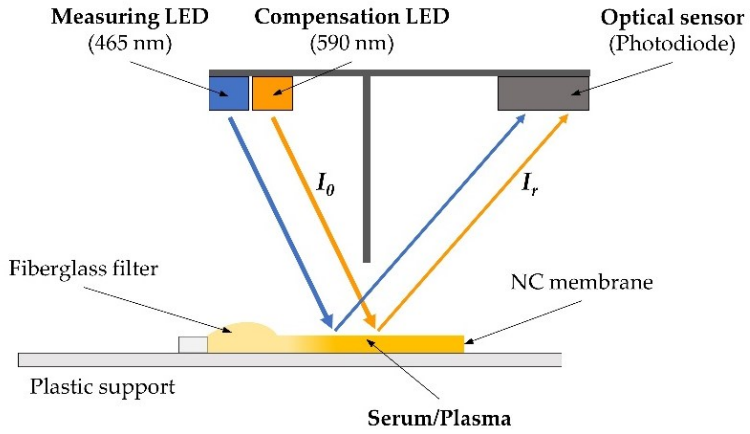

Figure 23. A schema of the reflectance photometer used in the experiments. The two discrete LEDs irradiate the sample after membrane saturation is detected, then the photodiode inside the optical chamber measures the intensity of reflected light.

2.7.2.2. *Test samples*

A panel including five different levels of bilirubin concentration and five different levels of hemoglobin concentration was prepared immediately before the experiment.

Commercially purified bilirubin (Bilirubin powder ≥ 98%–Code B4126, Merck KGaA, Darmstadt, Germany) was dissolved in DMSO to prepare a stock bilirubin solution. Simultaneously, 12 mL of blood was drawn from an adult volunteer into a tube containing K3 EDTA as an anticoagulant. After centrifugation, five plasma aliquots were transferred to separate test tubes. Varying amounts of the bilirubin stock solution were added to each tube to achieve different bilirubin concentrations. To create a stock hemoglobin solution, the same blood sample was lysed and centrifuged again to remove lysed cell fragments, and the resulting hemoglobin-rich plasma was used to prepare five distinct hemoglobin concentrations for each test tube. The hemoglobin concentration in each sample was confirmed using a commercial colorimetric assay (Hemoglobin Colorimetric Method–Code HG1539, Randox Laboratories, Ltd., Crumlin, United Kingdom). The final panel of samples, shown in Table 8, was tested in five replicates per sample.

Sample #	Bilirubin concentration [mg/dl]	Hemoglobin concentration [g/dl]
B1H1 – B1H5	4.96	0.06, 0.29, 0.50, 0.75, 0.99
B2H1 – B2H5	9.67	0.06, 0.29, 0.50, 0.75, 0.99
B3H1 – B3H5	14.47	0.06, 0.29, 0.50, 0.75, 0.99
B4H1 – B4H5	19.33	0.06, 0.29, 0.50, 0.75, 0.99
B5H1 – B5H5	28.00	0.06, 0.29, 0.50, 0.75, 0.99

Table 8. The panel of samples generated for this experiment. For each of the five bilirubin levels, five different levels of hemolysis were produced, and each sample was repeated five times.

2.7.2.3. *Hemoglobin interference compensation algorithm*

The reflectance photometer's response to different bilirubin concentrations was evaluated by testing non-hemolyzed samples across a broad range of bilirubin levels for this experiment. Specifically, the 465 nm wavelength was used due to its proximity to the bilirubin absorption peak [139]. An exponential function was employed to approximate the relationship between the 465 nm reflectance and bilirubin concentration, creating a reflectance–bilirubin calibration curve for estimating bilirubin concentration, as shown in Figure 24. In a previous proof-of-

concept study [109], the same reflectance photometer and test strips were used to explore the possibility of achieving compensation using just two wavelengths; however, in such instrument, the compensation wavelength was 575 nm instead of 590 nm. This preliminary effort was helpful in confirming the feasibility of this approach despite its limited accuracy in compensation due to a non-optimal choice of the compensation wavelength. In particular, 570 nm showed a slight sensitivity to bilirubin, leading to the impossibility of identifying a unique compensation law dependent only on hemoglobin concentration. Further preliminary research demonstrated that while at 465 nm, significant absorption is observed for both bilirubin and hemoglobin; at 590 nm, absorption is predominantly attributed to hemoglobin with bilirubin's effect being theoretically negligible [115]. Consequently, the presence of a specific concentration of hemoglobin leads to a noticeable reduction in reflectance at both wavelengths (indicated as ΔR_{590} and ΔR_{465}, respectively) compared to a non-hemolyzed sample, which would cause a measurable decrease in reflectance only at 465 nm. In order to accurately measure bilirubin concentration without interference from hemoglobin at 465 nm, it is essential to establish a relationship between ΔR_{590} and ΔR_{465}.

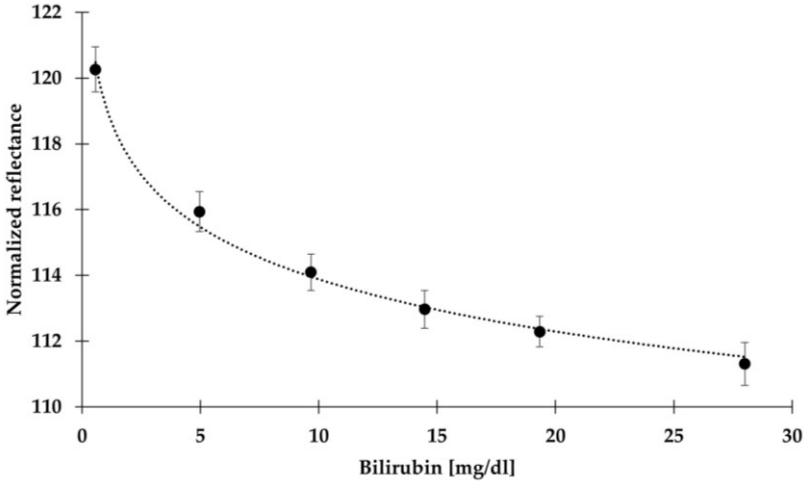

Figure 24. The exponential law used to approximate the relationship between bilirubin and normalized reflectance (dimensionless number). Black dots represent the averaged values for each bilirubin concentration (0.56 to 28.00 mg/dL). Error bars represent the standard deviation for each level. The normalized reflectance values exceed 100 due to the normalization procedure; blank reflectance is measured using the compensation wavelength of 590 nm, which due to the current supply of the LED, has a lower luminous intensity compared to the measurement wavelength of 465 nm. Consequently, for all tested bilirubin levels, the blank reflectance values used for normalization are lower than the actual reflectance values recorded during the measurement at 465 nm, resulting in values above 100.

Reflectance values for non-hemolyzed samples, indicated as B1H1, B2H1, ..., B5H1 in Table 8, serve as reference points for 590 and 465 nm wavelengths, referred to as $R_{590,\,ref}$ and $R_{465,\,ref}$, respectively. For each of the other tests, ΔR_{590} and ΔR_{465} are calculated as reported in Equation 5 and Equation 6, where $R_{590,\,[Hb]}$ and $R_{465,\,[Hb]}$ represent the measured reflectance values for a specific hemoglobin concentration at each respective wavelength.

$$\Delta R_{590} = R_{590,\,ref} - R_{590,\,[Hb]} \qquad \text{Eq. 5}$$

$$\Delta R_{465} = R_{465,\,ref} - R_{465,\,[Hb]} \qquad \text{Eq. 6}$$

Equations 5 and 6. The equations used to define the linear function between the reflectance decreased at 590 and 465 nm for a certain hemoglobin concentration.

Following this, ΔR_{590} and ΔR_{465} are correlated using a linear function. This method enables the association of a specific difference between $R_{590,\,[Hb]}$ and $R_{590,\,ref}$ with the corresponding difference between $R_{465,\,[Hb]}$ and $R_{465,\,ref}$, allowing the

determination of the reflectance change at 465 nm induced by hemoglobin. Subsequently, ΔR_{465} is added to the measured reflectance value, and the bilirubin concentration is calculated using the established exponential calibration law. This process accounts for hemoglobin interference by leveraging the difference in reflectance caused by hemoglobin absorption at 590 nm and applying the derived correction to the measurement at 465 nm, ensuring accurate bilirubin quantification.

2.7.3. Results

Six non-hemolyzed bilirubin plasma samples, tested in repetitions of five, were used to calibrate the reflectance photometer. Specifically, the curve was constructed using the five bilirubin levels in the panel plus an additional lower level (0.56 mg/dL). An exponential law was used to approximate the relationship between normalized reflectance and bilirubin concentration, yielding a significant correlation ($R^2 > 0.99$) (Figure 24).

A total of 125 single tests were performed. The calibration curve was used to calculate bilirubin values for both reference and hemolyzed plasma samples. A significant influence of hemoglobin on the bilirubin results was found, leading to major overestimation errors. Table 9 shows the averaged results without any compensation for each bilirubin level and the associated root mean square error (RMSE).

Expected Bilirubin [mg/dl]	Measured Bilirubin [mg/dl]	RMSE [mg/dl]
4.96	7.52 ± 2.92	3.12
9.67	13.09 ± 2.81	2.63
14.47	20.07 ± 3.22	4.43
19.33	24.27 ± 2.99	5.77
28.00	34.27 ± 2.44	6.73

Table 9. Non-compensated bilirubin results presented as mean value and standard deviation for each level, as well as root mean square errors with respect to the expected value.

A significative correlation was found between ΔR_{465} and ΔR_{590} ($R^2 = 0.74$, $p < 0.05$), despite a considerable dispersion of values across different bilirubin levels (Figure 25).

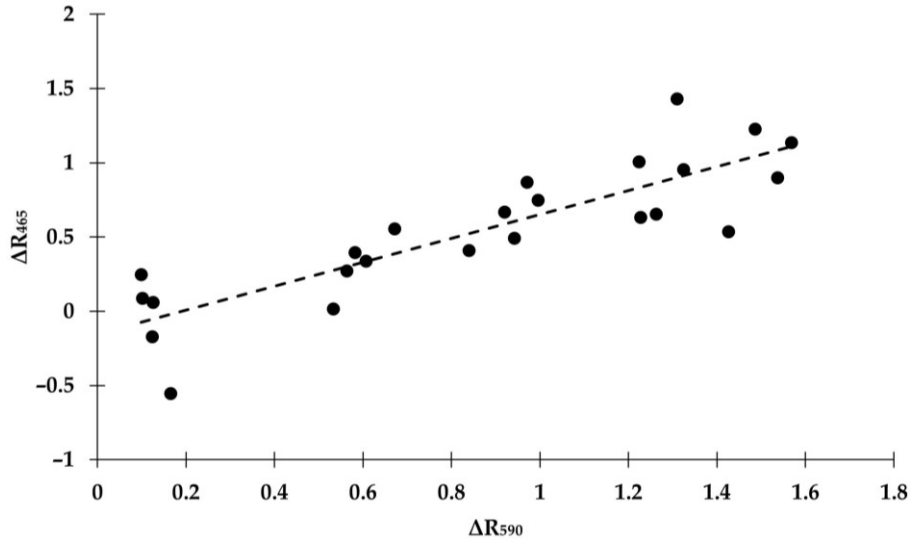

Figure 25. Black dots represent ΔR_{465} and ΔR_{590} for every sample in the test panel. Each point is the mean of the five single tests in the sample. The dashed line represents the linear equation used to approximate the relationship between ΔR_{465} and ΔR_{590}.

The compensation algorithm was applied and the corrected reflectance at 465 nm ($R_{465,\,ref}$) was calculated using the linear relationship shown in Figure 24. Table 10 presents the mean values and standard deviations for the compensated results, as well as the root mean square errors for comparison with non-compensated data. Figure 26 shows the Bland–Altman plot for both the non-compensated and compensated results. Overall, compensated results show reduced standard deviation values at all bilirubin levels except for the highest. More importantly, however, the root mean square errors are less than half of those without any compensation across all levels tested.

Expected Bilirubin [mg/dl]	Measured Bilirubin [mg/dl]	RMSE [mg/dl]
4.96	5.04 ± 0.95	0.95
9.67	9.98 ± 0.50	0.59
14.47	15.08 ± 0.35	0.70
19.33	18.92 ± 1.26	1.33
28.00	26.97 ± 3.17	3.33

Table 10. Hemoglobin-compensated bilirubin results presented as mean value, standard deviation, and root mean square errors for each level, with respect to the expected value.

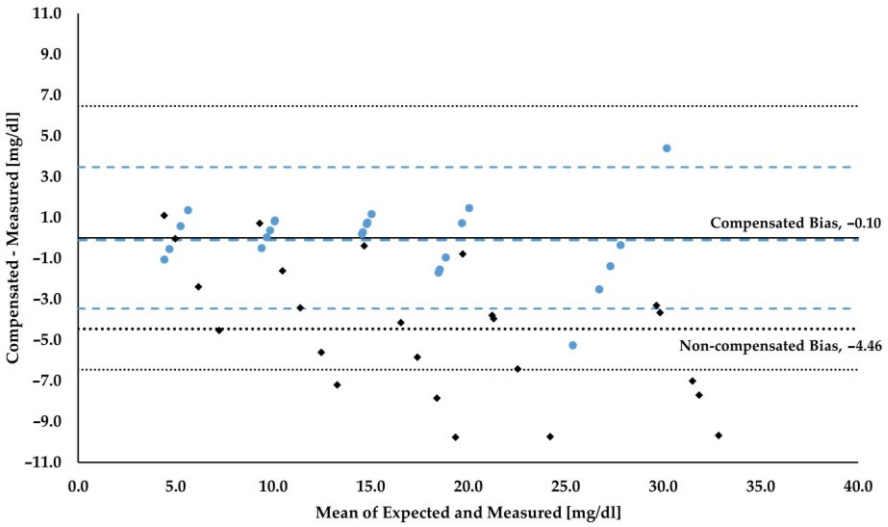

Figure 26. Bland–Altman plot showing both non-compensated and compensated results. Black diamonds represent non-compensated results; blue circles represent compensated results; thin dotted black lines represent upper and lower limits of agreement for non-compensated results (6.46 and −6.46 mg/dL, respectively); thin dashed blue lines represent upper and lower limits of agreement for compensated results (3.46 and −3.46 mg/dL, respectively); thick dotted black line represents bias for non-compensated data (−4.46 mg/dL); thick dashed blue line represents bias for compensated data (−0.10 mg/dL).

2.7.4. Discussion

In this study, we assessed the performance of an algorithm designed to compensate for hemoglobin interference in bilirubin measurements using a simple and portable two-wavelength reflectance photometer. This device was capable of performing measurements on 30 µL samples without the addition of reagents. A panel of plasma samples, comprising five different concentrations of bilirubin and five different degrees of hemolysis, was tested, totaling 125 tests. A commercial discrete LED emitting light at 465 nm was used to measure bilirubin concentration,

while another discrete LED emitting light at 590 nm was used to estimate hemoglobin concentration, as bilirubin shows no absorption at this wavelength. The proposed algorithm combined reflectance data from the two wavelengths to subtract the influence of hemoglobin on the results.

Non-compensated results showed significant overestimation errors, particularly at higher bilirubin levels, which can lead to the misdiagnosis and potential overtreatment of patients. Compensated results, on the other hand, showed a substantial increase in accuracy at all levels. The highest level, with an expected bilirubin concentration of 28.00 mg/dL, retained a non-negligible RMSE, although it was less than half compared to the non-compensated data (3.33 vs. 6.73 mg/dL). A potential factor to consider is the calibration curve presented in Figure 24. While the exponential model effectively captured the relationship between normalized reflectance and bilirubin, it showed a slight tendency to underestimate the concentration of 4.98 mg/dL and slightly overestimate the concentration of 28.00 mg/dL. However, due to the minimal nature of such deviations, it can be speculated that this aspect did not significantly detract from the overall accuracy of the model and thus of the system. On the whole, the proposed algorithm demonstrated good performance in compensating for hemoglobin interference across a wide range of bilirubin concentrations, covering nearly the entire range of clinical diagnostic interest.

To the best of our knowledge, few recent studies have specifically addressed hemoglobin interference on bilirubin measurements using simple devices, despite its relevance for developing countries and resource-constrained settings. Kudavelly and Balakrishnan proposed a simple, low-cost, and two-wavelength spectrophotometer working with just 5 µL plasma samples and reported hemoglobin compensation capabilities; however, the performance of the device in this regard was not disclosed by the authors [91]. Keahey et al. reported a three-wavelength instrument tailored

for low-resource environments like Africa and South Asia, working with 50 µL whole blood samples and featuring one dedicated wavelength for hemoglobin measurement. While positive results in bilirubin determination were demonstrated in a pilot study in Malawi, the specific impact of hemoglobin was not thoroughly discussed [63]. Lastly, Tan et al. proposed a low-cost paper-based assay system with great tolerance to hemoglobin interference and satisfactory accuracy in bilirubin measurement. However, this method was based on Jendrassik–Grof diazotization, requiring the use of reagents before analysis and an external device for quantitative reading, such as a scanner or a smartphone with a camera [140]. These devices show promising potential in terms of performance, low cost, and ease of use—critical features for harsh and under-resourced settings. However, only the latter study disclosed the performance of hemoglobin compensation, though it involved the use of reagents and additional machinery.

We believe that this system, comprising the reflectance photometer and compensation algorithm, could be highly valuable in under-resourced settings, such as LMICs, where the burden of NH is greatest. The system's evaluation against the WHO's A.S.S.U.R.E.D. guidelines yield positive outcomes—affordability, the primary criterion, is achieved due to the system's simplicity and the lack of complex optical or electronic components, as well as the elimination of the need for reagents or sample preparation in real-world applications. The algorithm's compensation performance ensures that the system meets the required sensitivity and specificity, the second and third criteria, respectively, at least in terms of bilirubin concentration measurement and hemoglobin interference rejection. Additionally, the system satisfies the user-friendly and equipment-free criteria due to its simplicity. The automated nature of the system, which performs analyses and retrieves results in a very short time, further reinforces these advantages.

A limitation of this study was the limited precision of the 590 nm wavelength in estimating hemoglobin concentration, which led to a dispersion of data points, as shown in Figure 26. This limitation in precision did not emerge in our preliminary study, which also investigated the performance of three other wavelengths (570, 575, and 605 nm) [115]. In that work, 590 nm was concluded to be the best overall choice among those tested. This dispersion resulted in higher, although acceptable, standard deviations and root mean square errors for the compensated data.

Future efforts will focus on increasing the precision of hemoglobin estimation and applying the algorithm to higher concentrations of hemoglobin. Subsequently, the reflectance photometer used in this experiment will be evaluated in real-world clinical settings to assess the robustness and usability of this method.

2.8. Temperature influence estimation on a reflectance photometer for bilirubin measurement [141]

2.8.1. Introduction

Bilirubin is the major product of erythrocytes breakdown; under normal conditions UCB is released in plasma where bounds to albumin, until it is excreted in bile as conjugate bilirubin [1,52]. In neonates, this metabolism is stronger and UCB forms in higher concentrations: while a temporary and controlled increase is known to be physiological during the first days of life, an abnormal concentration of UCB can lead to a pathological condition known as hyperbilirubinemia; due to the neurotoxicity of bilirubin, this condition can lead to kernicterus or death [1,2,60]. More than half of neonates develops benign hyperbilirubinemia during the first week of life, and roughly one in ten newborns develops clinically significative hyperbilirubinemia [2,60]. In these cases, frequent monitoring of serum bilirubin is

needed to establish a proper treatment and reduce chances of neurological damage [15,110].

Several methods were developed to measure bilirubin concentration, both with invasive and non-invasive approaches. Currently used invasive methods are based on diazo reactions or vanadic acid reactions with bilirubin, while non-invasive methods, like transcutaneous bilirubinometers, have been on the market since 1980s [73,77]. An alternative invasive method is direct photometry which presents some advantages: a) it operates directly on plasma or serum without reagents and sample volume can easily be minimized to microliters; b) its complexity and cost are reduced due to the use of visible wavelength; c) it is suitable for compact portable devices. On the other hand, disadvantages are: a) some substances in plasma can interfere with bilirubin, such as oxyhemoglobin; b) any opalescence resulting from sample treatment can limit the accuracy; c) it is only valid for neonates due to the presence of other interfering substances, such as carotenoids, in children and adults [77,94,95,142]; d) it is influenced by temperature as stated in the Lambert-Beer law.

The use of direct photometry for bilirubin assay traces back to 1960s [95]; since then several invasive and non-invasive applications of this method have been proposed [94,142–144]. However, no literature concerning temperature influence on such systems was found.

Bilirubin measurement devices in clinical settings operate under controlled environment rooms where temperature is almost constant but, as aforementioned, direct photometry can be applied to portable and field instrumentation, which can be used both inside and outside clinical facilities, thus in environments with diverse temperatures.

The aim of this work is to determine the effect of external temperature on the measurement of bilirubin concentration using a simple two-wavelength reflectance photometer.

2.8.2. Materials and Methods

2.8.2.1. *The reflectance photometer*

A set of eight identical photometers was used to ensure the repeatability of evidence found during the experiment. Each photometer was composed by an optical chamber, two LEDs (KPHHS-1005QBC-D-V and KPT-1608CGCK, Kingbright Electronic Co., Ltd., Taiwan), a photodiode (TEMD6200FX01, Vishay Intertechnology, Inc., USA), and other electronic components necessary for the acquisition of the signal (Figure 27). The LEDs emitted light at 465 nm and 570 nm, hence blue and green light respectively, and irradiated the sample inserted in the chamber; since no light was transmitted through the sample, the fraction of light not absorbed by the sample was reflected towards the photodiode; the output current of the photodiode was converted to a tension, then digitized with 0 to 3 V range. In this way, the photometer acquired the intensity of reflected light: a high intensity indicated high reflectance, or equivalently low absorption, and vice versa.

A temperature sensor with 0.25 °C resolution (LM73, Texas Instruments, Inc., USA) was placed on the electronic board of each photometer, adequately far from heat sources like microcontrollers or power supplies. Such placement was deemed better than using a single sensor for all instruments: the measurement of "ambient" temperature, intended as the temperature of the environment in which the instruments were placed, could have differed considerably from the air immediately surrounding the instruments themselves; placing a temperature sensor as near as possible to the optical chamber produces more accurate results [145,146].

Finally, each photometer was provided with a 16-bit ADC and a microcontroller (MKL15Z32VFT4, Freescale Semiconductor, USA) that sent intensity values to a single computer that stored all data.

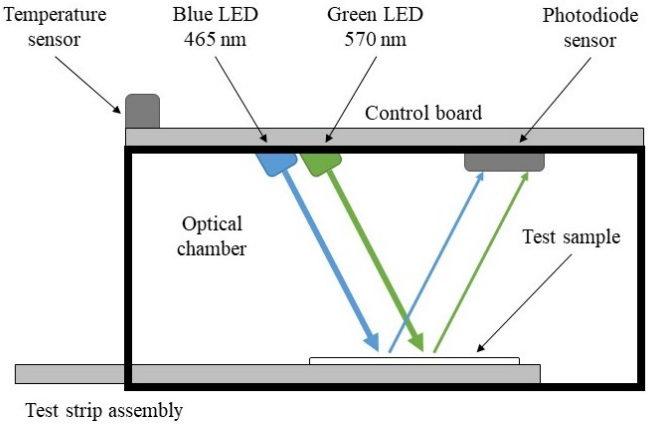

Figure 27. A schematic representation of one of the photometers used in the experiment. The test strip is inserted into the optical chamber where two LEDs irradiate the sample; a fraction of the light is reflected and detected by the photodiode.

2.8.2.2. *Test samples*

A set of eight paper test strips was fabricated, simulating different levels of absorption by bilirubin distributed across the input scale of the photometers. Considering that the study is focused on the identification of temperature impact on the measurements, the use of plasma or diluted bilirubin was excluded; this choice allowed to avoid errors due to biological samples preparation, treatment, and conservation. Additionally, "real" samples would not have maintained chemical and physical stability throughout the experiment: bilirubin oxidates when exposed to blue light, bringing further interference to the system [15,60,73].

As demonstrated in Figure 28, eight different patterns were created to form a logarithmic greyscale from an almost white to a very dark shade, then printed with laser printers on normal paper; the patterns were then cut and laid down on test strips assemblies. Since all eight photometers were subjected to the test contemporarily, eight test strips were prepared for each of the eight levels, thus 64 in total. This method had some advantages, two were the most important: a) printing the pattern on paper led to repeatable reflectance values among different

strips with the same grey level; b) reflectance values were stable during the whole experiment and any damaged strips could have been replaced easily.

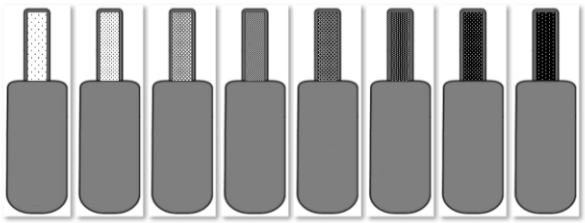

Figure 28. The greyscale pattern created for the experiment and the test strips, which shape was suitable to fit the optical chamber. The strips were enumerated from 1 to 8 in order of absorbance.

2.8.2.3. *Experimental procedure*

To measure the influence of external temperature on intensity value, the photometers were placed inside a temperature test chamber. At the beginning of each test, one of the eight groups of test strips was loaded, and the photometers were cooled at 15 °C, maintaining low levels of humidity to avoid condensation of water on the electronic boards and inside the optical chambers. After cooling, they were immediately connected and powered on, and the temperature test chamber was set to 40 °C: in this way, during the heating process, the instruments could reach thermal equilibrium with the test chamber starting from 15 °C or slightly under. Simultaneously, their firmware was started: with a period of 10 s, the instruments executed four consecutive instantaneous readings with the 465 nm LED and another four with the 570 nm LED; the four readings made with each wavelength were arithmetically averaged and sent to the central calculator, as well as timestamp data and temperature data. In other words, every 10 seconds the calculator received eight "rows" of information, one from each instrument, containing timestamp, temperature, blue light intensity, and green light intensity. The experiment was stopped when all temperature sensors provided a temperature above 30 °C. The photometers were consequently powered off and let chill again. This described workflow was repeated eight times, one for each test strip group. To avoid

bias errors due to experimental design, such as instruments hysteresis, all the acquisitions for all experimental settings were also performed by starting from 30 °C and cooling the devices until reaching temperatures below 15 °C, hence reversing the described process.

Before and after each test all the test strips and the optical chamber were visually inspected to assess the absence of moisture, condensation, or damages. During the execution of each test both the temperature test chamber and the instruments inside were not moved or handled to avoid producing motion or vibration artifacts.

For each instrument, each test strip, and each wavelength the same procedure was used for the analysis. Any measure below 15.0 °C or above 30.0 °C was excluded from the analysis. Then, 15.0 °C was adopted as reference temperature (T_{ref}): the lower limit of temperature range was set at 15.0 °C as cooling the devices at lower temperatures caused frequent condensation inside the optical chamber of the instruments, or in the paper test strips. For each test, all blue and green measures executed at exactly T_{ref} were averaged in order to find an intensity reference for blue and green data, respectively, identified as $I_{ref,b}$ and $I_{ref,g}$.

As the temperature inside the test chamber increased, each i-th measure was defined by a T_i temperature and an intensity value, $I_{i,b}$ for blue light and $I_{i,g}$ for green light. Consequently, the variation of temperature and blue and green intensity from their respective reference were calculated for each i-th measure (Equation 7):

$$\begin{cases} \Delta T_i = T_i - T_{ref} \\ \Delta I_{i,b} = I_{i,b} - I_{ref,b} \\ \Delta I_{i,g} = I_{i,g} - I_{ref,g} \end{cases} \quad \text{Eq. 7}$$

Equation 7. The equations describing how intensity variations are computed.

2.8.3. Results

Over 90.000 measurements were performed by the eight photometers testing all eight test strip groups. Intensity values for each instrument and each test strip were plotted against time and inspected. The decreasing trend of measured intensity was observed for higher external temperature values, highlighting an increase in absorbance for higher temperatures. Figure 29 shows the temporal trend of intensity and temperature for the lightest strip (Strip 1) irradiated with 465 nm light in one of the eight instruments.

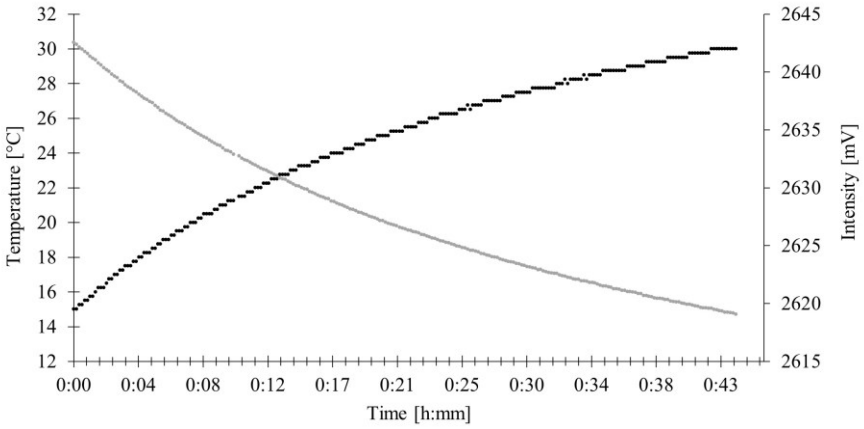

Figure 29. An example of the typical temporal trend resulting from the experiments, intensity vs. time (grey) and temperature vs. time (black).

In Figure 30 an example of ΔI for blue and green light plotted against ΔT is reported, regarding one of the instruments measuring the lightest strip. A negative relation can be observed between intensity and temperature causing underestimation for temperatures higher than the reference one.

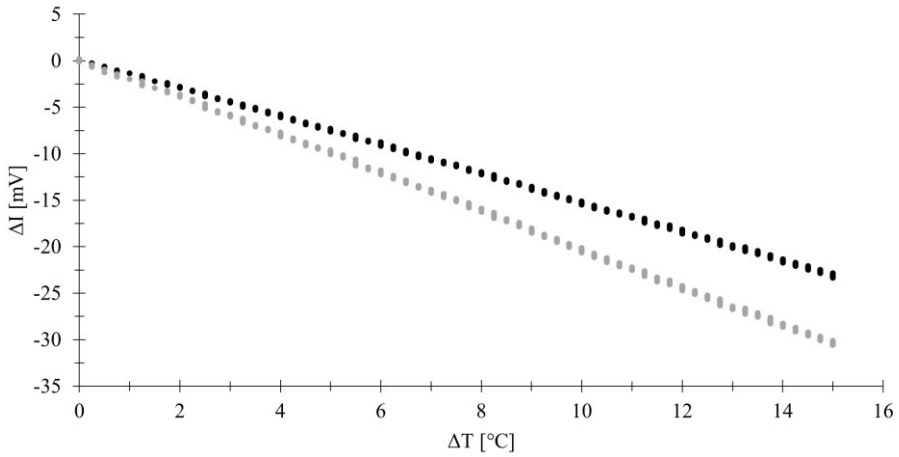

Figure 30. ΔI_b vs. ΔT (black dots) and ΔI_g vs. ΔT (grey dots). The quadratic behaviour of the relation between green intensity and temperature is noticeable especially in ΔT included in the range 0-4 °C. Data is extrapolated from one of the instruments and refers to the lightest strip.

Blue intensity was differently affected by temperature with respect to the green intensity, with the latter showing a more pronounced quadratic behaviour especially for small ΔT, while the first being linear. Linear functions were then used to approximate the relationship between ΔI_b and ΔT, while quadratic functions were used to approximate the relationship between ΔI_g and ΔT; in every test the approximation resulted in a coefficient of determination R^2 greater than 0.95.

Lighter test strips caused wider deviations from the intensity reference, while darker ones were less influenced by temperature. Table 11 indicates that the relation between ΔI and ΔT depended on the test strip group, hence from the concentration of the sample: for higher concentrations the effect of temperature decreased. This was valid for both blue and green data despite the difference in terms of approximation function degree; the first-grade polynomial coefficient (m for blue, b for green) exhibited a coherent dependence on strip type.

Finally, the analysis of reversed experiments, therefore with temperature starting at 30 °C until 15 °C, showed no significant differences with the regular setup suggesting the absence of instrument hysteresis effects.

	Blue light (465 nm)		Green light (570 nm)		
	m	q	a	b	c
Strip 1	-681.647	43.862	6.808	-1077.09	0.672
Strip 2	-488.149	64.625	5.915	-811.407	21.209
Strip 3	-421.097	61.836	5.108	-718.362	19.693
Strip 4	-384.226	43.467	3.79	-642.316	52.764
Strip 5	-358.341	33.193	3.913	-607.721	44.35
Strip 6	-351.935	8.435	3.035	-558.412	-17.251
Strip 7	-311.295	39.456	5.058	-564.956	29.77
Strip 8	-335.417	9.1	5.184	-562.882	-13.577
Mean	-416.513	37.997	4.858	-692.893	17.203
±SD	±32.998	±58.271	±1.05	±35.098	±46.433

Table 11. Polynomial interpolation results. Strip 1 is the lightest, while Strip 8 is the darkest. For blue light m is the first-degree polynomial coefficient, and q is the zero-degree one. For green light a is the second-degree polynomial coefficient, b is the first-degree polynomial coefficient, and c is the zero-degree one. Stated values are the result of the average of the values provided by the single photometers.

2.8.4. Discussion

NH is known as one of the burdens of developing countries, affecting tenths of thousands of newborns and inducing permanent damages to many of them [1]. In developed countries instead, where the incidence is much lower and management protocols are well-established, it is essential to provide effective solutions for reducing costs related to diagnosis and treatment [73].

For these reasons a broad range of methods for the measurement of bilirubin in neonates have been developed, reflectance photometry being one of them. Although being a promising method no evidence was found regarding temperature influence on such systems; this aspect is believed to be fundamental, especially when considering that this method is applicable to portable instruments, which could be used in various environments and not only in clinical laboratories. Previous literature facing temperature influence on optical sensors and spectrometers was found, even though not involving medical systems but agricultural systems [145,147].

The focus of this work was to correlate external temperature and reflectance readings of a series of photometers for bilirubin measurement application. Placing temperature sensors directly on-board allowed to measure the temperature of air immediately surrounding the instruments rather than generic air temperature. Investigating photometers behaviour at temperatures from 15 to 30 °C was necessary to cover different scenarios of use, inside and outside clinical facilities; a large amount of data was consequently produced and allowed a robust analysis.

A first result was how blue and green light were influenced by temperature regardless of the strip type: blue light showed a linear behaviour, while green light was correctly interpolated by quadratic function. In any case, the common feature was a reduction in reflectance for higher temperatures: a reduction of reflectance by the sample is associated to an increase of its absorbance, hence to greater concentration of bilirubin in the sample itself. In other words, as temperature increases the instrument tends to overestimate bilirubin concentration.

Since blue and green LED measures were executed with a delay of just tenths of a second from each other on the same strip and at identical external conditions, the difference could be traced back to the LEDs characteristics: 465 nm LEDs are less sensitive to temperature than 570 nm LEDs or, in other words, the relative luminous intensity of the first is less dependent from temperature and more linear than the latter.

The second result is how test strips type correlates with temperature, or equivalently how the result of the measurement of a sample varies with temperature. Table 11 demonstrates how a lighter sample, which reflects most of the incident light, is more temperature dependent than a darker one, producing a steeper relationship. This phenomenon should be associated with the relationship between sample absorbance and temperature: a sample containing a certain concentration of

bilirubin provides a certain absorbance dependent to its temperature, as defined by the Lambert-Beer law.

In conclusion, we identified the dependency of reflectance on temperature in these devices. The results showed that measurements performed at higher temperatures induced reduction of measured reflectance, leading to potential overestimation of bilirubin. Future research should be focused to develop mitigating strategies to compensate the effect of temperature on reflectance photometers designed for bilirubin measurements.

Chapter 3. HEMATOCRIT ESTIMATION IN THE NEWBORN FROM A BLOOD MICROCAPSULE

3.1. Introduction

3.1.1. Background

HCT, along with hemoglobin concentration, is one of the most commonly performed laboratory tests in both adult and neonatal or pediatric clinical care.

The first description of HCT is credited to Dr. M.M. Wintrobe, who, in 1929, defined the proportion of a blood sample occupied by erythrocytes as the "volume of packed red blood cells" [148]. The term "hematocrit" originally referred to a specially designed glass capillary tube used for this measurement. Over the following decades, the hematocrit method became so widespread that the term came to represent the clinical measurement itself. This manual procedure involves collecting a whole blood sample, which is then centrifuged for a defined duration and force within a graduated hematocrit tube. Centrifugation separates the blood into three distinct components: red blood cells, white blood cells and platelets, and plasma. After centrifugation, the graduated scale on the capillary tube is used to calculate the fraction of the total blood volume occupied by red blood cells (Figure 31).

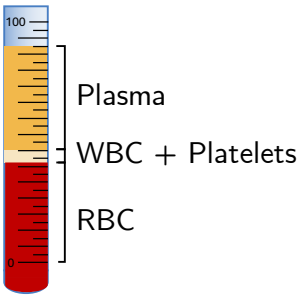

Figure 31. A representation of a whole blood sample after the centrifugation process in a graduated hematocrit tube.

3.1.2. Current HCT measurement methods

The method proposed by Wintrobe has remained in use to this day with minimal modifications, owing to its simplicity and standardization. Despite the development and increasing use of more automated and rapid methods, it is still considered the gold standard [36,149,150]. The manual method, commonly known as micro-HCT or microhematocrit, continues to be widely used, particularly in low-resource settings where automated analyzers are less available [37,151,152]. The original Wintrobe method used a larger capillary tube, whereas the microhematocrit technique utilizes a smaller tube, typically 1 mm in diameter, requiring less sample volume [38]. Additionally, unlike the Wintrobe tube, which was graduated for direct measurement, the microhematocrit tube is not graduated. Therefore, the operator must use a ruler or graph paper to measure the HCT. Various potential issues have been highlighted in both recent and older literature, primarily related to: i) the manual nature of the method itself, and ii) the settings and operation of the centrifugation process.

Regarding the first point, the accuracy of this method heavily depends on the sample collection, the capillary tube filling process, the handling of the tube before and after centrifugation, and the tools used to measure the ratio of the whole sample to the packed red blood cells [153]. A key source of error is the handling of the tube after centrifugation, as any agitation may disrupt the packing of RBCs, leading to inaccurate HCT measurements. Another potential issue is the operator's ability to precisely measure the two portions of the sample post-centrifugation. Errors can arise from visual misalignment, incorrect distance from the measuring instrument (e.g., a ruler or graph paper), or the precision of the instrument itself.

Secondly, in terms of the centrifugation process, it is well known that the duration, angle, and force of centrifugation directly influence the results [154]. This is mainly due to a small but significant amount of plasma trapped within the RBC

matrix, which cannot be fully separated [155]. This can account for a 1-6% overestimation error, which clinicians must consider before making clinical decisions based on the HCT value [156,157].

Since the introduction of the manual HCT method by Wintrobe, which later evolved into the microhematocrit technique, automated methods have been developed and widely adopted in clinical practice, especially in developed countries (Figure 32). Modern automated laboratory blood cell counters measure a variety of blood-related parameters, including HCT, using the principle of flow cytometry, which is based on either optical measurements, impedance measurements, or a combination of both [36,158]. In flow cytometry, the blood sample is diluted and red blood cells (RBCs) are fixed with specific reagents. The solution passes through a flow cell, where the laminar flow arranges the cells in a single file. In the impedance-based method, changes in electrical impedance are recorded as each cell passes through, and the HCT value is calculated by summing the electrical pulses [159,160]. In the optical approach, cells are classified based on how they scatter light from a laser beam, with the scattering angle and intensity providing detailed information about cell characteristics [159,160]. It is important to note that in such instruments HCT results from calculations and internal algorithms, therefore is an indirect measurement.

Figure 32. An example of a clinical laboratory automated hematology analyzer.

Despite their full automation, high throughput, and the increasingly broad range of parameters measurable from a single blood sample, clinical laboratory blood cell counters still face several issues and limitations. Firstly, as previously mentioned, these instruments estimate HCT through algorithms based on the total count and classification of cells. While this method typically produces accurate results [161], HCT remains an indirect calculation rather than a direct measurement. Consequently, errors in cell counting or classification can lead to inaccurate HCT results. This potential for error has been observed in cases involving morphologically abnormal red blood cells, polycythemia, various types of anemia, and red blood cell agglutinates [162,163]. Despite the advantages of automated blood cell counters and hematologic analyzers, their primary limitation in LMICs is their reliance on centralized clinical laboratories. In these settings, turnaround times for samples sent to equipped laboratories can take days, making it impractical to rely on them for screening analyses, follow-up protocols, or, most critically, for patients requiring immediate treatment [164]. Moreover, in lower-resourced countries, where healthcare costs are largely covered by private actors or the patients themselves, the expense of performing a complete blood count analysis can be prohibitive. Even if we were to ignore the analytical performance disadvantages of these systems, their overall cost and impracticality make them inaccessible for a vast portion of the population in developing countries, especially those in rural areas or far from major cities [164,165].

A third option is offered by POC automatic blood gas analyzers, which differ from traditional laboratory equipment in several procedural and technical aspects. Due to their compact size and minimal use of reagents, these devices are frequently employed in Neonatal Intensive Care Units, lower-level laboratories, and neonatal and pediatric hospital wards (Figure 33). Additionally, they require smaller sample volumes compared to laboratory analyzers—typically in the range of tenths of microliters—and no sample preparation is needed before analysis. Another

advantage of blood gas analyzers is their ease of use, allowing multiple measurements, including HCT, to be performed without the need for specialized laboratory personnel. This increased accessibility, combined with the proximity of the instrument to the patient, results in very short turnaround times, often within a few minutes from sample collection to result retrieval. Typically, the whole blood sample is hemolyzed via ultrasound, and multi-wavelength spectrophotometry is used to determine hemoglobin concentration. HCT is then indirectly calculated through internal algorithms, similar to laboratory equipment [160,166].

Figure 33. An example of a compact, POC automatic blood gas analyzer.

Lower purchasing and per-measurement costs, combined with ease of use and reduced complexity, have contributed to the increased diffusion of blood gas analyzers in resource-constrained settings. However, these instruments are not without their disadvantages, and concerns remain about their overall benefit. Several studies have compared specific commercial models to clinical laboratory equipment, yielding mixed results [165,167–169]. The most common finding is that the results obtained by the two methods, particularly for HCT measurement, are not equivalent, meaning POC instruments cannot fully replace central laboratories. Additionally, aside from method comparison, the accuracy of blood gas analyzers

remains under debate. Many studies conclude that while these instruments can be beneficial for daily routine, screening, and urgent medical decisions, their accuracy depends heavily on rigorous and proper sample collection and handling [170,171]. Another critical issue is calibration and quality assurance. POC instruments often require frequent calibration, sometimes daily, and must be integrated into quality assurance programs, whether internal or external, just as clinical laboratory equipment is [171,172]. Given the growing importance of POC testing and its increasing use by doctors and nurses, there should be no question about including these instruments in external quality assurance controls and general quality management. While higher-income countries have begun implementing such protocols, in LMICs, this remains far from reality due to several challenges: quality assurance and management are costly, and these expenses would likely fall on the patient or private organizations. Additionally, there is a need for trained experts, established guidelines, and, crucially, devices designed with resource-limited settings in mind to minimize the workload and consumables required for such assessments [173].

3.1.3. Hematocrit measurement in the neonate

In the previous section the most diffused methods and techniques for the measurement of HCT were described along with the respective advantages, disadvantages and limitations related to their application and usability in low-resource settings. Generally, such methods are applicable, thus used in clinical practice, both for adults and neonates.

Another significant factor in HCT analysis in newborns, aside from the measurement method, is the sampling method (venous, arterial, or capillary blood). In a prospective study [174], 141 subjects were stratified into four groups based on postnatal age at measurement (7, 14, 21, and 28 days, respectively), and a complete blood count was performed using an automated hematological analyzer. For each

subject, both capillary and venous blood samples were collected simultaneously and analyzed in parallel. The results demonstrated that capillary samples yielded up to 12% higher HCT values compared to venous samples on postnatal day 1, and 5-7% higher on postnatal days 7, 14, 21, and 28. Additionally, HCT and hemoglobin values decreased by an average of 25% from day 1 to day 28 postnatally. These latter results were subsequently confirmed by another large-population study, which, however, did not distinguish between sampling sites [32]. When performing HCT measurements on capillary samples, doctors and nurses must be aware of the discrepancies with other sampling sites. Furthermore, capillary HCT may be less reproducible and informative under certain conditions, such as poor skin perfusion or preterm birth [175].

In light of these considerations, it is clear how challenging HCT measurement in newborns can be, and that relying on technology alone is often insufficient to meet this urgent need, especially in resource-limited settings. Designing an effective solution for this analysis must begin with defining sample requirements and handling procedures. Although not ideal, as briefly described earlier, capillary samples are routinely used due to their less invasive, less painful nature, and their lower risk of infection or complications. They are also easier to collect, and in the case of very small volumes, they do not require syringes or test tubes, as venous or arterial samples do. These characteristics are particularly beneficial when the patient is outside of equipped facilities or hospitals. Another important parameter that needs to be defined is the HCT range, which, from a measurement device design standpoint, corresponds to the input value dynamic. In most medical measurement systems, ranges are typically based on normal values reported in scientific literature, as this is the standard approach for ensuring accurate design. However, this approach is not straightforward for neonatal HCT due to the specific clinical and ethical complexities faced in the definition of such ranges.

The clinical rationale for performing HCT testing differs significantly between adult and neonatal populations. In adults, HCT may be measured for routine screening or periodic check-ups, often on healthy, voluntary subjects. In neonates, however, this test is performed to address a specific clinical question or on the basis of a medical condition that justifies blood sample collection. Unlike in adult general medicine, "normal ranges" for HCT do not exist in neonatology. Instead, "reference intervals" are used, representing the 5th to 95th percentile values from laboratory tests conducted on selected subjects [32,176,177]. In other words, while normal ranges for adults are derived from studies typically involving healthy participants, reference intervals for neonates are based on data from subjects with specific clinical conditions that warranted HCT testing. These reference intervals serve as approximations of normal ranges in clinical practice but must be interpreted in the context of other factors, such as gestational age, birth weight, postnatal age, and the presence of underlying illnesses [177]. In addition to the sampling site differences and constraints previously described, these factors necessitate the provision of a wide range of measurable HCT values. Figure 34 presents results from a large multicenter population study, outlining HCT reference ranges for preterm and term infants during the first 28 days of life [32]. These ranges can be confidently used to define the input value dynamic for a neonatal HCT measurement device.

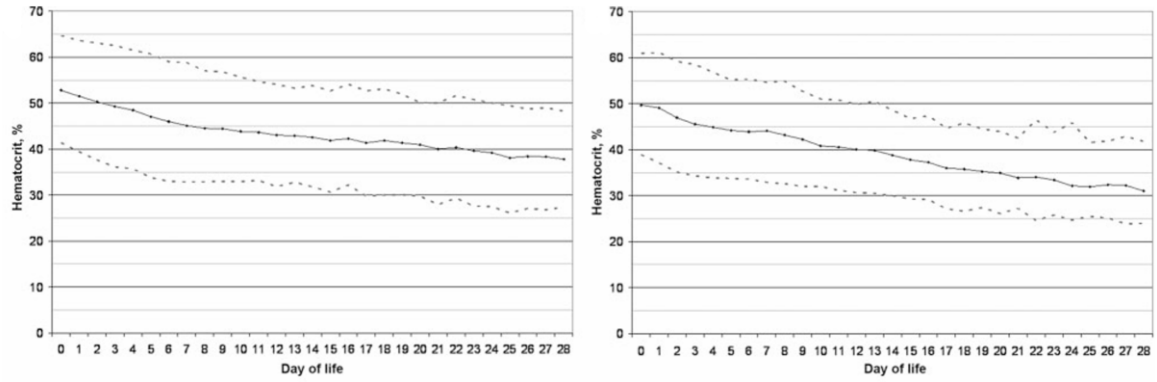

Figure 34. On the left reference ranges for late-preterm and term infants (35-42 weeks' gestation); on the right reference ranges for preterm infants (29-34 weeks' gestation). Solid line indicates average values while dashed lines indicate 5% and 95% confidence intervals, respectively. Adapted from [32].

This section has outlined HCT and its clinical significance, along with the most common measurement methods used in clinical practice, highlighting their advantages and disadvantages in relation to low-resource settings. The following section presents a novel approach for neonatal HCT measurement, along with a discussion of its implications and potential perspectives.

3.2. A NOVEL APPROACH FOR NEONATAL HEMATOCRIT SCREENING [178]

3.2.1. Introduction

HCT is commonly used as a general indicator of a patient's health status in relation to specific reference ranges for adults and newborns [32,34,160,179]. Deviations from these ranges can be used to aid diagnosing certain conditions related to health status in general clinical practice as well as in neonatology. The main reasons for increased levels of HCT include dehydration, burns, diarrhea, postpartum eclampsia, and polycythemia vera; a high HCT level also indicates risk for heart and cerebral infarction because of hemoconcentration. Furthermore, increased HCT is a factor of thrombus formation and increases risk for thrombosis.

This condition is especially dangerous for patients with artificial heart, in dialysis, and during open-heart surgery [179]. On the other hand, when the HCT level is reduced, symptoms of anemia and bleeding are usually suspected, as well as diseases of the bone marrow, leukemia, malnutrition, and overhydration. Furthermore, each change of HCT value affects the safe control of the blood pump [33,179,180]. This physical parameter is commonly used, for example, to decide whether to administer blood transfusion or partial exchange transfusion [36], and it should be considered in the presence of risk factors of numerous pathological conditions, such as hyperbilirubinemia [8,35]. Since changes in HCT reflect acute or chronic alterations in the patient's state of health, a quick HCT estimation is critical to establish a prompt and adequate approach [36] or, at least, to suggest further investigations. Therefore, HCT could have even more importance and significance in neonatology, although recent literature shows that it may not yet be used to its full potential; for example, the HCT of infants under phototherapy is often not thoroughly considered in clinical practice: Lamola et al. [35] speculate that going from a HCT of 40% to 60% could mean a twofold reduction in the absorption of light by bilirubin; in other words, a twofold increase in irradiance or duration of exposure would be required to achieve the same amount of light absorbed by bilirubin for an infant with an HCT of 60% versus an infant with an HCT of 40%. Nowadays, there are two most common approaches for HCT measurement in clinical use: i) direct measurement by centrifugation of a blood-filled microcapillary tube and visual examination using a ruler (micro-HCT) and ii) automated calculation performed by modern blood analyzers [36–38]. Both are considered accurate and reliable enough to be used in clinical decision processes, although presenting some disadvantages: the first, being completely manual, requires the presence of a skilled operator; hence, it is susceptible to operator-related errors or technical errors, such as incorrect positioning of the capillary in rotors or incorrect setting of the centrifuge. Two other non-negligible downsides are biohazard risk introduced by broken glass capillaries

and errors due to aberrant red blood cell morphologies [36,181]. The second is susceptible to overestimation if certain clinical conditions are present, such as high concentration of platelets or white blood cells; on the other hand, this method is susceptible to underestimation in the presence of red blood cell agglutinates [36,162]. Another concern is with regard to consistency and agreement between different methods. In particular, despite being widely used, POC automated blood analyzers based on different analytical methods can produce divergent results, which can lead to different clinical decisions [160,166]. Other than these weaknesses, the most interesting aspects for this study are turnaround time and complexity: for micro-HCT, the minimum technical time to execute the measure could be about 10 min, having a dedicated operator that collects the blood sample, fills and seals the capillary tube, centrifuges it, and reads the resulting centrifuged sample without any downtime. However, the time taken to complete this process is easily two- or threefold increased due to other parallel activities, and depending on the organizational aspects of the facility, the interval between collection and reading influences results itself, as blood changes its properties over time [181]. Conversely, for automated methods, turnaround time is strongly dependent on the sample collecting and handling process, laboratory distance, and quality of the instrumentation available; in this case, complexity is obviously much greater. These aspects could considerably limit the applicability of the aforementioned methods in LMICs, which often lack instrumentation, facilities, and trained professionals and where healthcare access is generally poor [182–184]. Few alternative technologies have been developed to address the restrictions and constraints specific to LMICs, among them paper-based devices; in particular, lateral flow assays are rising in scientific and clinical interest. Recent applications of paper-based devices were found in the literature, capable of detecting proteins [185], microRNA biomarkers [186], micronutrients in food [187], and HIV virions [188]. Lateral flow test strips have many advantages: they require very small samples, the time necessary to obtain a

result is shorter than the traditional laboratory turnaround time, they do not require or require very little consumables or reagents, they are easier to use and maintain than laboratory equipment, and they are inexpensive and easier to dispose of; these design features become constraints to be considered in LMICs, as evidenced in the IEEE 21st International Conference on Nanotechnology [19] and stated by Murray and Mace [44]. An aspect of interest for this study is that, in most cases, lateral flow assays provide qualitative or semiquantitative outputs, for which human intervention is necessary to adequately interpret the results. For this reason, a method based on lateral flow test strips that extends their advantages by integrating automation and quantitative response capabilities is desirable in LMICs. Four previous studies were found in the literature: Berry S.B. et al. [189] developed a low-cost thermometer-style device that enables semiquantitative evaluation of HCT in 30 min from a 50 µL sample, working with HCTs in the 28–57% range; further refinement [190] improved device features, reducing both the sample size and the time required to 10 µL and 10 min, respectively. Differently, Del Ben F. et al. [191] proposed a method based on image analysis requiring a scanner and filter paper for dried blood spot collection, which resulted in good accuracy, precision, and reproducibility within 23–48% HCT interval. Then, Miller IV, J.H. [192] used Whatman 903 filter paper and a scientific-grade spectrometer to calculate HCT from dried blood spots in the 25–75% range, taking a 50 µL whole blood sample. Finally, Punter-Villagrasa J. et al. [193] presented a solution for the instantaneous detection of HCT based on three electrodes measuring the impedance of a 50 µL whole blood sample, capable of giving a −0.96 Pearson's correlation coefficient testing a 14.2–50.6% input range, even though the results provided were limited to 45%. The solutions reported in the aforementioned studies might also be valid for neonatal population, but they were principally focused on normal adult population ranges, which are typically lower than neonates [194]. Indeed, a large study [32] on more than 20,000 neonatal patients indicates a HCT reference range of 42–65%. In

general, assaying neonate HCT adds further constraints to the development of a valid alternative for, and not only, LMICs: i) sample collection from neonates must be minimized in terms of both frequency and volume to reduce pain, stress induction, and infection probability; ii) neonates present higher HCTs than adults; iii) having a low-cost, low-complexity, and fast estimation method becomes more important as local health accessibility decreases. The aim of this study is to describe and validate a novel HCT screening method based on penetration velocity in lateral flow test strips and quantified using a light reflectance meter.

3.2.2. Materials and Methods

3.2.2.1. *HCT Estimation Method*

The method for HCT determination was based on the plasma penetration velocity in a lateral flow test strip and a light reflectance meter. The lateral flow test strip was composed of a filter coupled with a membrane (Advanced Microdevices Pvt., Ambala, India). The filter was made of white fiberglass having a thickness of 570 ± 80 µm and a tare weight of 10.5 ± 3 mg/cm3; the membrane was made of nitrocellulose having a thickness of 105 ± 15 µm, a pore size of 15 µm, and a mean wicking time of 100 ± 25 s measured on a 4 cm distance with normal saline solution. The filter and the membrane were hand-cut to the same width and vertically coupled with a small overlap, allowing plasma to permeate from the filter to the membrane, as shown in Figure 35. The filter-membrane system was placed on a plastic support, guaranteeing mechanical rigidity during the experiment. A whole blood sample (35 µL) was loaded onto the filter, which retained the corpuscular part of the blood, allowing only the plasma to enter the NC membrane until its complete saturation, as illustrated in Figure 36a.

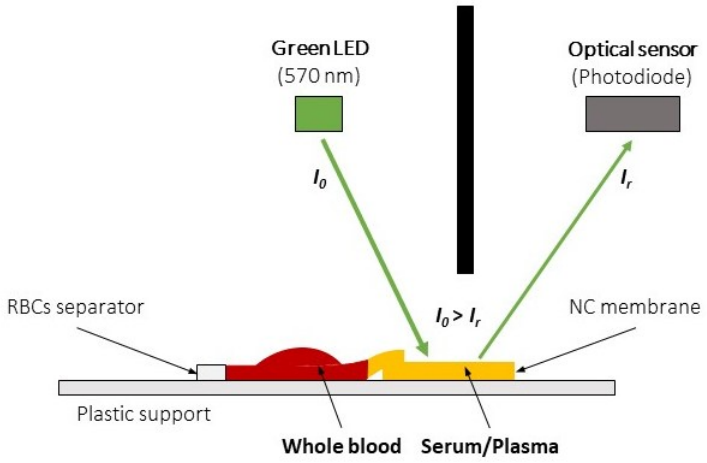

Figure 35. The optical measurement system. The LED light source irradiates the membrane filled with plasma forming the sample; an optical sensor positioned in the same chamber measures the amount of reflected light, enabling the calculus of sample absorbance.

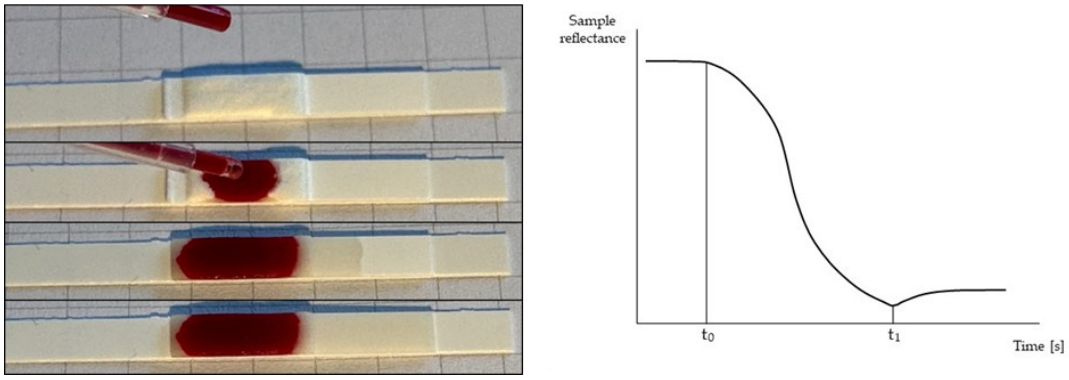

Figure 36. (a): from top to bottom, a blank strip having the filter in the center, in contact with the NC membrane extending to the right; the loading instant; plasma entering the membrane; the membrane has been saturated by plasma(b): characteristic reflectance-time pattern; t0 is defined as the instant in which plasma starts filling the NC membrane, associated with a decrease in reflectance; t1 is defined as the instant in which plasma saturates the NC membrane, associated with a minimum point in reflectance signal. Δt = t1- t-t00.

The entrance of plasma in the NC membrane was monitored using a light reflectance meter. The instrument irradiated the NC membrane with an LED emitting light at 570 nm; the reflected light intensity was measured by an optical sensor. A representation of the measuring principle is reported in Figure 35. The data for the present study were collected by instructing the optical system to

perform four readings per second, therefore with a period of 250 ms. This sampling period was determined after a pilot analysis, which resulted in high measurement error using a sampling period of 500 ms (data not shown). During the data collection, the trend of reflectance values was monitored, and the train of readings was interrupted when a series of equal readings occurred, a condition that indicated a stationary condition in the system, hence the saturation of the strip. Penetration velocity was indirectly calculated based on the time difference (Δt) between instant t0 and instant t1. The first indicated the entry of plasma into the NC membrane, which produced a progressive reduction of reflectance from the initial steady-state condition of the system. The latter indicated the complete saturation of the NC membrane: this final condition was identifiable as a minimum point in reflectance data. The nature of this behavior is physical and attributable to plasma reflectance: approaching membrane saturation, the reflectance was minimum as the quantity of plasma absorbing light was maximum, while immediately after saturation, a layer of plasma progressively formed over the membrane, producing a more reflective "glossy" surface. This temporary increase in reflectance anticipated the final equilibrium condition of the system and thus the end of a run. For this reason, all data points acquired after the minimum point t1 were irrelevant for our aim. In Figure 36b, a typical pattern of reflectance signal versus time is shown, and t0 and t1 are indicated.

If, during the analysis of the results, a run was particularly different due to lack of saturation of the strip or lack of blood flow through the filter, the run was rejected. In any case, the strips were observed at the end of each test to check the state of membrane saturation and any presence of hemolysis.

3.2.2.2. *Data acquisition, calibration, and clinical test*

Whole blood samples were collected from 105 healthy neonates over 37 weeks' gestational age born at IRCCS Materno Infantile "Burlo Garofolo" of Trieste, Italy.

Tests were performed in duplicate. However, knowing that each prick causes suffering and stress to the neonate, the number of samples collected during the study time was minimized by waiting for a blood sample to be available rather than collecting one strictly for the study purpose. The sample collection period was over 3 months, from February to May 2022. Blood samples were collected by puncture on the patient's heel in two heparinized capillary tubes. One capillary was subjected to analysis with a blood gas analyzer (Radiometer ABL90 Flex), as a reference method for this study, while the other was estimated by the proposed method. In this case, the sample was transferred from the capillary tube to the test strip using an automatic pipette to minimize hemolysis and the formation of bubbles. Each measurement, with both one method and the other, was performed by trained personnel, and the data obtained were merged for comparison. With reference to the tested method, during the deposition of the sample, the personnel were instructed to observe the behavior of the blood drop permeating through the filter to detect any abnormality. Subsequently, at the end of each measurement performed by the reader, the strip was observed to detect incomplete saturation, hemolysis, or anomalies. Figure 37 summarizes the procedure from sample collection to data analysis.

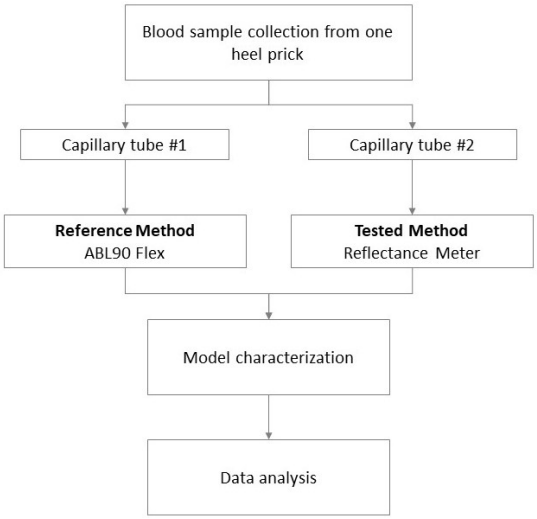

Figure 37. Workflow of procedure for data acquisition, model characterization, and clinical test.

Considering the total amount of acquired samples, 20% of them were used to perform the system calibration and calculate the model (calibration data), and the remaining 80% were used to perform a comparison with the reference method (test data). The samples used for the calibration were selected as described: the input HCT range was equally divided into four levels, from each of which at least five samples were randomly selected.

3.2.3. Results

A total of 192 runs were performed. Following the described protocol, a total of 28 runs were excluded due to visible hemolysis and erythrocyte presence in the plasma-filled membrane, while another 12 runs were excluded due to bubble formation during the deposition of the sample on the test strip. During data analysis, 7 more runs were excluded, showing outlying behavior. From the remaining 145 runs, as described in Materials and Methods, 29 were extracted randomly to create the model as 20% of the total, while 116 were used as test data.

In Figure 38, the measured HCT was plotted against Δt. A nonlinear relation was observed between HCT and Δt, and it was estimated by a third-degree polynomial equation ($R^2 = 0.912$). Having considered the range of the Δt and HCT values used for the calibration, which reflect the range of interest for this application, hence 30% to 70% HCTs, the following model in the range ($15s < \Delta t < 58s$) was proposed and reported in Equation 8:

$$HCT(\Delta t)\% = 0.001 \times \Delta t^3 - 0.1473 \times \Delta t^2 + 7.218 \times \Delta t - 49.07 \qquad \text{Eq. 8}$$

Equation 8. The mathematical model used to estimate the HCT.

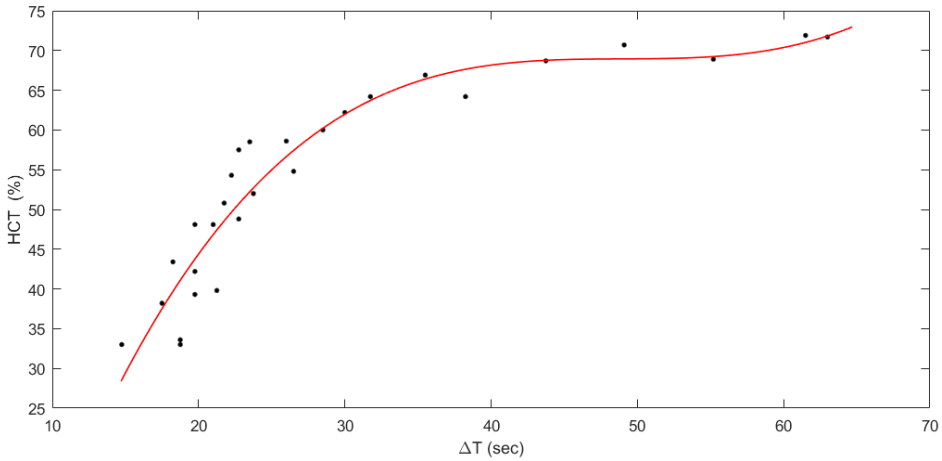

Figure 38. The measured HCT was plotted against Δt (black dots—calibration data) and fitted with a third-degree polynomial equation (red line).

The identified model was subsequently used to estimate HCT values (HCTest) on a test set, which were then compared with measured ones (HCTmeas). In Figure 39a, the estimated hematocrit HCTest values were plotted against HCTmeas for each measurement. The results showed dispersion around the identity line, and a significant linear correlation was observed between HCTest and HCTmeas ($r = 0.87$, $p < 0.001$). The mean absolute error was 4.29%, while the maximum absolute error was 10.69%. The comparison of HCTest and HCTmeas by Bland–Altman analysis (Figure 39b) showed a good agreement with a low mean difference of $0.53 \pm 5.04\%$ and a slight trend of overestimation for higher HCT values.

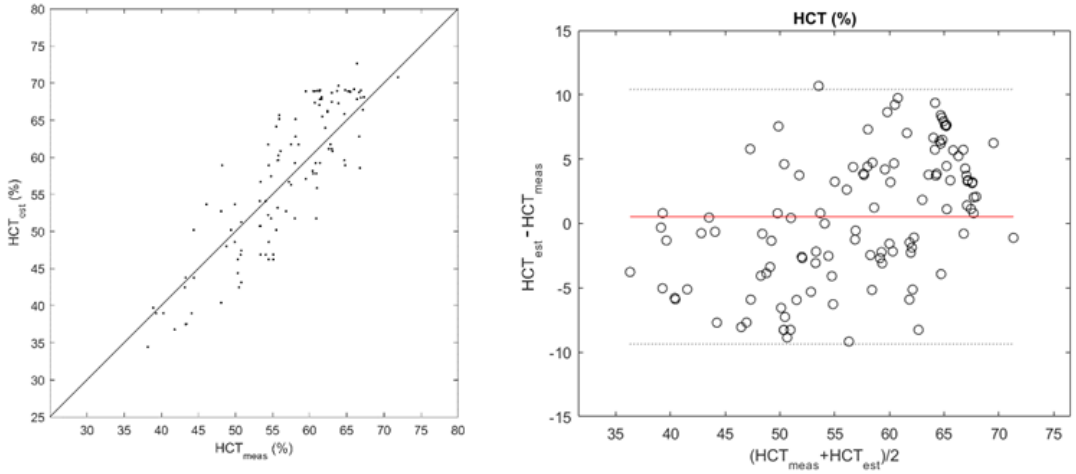

Figure 39. (a) Estimated HCT vs. measured HCT; (b) Bland–Altman plot for the estimated HCT (HCTest) and measured HCT (HCTmeas). The red line indicates the mean difference between the two datasets, and the black dotted lines indicate 95% confidence intervals.

3.2.4. Discussion

HCT is a crucial physical parameter that provides information about health status and pathological conditions in both adults and newborn patients. While modern countries are equipped with gold standard measurement methods, such as automated laboratory analyzers, in LMICs, there is often a lack under structural, technological, and organizational aspects. For these realities, the need for inexpensive, fast, and portable POC devices is strong [19,44,184]. Taking these requirements as a starting point, the aim of this work was to develop a system capable of meeting them and addressing a newborn's specific needs.

In this work, we proposed a novel HCT estimation method based on penetration velocity in lateral flow test strips and a light reflectance meter complying with the requirements in LMIC scenarios. The comparison in a clinical environment conducted in the present study confirmed the technical feasibility of this approach and its applicability for the screening of newborns in difficult scenarios, such as those found in LMIC, even though its accuracy has great margins of improvement.

In particular, the test phase using 20% of collected data resulted in a coefficient of determination of 0.912, which may have been limited by the need for a third-grade interpolation function to properly fit input data; the function itself (as reported in Figure 38) features a higher slope in the 30%–60% HCT range while being flatter for higher levels reaching saturation for 70% HCT; this aspect itself might not prevent the usage of this method in clinical practice if intended as a screening tool for newborn patients, having observed reference ranges defined in previous literature [32]: in the first day of life, the average HCT value is about 53%, reducing monotonically in the following 28 days, and the 95% reference range is below 65% in the worst case. The subsequent comparison with a reference method performed in a clinical environment demonstrated the applicability of the proposed method, resulting in a good agreement between estimated and measured HCT values. In spurious cases, the measured value discarded by around 10% or more with respect to the real value provided by the reference method. Observing the distribution of errors in the Bland-Altman plot, its increased density in 65%–70% HCT can be interpreted as a consequence of the reduction in slope of the model characteristic. Furthermore, it is not possible to exclude that some errors derive from abnormal conditions, including singular blood sample features or imprecise sample loading on the test strip.

All the methods taken as reference were capable of effectively measuring HCTs below 35%, with [190] being the best of them, reaching 14.2%. On the other hand, only one of them tested HCTs equal to or higher than those tested by this study [189], a level at which this method presents its better accuracy; three of them tested ranges of HCTs having maximum values of approximately 50%, hence partially covering reference ranges for neonates [44,182,190].

Timewise, it was confirmed that this method allows a fast response and a shorter turnaround time with minimum effort required: not considering that the amount of

time required to collect the sample, which is present in any method, results could be retrieved within 3 min. The paper-based method proposed by [185,186,189] presented a longer turnaround time of 30 min, subsequently reduced to 10 min. The image-analysis-based method by [191] was not determined in these terms, but it could be speculated that about 5 min is necessary for sample deposition, sample analysis, and elaboration. The fastest method among those chosen as a reference was the impedance-based device, which, according to authors, is instantaneous [190].

Another point of view is portability: the paper-based device from Berry, S.B. et al. was easily the most portable due to its pure paper design that did not require any energy supply [189]. The proposed method is based on lateral flow test strips and a reflectance meter, which needs a source to power its electronic components. Being a relatively simple device, the reflectance meter is so small that it can be proposed as a handheld device powered by batteries. In this way, portability would be preserved, and the constraints highlighted in pertinent literature are satisfied [19,44]. Devices that incorporate reflectance photometers, such as the device reported in a recent study [195], can be available for LMIC scenarios. The impedance-based device also shows good portability and low energy requirements [190]. All other aforementioned methods did not directly address this concern.

The last comparison is made from an accuracy perspective: the thermometer-style device ensured a good linearity with both plasma and whole blood, being understood that the nonquantitative principle of the system could lead to user errors [19]. This proposed penetration-velocity-based method did not reach such high performance, suggesting the need for future research and improvement of the algorithm underneath.

Overall, with respect to the others, this method operates in an adequate range of HCT for neonatal screening, and its turnaround time is shorter than both the majority of compared methods and the most diffused state of the art methods.

Moreover, it is deemed to be applicable in LMICs due to its portability, hence its usability both in- and outside clinical facilities. The proposed method showed a significantly lower accuracy than gold standards, and in its current state of development, it is not suitable for diagnostic purposes; nevertheless, it could be useful if intended as a fast, portable, inexpensive, and easy-to-use screening tool. In this sense, clinical infrastructures and facilities that already have such a system would gain a secondary functionality at no further costs, with no hardware changes on the reader or on the test strips. Future research will deepen the knowledge on this method, mostly in the following aspects: i) enhancement of the algorithm to reach better accuracy; ii) enhancement of optical measurement hardware, such as test strips and LEDs; and iii) reproducibility of the results.

Chapter 4. DIAGNOSTICS DIFFUSION IN LMICs

4.1. Introduction

It is widely recognized that lower-income regions, such as Africa and Southern Asia, continue to lag significantly behind wealthier, industrialized countries in terms of health outcomes. However, this disparity is often underestimated or interpreted superficially, despite the availability of extensive studies and statistics from large supranational organizations such as the WHO and UNICEF. Despite the substantial number of development projects, funding initiatives, and charity efforts—both privately and publicly financed—health outcomes have shown only modest improvement over the past few decades when viewed from a broad perspective. The complexity and multifaceted nature of this "health" issue make it extraordinarily difficult even to define what the real objectives should be.

If the core issue is the "lack" of health, the right approach should ensure the most consistent improvement in health conditions within the financial, technological, and structural constraints of these regions. The optimal solution cannot be purely financial, technological, or structural. Financial aid from non-governmental organizations or wealthier nations, along with increased healthcare spending, can positively impact a region's healthcare system and capabilities, but the infusion of money alone often does not result in an overall improvement in population health [196,197]. Similarly, increasing the availability of technology—such as medical devices, IVDs, or drugs and vaccines—does not necessarily lead to improved prevention, diagnosis, or treatment for citizens and patients, and therefore does not, on its own, guarantee a reduction in the many health burdens of developing countries. This has been clearly demonstrated by the practice of donating medical devices and equipment from high-income countries to LMICs, a practice still

debated for its usefulness and potential to be even detrimental to the receiving facilities and patients [198–200]. Ultimately, at a higher national level, the severe lack of regulation, procurement, and management policies represents a third major issue to be addressed. Even if a medical device is well-designed for the constraints of LMICs and available on the global market, and even if a health facility or organization has the financial capacity to purchase it, these factors can be undermined by the absence of regulatory frameworks and defined procurement processes. Additionally, management challenges related to the device's proper operation, maintenance, repair, and, when necessary, calibration and quality assurance further complicate its effective use [201].

The complexity of achieving meaningful improvements in health conditions for these populations stems from the involvement of multiple stakeholders, each pursuing its own interests. If one were to model this ecosystem, five principal actors would emerge: i) manufacturers, typically based in Western countries, who aim to design, develop, and market their solutions in a profitable manner; ii) non-governmental organizations and suppliers, who must identify safe and effective solutions based on local and regional health needs while operating within economic constraints dictated by funding and donations; iii) NRAs in LMICs, where they exist and are sufficiently developed, responsible for regulating and overseeing the entry and distribution of medical devices, often requiring support with registration and surveillance procedures; iv) health workers, who use the supplied devices, ideally after receiving proper training and knowledge; and v) citizens and patients, who expect and need prevention, diagnosis, and treatment capabilities from their health systems. This simplified description is somewhat sequential and mirrors the typical lifecycle of a medical device dedicated to low-resource settings, from design to its use in clinical practice (Figure 40).

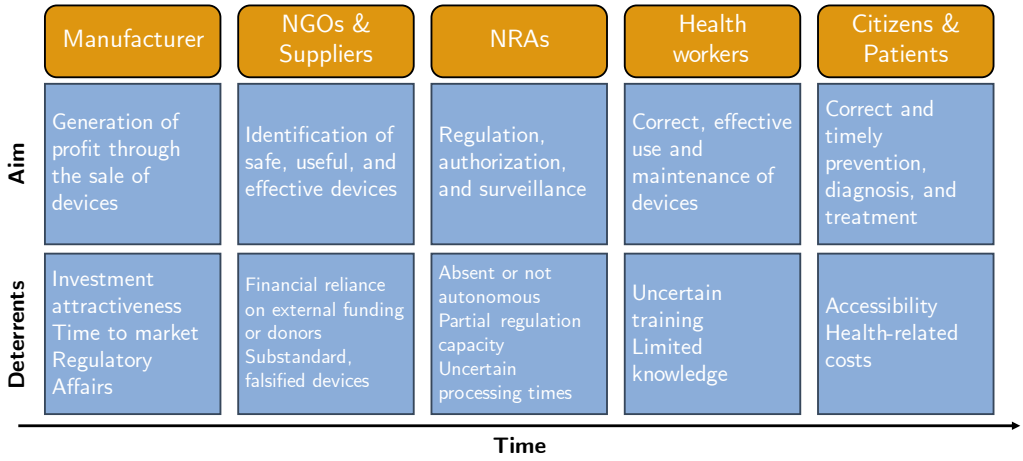

Figure 40. The five most important stakeholders of the diffusion process of medical devices and instruments in LMICs.

Each of these steps presents critical aspects, which will be addressed in the following sections, particularly from the perspective of a manufacturer aiming to develop a device specifically for LMICs.

4.2. Income, Wealth, and Health Inequalities in Developing Countries

For a fair and comprehensive understanding of health inequalities between wealthier and poorer countries, it is essential to identify the latter and recognize the proportion of the global population living in these areas. The World Bank Group, among others, collects and aggregates data from various reliable sources and publishes periodic reports on numerous topics, including population, economics, and health. The latest report on country classification by income, similar to previous reports, highlights the stark distinction between the African continent, South Asia, and the rest of the world [202]. In this classification, countries are categorized by Gross National Income (GNI) per capita into four groups: Low Income (less than 1,145 USD), Lower-Middle Income (1,146 to 4,515 USD), Upper-Middle Income (4,516 to 14,005 USD), and High Income (more than 14,006 USD). Even at first

glance, it is evident that, over the past twenty years, much of Asia, including Russia, has transitioned from predominantly lower income to higher income. However, populous countries such as India and Pakistan have not experienced significant overall wealth growth during this period (Figure 41). In contrast, while there has been some improvement in Africa, the continent remains the poorest region in the world, with most sub-Saharan countries still suffering from exceptionally low-income levels.

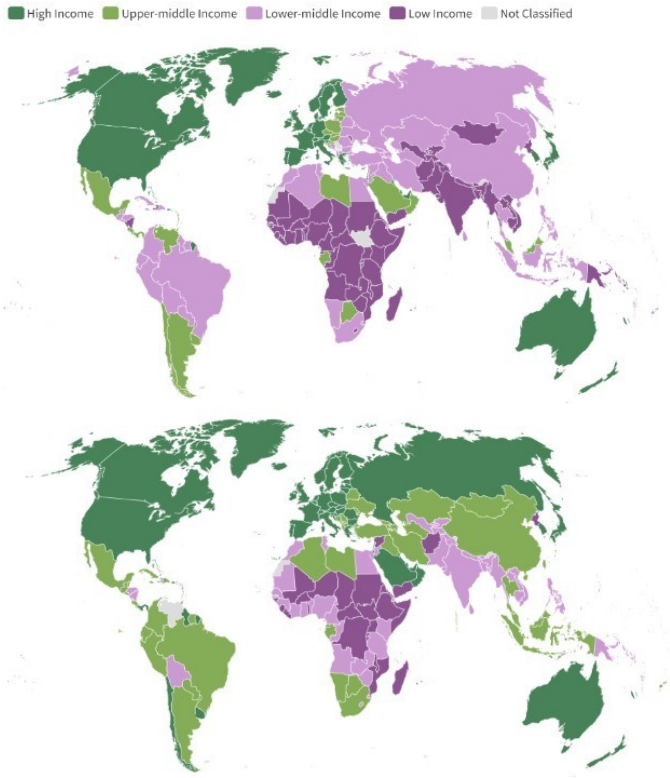

Figure 41. On the top, map of the countries classified by income in 2003; on the bottom, the same classification in 2023. Adapted from [202].

In terms of population growth, from 1960 to 2022, the population in low-income countries increased by 418%, and by 252% in LMICs, compared to just 60% in high-income countries [203]. In absolute terms, the global population was estimated at nearly 8 billion in 2022, with almost half residing in low or LMICs.

High-level aggregated data, like those presented, are crucial for understanding the broad scope of health inequalities across different regions of the world. However, as with any averaging statistic, there is a significant loss of essential details regarding the distribution of the phenomena under examination—in this case, healthcare accessibility. Even excluding the lowest income tail of the global population, wealth distribution in developing regions is far more uneven than in wealthier areas like Europe, where healthcare is typically universal or, at the very least, a basic level of care is guaranteed for all citizens. In less developed countries, access to healthcare is often limited to those who can afford it and who have physical access to medical services. Recent survey-based data on wealth distribution further illustrate these disparities: in 2022, the richest 10% of the population controlled about 30-35% of the income in European countries, compared to well over 60% in southern African nations and some Central and South American countries [204]. Moreover, the wealthiest individuals are often excluded from such statistics, creating an inherent bias that makes the data appear more favorable than it is in reality. This bias is partly due to the extremely small number of ultra-wealthy individuals, but also because they may deliberately avoid inclusion in these reports. This issue is even more pronounced in lower-income countries, where a vast proportion of wealth and influence is concentrated among a very small, elite segment of the population, and the reliability of survey-generated data is questionable [205].

This picture becomes even more complex when considering time and annual trends. While global wealth inequality is generally believed to be decreasing, this is not the case for poorer regions and is significantly worse for rapidly growing economies like China and India (Figure 42). In these countries, although the overall economic and income figures appear promising, the reality is that wealth gains are increasingly concentrated in a small fraction of the population. This widens the gap between the wealthy, who reside in advanced urban centers, and the poorest, who remain in rural and remote areas.

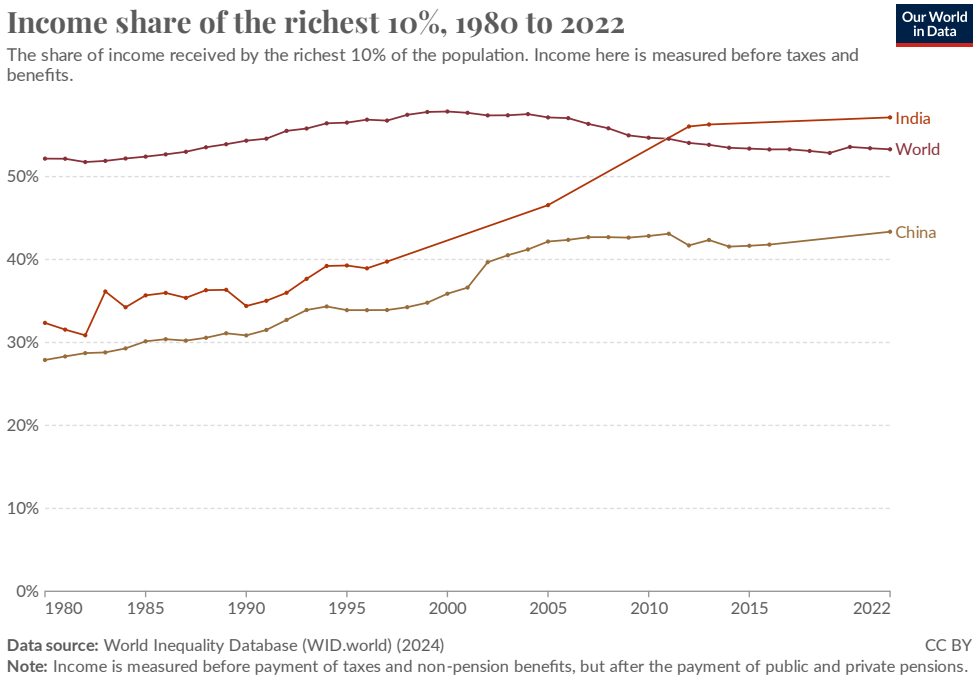

Figure 42. The income share of the richest 10% at a global level, for India, and for China from 1980 to 2022. Adapted from [204].

The presented data highlights how income and wealth are distributed, with poorer countries experiencing the widest disparities. Unlike in developed countries, the economic resources of an individual or a household significantly impact healthcare access in these regions, as universal healthcare coverage remains far from reality. Recent data shows that average health insurance coverage in low-income countries is as low as 7.9%, with LMICs at 27.3% and upper-middle-income countries at 52.5% [206]. The main consequence of this lack of coverage is the further impoverishment of households, which are often forced to pay out-of-pocket for medical care. In fact, out-of-pocket health spending is one of the largest, if not the largest, sources of healthcare financing in low-income countries. For example, in 2020, around 50% of health expenditure in India was privately financed through out-of-pocket payments, with figures reaching or exceeding 60% in African countries such as Nigeria, Sudan, Cameroon, and Egypt [207]. Viewed from another perspective, it is estimated that 2 billion people worldwide face financial hardship

due to out-of-pocket health spending, pushing many individuals and households below the poverty line [208]. The impact of such expenditures exacerbates health outcomes at both individual and public levels: households barely able to afford medical care are often compelled to neglect their healthcare needs unless absolutely necessary. Preventative care is virtually non-existent, as it is typically sought while one is still healthy. Non-communicable diseases, such as cardiovascular diseases and cancer, have the most severe financial and health impacts, leading to further impoverishment. Meanwhile, communicable diseases, such as malaria and tuberculosis, have higher incidence rates and also contribute to deepening poverty [209]. In addition, these diseases disproportionately affect the poorest communities, which have the least financial capacity to address them.

The disparities discussed in the previous paragraphs result in differing diseases and clinical conditions experienced by the populations of wealthier and poorer countries, which in turn lead to differences in the most common causes of death. In its 2024 annual report, the WHO ranked the ten leading causes of death by income group [210] (Figure 43).

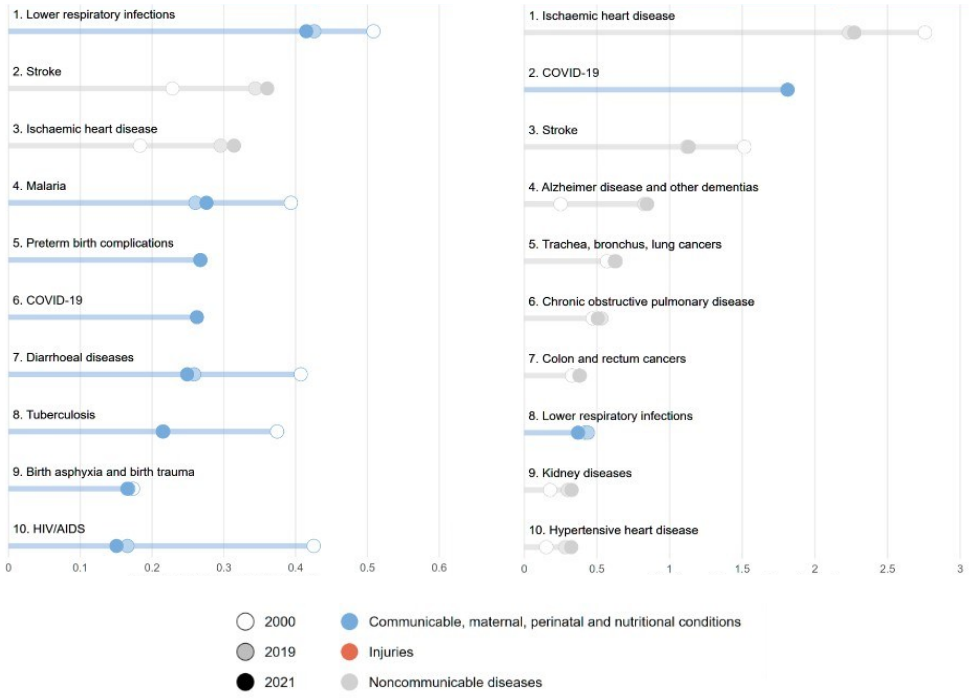

Figure 43. On the left, the ten leading causes of death for low-income countries; on the right, the same raking for high-income countries. Values are expressed in millions of deaths. Adapted from [210].

Notably, people in poorer countries remain significantly more likely to die from communicable diseases, which account for eight of the ten leading causes of death. In the coming decades, a double burden is expected to emerge in these regions, characterized by the persistent incidence of infections and communicable diseases alongside a rising prevalence of non-communicable diseases, such as stroke and ischemic heart disease, conditions historically associated with wealthier populations [211]. While HIV and malaria still claim hundreds of thousands of lives annually, their impact is now overshadowed by cardiovascular diseases, which have nearly doubled their burden over the past two decades. Shifts in lifestyle, uncontrolled urbanization, smoking, consumption of unhealthy and processed foods, and other typically "Western" habits are increasingly affecting lower-income countries. This shift is particularly concerning, as health systems in these regions are often neither mature nor adequately prepared to manage long-term chronic diseases or patients with multimorbidities [212].

Focusing on neonatal mortality rates—the number of children who die within their first 28 days of life—reveals similar patterns of disparity between income regions. Key determinants of neonatal mortality include income, geographical location, maternal education, and place of delivery [213,214]. More than half of all neonatal deaths occur in just five high-burden countries: India, Nigeria, Pakistan, China, and the Democratic Republic of Congo, which together account for over 1.5 million deaths annually [215]. In relative terms, neonatal mortality rates in 2022 ranged from an average of 0.1% in European countries to nearly 4% in Pakistan, Afghanistan, and sub-Saharan countries [216] (Figure 44). Globally, around 4.9 million children under the age of five died in 2022, with 2.3 million of those deaths occurring in the first month of life. A child born in the highest-mortality country is 80 times more likely to die before the age of five compared to a child born in the lowest-mortality country [217].

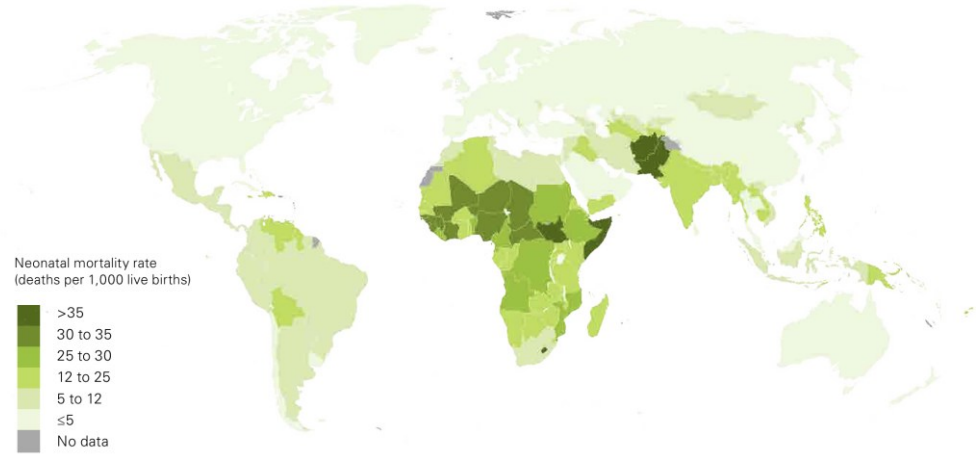

Figure 44. Neonatal mortality rate by country for year 2022. Adapted from [217].

This data-based analysis, though brief and not exhaustive, effectively highlights the immense disparities between wealthier and poorer countries, where a multitude of factors converge to produce a severe lack of healthcare coverage and medical assistance. One potential avenue for significant improvement lies in the increased diffusion of diagnostics, provided that such diagnostics are both effective and usable

in resource-constrained environments. This has been demonstrated by several successful examples in recent years. For instance, HIV infection control has greatly benefited from the introduction of simple, POC HIV rapid tests [218], and sexually transmitted infections have also been reduced through the development of appropriate POC diagnostics [219]. Building on this foundation, the following discussion will focus on the critical need for diagnostics in LMICs and the strategies manufacturers should adopt to design and implement devices that are not only accurate and robust but also affordable for developing countries, while remaining commercially viable for manufacturers.

4.3. The role of manufacturers: from donations to ad-hoc diagnostics

4.3.1. Lights and shadows of medical equipment donation

It may seem intuitive that the lack of diagnostic capabilities in health systems and facilities in developing countries could be addressed, or at least mitigated, through the donation of medical devices and IVDs.

This practice is indeed common, with donations coming from various entities such as governments, non-governmental organizations, private voluntary organizations, and manufacturers. To regulate and standardize these donations, the WHO published a guideline in 2011, outlining best practices for donors to follow in order to maximize the benefits for recipients [220]. In essence, the guideline proposed essential elements that both donors and recipients should consider when developing their respective policies. One key recommendation is that donations should align with the receiving country's regulations, acceptance or purchasing policies, and public health needs and plans. However, despite the guideline's optimistic intent, this requirement may be unattainable for many sub-Saharan and South Asian

countries, which often have limited or nonexistent regulatory frameworks for medical devices and lack comprehensive public health plans. In a subsequent 2017 publication [23], WHO once again addressed the issue of donations, raising concerns about substandard and "unwanted" devices. It acknowledged that, in some cases, donated equipment was so detrimental and useless for receiving countries that some nations banned donations altogether, aiming to avoid becoming dumping grounds for obsolete or malfunctioning equipment. The proposed solution, as before, was that donated equipment should comply with all regulatory requirements for safety, quality, and performance, and that the supply process should mirror that of regularly purchased equipment.

Despite the widespread dissemination of guidelines and efforts by WHO and other influential stakeholders to regulate and standardize donation practices, literature and various reports highlight dramatic outcomes that often lead to serious clinical challenges or, at the very least, unnecessary strain on already overburdened facilities. A case study from a Gambian hospital illustrates how well-intentioned donations can result in negative outcomes [221]. The hospital received more than twenty pediatric oxygen concentrators from a private group of philanthropists, yet none remained in use after just a few weeks due to technical issues. The donors later admitted that the equipment was not new, and some units were already malfunctioning at the time of donation. Additionally, a subsequent technical inspection revealed that the primary issue was the electrical incompatibility between the equipment and the facility's power supply.

The example provided is just one of many similar situations in LMICs, where healthcare facilities are increasingly becoming associated with "graveyards" for outdated, low-quality, and unused equipment from wealthier nations. It is estimated that up to 70% of medical equipment in sub-Saharan countries is donated, but only 10 to 30% of it becomes operational [222,223]. Moreover, flawed donation protocols

and acceptance procedures often result in equipment arriving without spare parts, or with parts that are difficult to source, as well as lacking manuals, instructions, proper training, and maintenance plans or capabilities [224,225].

In general, donors and recipients should communicate and collaborate from the very beginning, starting with the identification of needs and certainly before the shipment of donated goods, especially when the equipment includes electrical components and has specific functional and operational requirements, as most diagnostic devices do. In summary, five key points must be assessed: i) the availability of trained personnel to operate and maintain the equipment, from doctors and nurses to technicians; ii) the environmental conditions in relation to the operational requirements of the devices, such as power supply, water, temperature, and humidity; iii) the need for and availability of auxiliary equipment and spare parts; iv) the resources required for maintenance and repair, both economic and technical; and v) the capacity to train users in the correct operation and interpretation of results.

While the first and last points may be easier to address, at least for locations that are not extremely disadvantaged, the remaining three present significant challenges to the effectiveness of donations. Diagnostic devices and laboratory instrumentation are typically designed for higher-income countries, where electrical supply is stable and continuous, infrastructure is modern, and systems for water supply, waste management of reagents and samples, planned quality control, and routine maintenance are in place [226].

4.3.2. Designing diagnostics for the developing world

Manufacturers, as the producers of diagnostics, share the power and responsibility with distributors to ensure these devices reach areas where they are most needed. Without the active engagement of manufacturers, no significant improvement in healthcare access can be achieved. Two main challenges arise in this context: the

first is technological, concerning the design and development of effective diagnostics; the second is economic, relating to the financial viability and profitability of distributing devices in low-resource settings.

Despite the immense need for diagnostics in developing regions, turning a profit from selling devices in these markets is far from guaranteed. Many diseases, infections, and clinical conditions fall under the category of "non-profitable diseases," which refers to pathologies that, although addressable, lack the necessary leverage within health systems to be prioritized for monitoring or investment by manufacturers [227,228]. For example, around 500,000 people are infected annually by visceral leishmaniasis, with 90% of cases occurring in just five countries—India, Bangladesh, Nepal, Sudan, and Brazil. Without diagnosis and treatment, all of these individuals will die within years. However, because the burden is so concentrated in regions outside the developed world, there is insufficient market incentive to attract private sector investment [24]. This issue is further compounded by the surprisingly low amount of money spent on diagnostics, even in developed countries, despite their undeniable importance. A 2016 study found that while around 66% of diagnoses relied on IVDs, only 2.3% and 1.4% of total healthcare expenditures in the U.S. and Germany, respectively, were allocated to this sector [229]. Consequently, even if the share of diagnostics spending relative to overall healthcare costs were higher in developing countries, their healthcare budgets are so dramatically smaller than those of Western economies that even diseases with a heavy burden may attract little more than marginal interest from an investment perspective [230].

The severe economic constraints, combined with the technological challenges posed by infrastructural, management, and knowledge limitations discussed in the previous section, largely preclude the feasibility of using the same technologies and devices as those in wealthier, more organized countries. Exceptions are rare, limited

to national hospitals or tertiary care centers, which may be one or two for an entire population. The understandable temptation for manufacturers to design dual-use solutions that cater to both developed and developing countries rarely results in commercial success. High-income countries prioritize high-performance, high-accuracy diagnostics, often accepting higher costs and complexity in exchange for superior results. In contrast, lower-income countries are less likely to require maximum performance, instead valuing cost-effectiveness, ease of use and maintenance, and robustness. [184]. The more viable approach is to design diagnostics that are simple, portable, and yet sufficiently sensitive and specific, user-friendly, and requiring minimal maintenance and auxiliary equipment.

Manufacturers can refer to a cornerstone set of criteria published by WHO in 2003, initially designed for sexually transmitted diseases but applicable to any test intended for use in resource-constrained settings [24,231]. These criteria are encapsulated in the acronym "A.S.S.U.R.E.D.," with each letter representing a desirable feature that manufacturers should aim to fulfill to develop a diagnostic that is truly effective and usable (Table 12).

Criteria	Meaning
Affordable	Affordable to health systems and to end users
Sensitive	Few false negatives
Specific	Few false positives
User-friendly	Simple to perform and interpret, and requiring little training
Rapid and Robust	Results in the shortest time possible (within tenths of minutes) and working in harsh settings
Equipment free	No laboratory or additional equipment needed
Deliverable	Available and accessible to those who need it

Table 12. The WHO ASSURED criteria for the design of diagnostics for the developing world.

Despite the generic nature of the A.S.S.U.R.E.D criteria, which do not specify technical or technological details or set numeric thresholds, they represent a comprehensive and challenging benchmark for manufacturers and serve as a valuable guide for implementing their ideas effectively. It is unsurprising that affordability is the headline criterion, making it both the most important and, likely,

the most difficult to meet. Assessing the affordability of a test requires manufacturers to consider not only the final estimated price of a single test—already a demanding task—but also how much a health system is able and willing to pay. As discussed in previous sections, the payer may be the government, the patient, a non-profit organization, or a private donor. While all of these stakeholders aim to minimize costs, their willingness and ability to pay can vary significantly. Moreover, affordability should not be confused with cost-effectiveness. Affordability primarily refers to the monetary cost, whereas cost-effectiveness reflects the benefit derived from the diagnosis relative to the associated costs [45,98]. A test may be highly cost-effective but unaffordable for severely under-resourced settings, while an affordable test may not be cost-effective due to low specificity and sensitivity. Similar considerations arise when evaluating how critical a diagnosis is for the patient and where the diagnostic device fits into the clinical pathway. For first-line screening devices, end users may prioritize affordability over reliability and analytical performance, particularly specificity. In such cases, if the screening indicates a need for further investigation, the patient can be referred to higher-level facilities or subjected to more accurate, albeit more expensive, diagnostic methods. This controlled trade-off in favor of affordability can still be advantageous by enabling broader screening campaigns at lower costs [173]. It becomes clear that the perceived affordability of a device extends beyond its cost, encompassing its overall "value", which includes the benefit it provides to patients and the economic considerations of the healthcare provider. A key player in the procurement of diagnostics are non-governmental organizations, which purchase large quantities of devices from manufacturers and donate them where needed. In these instances, manufacturers must design and produce devices that meet the pricing requirements set by these organizations.

Two other important criteria are "User-friendly" and "Rapid and Robust". Both require careful design, beginning with a thorough understanding of the user, their

capabilities, and the environment in which the device will be used. Even if the end user is a doctor, nurse, or community health worker, their level of expertise in operating devices and handling samples should not be assumed. The worst-case scenario involves a minimally trained operator using the diagnostic in a rural area with limited or no access to electricity, water, or additional medical equipment. In such cases, the steps from sample collection to result readout must be minimized and simplified, with automation being a desirable feature.

First, sample collection must be feasible with minimal equipment and as non-invasive as possible, to reduce the risk of infections. For this reason, saliva, urine, or sweat are preferred when applicable. When blood samples are necessary, capillary specimens are preferable due to easier collection and a lower risk of infection compared to venous or arterial samples, which require sterile syringes and heparinized test tubes. However, collecting capillary samples via fingerstick or heel stick yields smaller volumes and increases the likelihood of hemolysis. Nonetheless, this should not be a limiting factor, as smaller sample volumes also contribute to user-friendliness [44].

Second, after sample collection, the user should not be required to further process the sample [232]. Sample processing may involve centrifugation, reagent addition, bacterial enrichment, or nucleic acid amplification—procedures that require additional equipment and increase the risk of user errors. Such errors, in the worst case, can lead to unnoticed sample degradation, resulting in false results or the need to repeat the test. For measurements performed on plasma or serum, the separation of the corpuscular part can be accomplished on-device using plasma separation membranes, as demonstrated by recent studies, including the reflectance photometer cited in this thesis for TSB measurement and HCT estimation [109,178,233,234]. Regarding reagents, diagnostics requiring wet reagents often fail to comply with the A.S.S.U.R.E.D. criteria due to the need for additional equipment, which reduces

user-friendliness. Wet reagents also frequently require more stringent storage and handling conditions. Cold chain management, while essential for the proper distribution of many medical products like medicines and vaccines, is often inefficient and unreliable in developing countries [235]. When reagents are necessary to enable a measurement or to enhance sensitivity and specificity, dry chemistry offers a valid alternative due to its less stringent handling requirements and greater tolerance to ambient storage conditions and temperature fluctuations [236,237].

Third, device operation refers to the sequence of steps the user must follow to obtain a result after adding the sample. While full automation is the most desirable option, it typically increases system complexity and requires additional components. Lateral-Flow Assays (LFAs) and Paper-based Analytical Devices (PADs or µPADs) can be engineered to accept samples and automatically perform simple tasks, such as plasma separation or reagent addition, through the design of the paper or nitrocellulose substrates themselves [238]. Despite significant advances in microfluidics, paper functionalization, and the promising development of multiplexed assays, paper-based devices without electronics or power supplies are generally limited to providing qualitative or semi-quantitative results [239]. Common result delivery methods include antibody test lines, colorimetry, meter-style distance scales, or counting-based systems [189,240–243]. Examples of these readout methods are shown in Figure 45. These methods enable diagnostic examinations to be completed at very low cost, typically quickly and automatically, using a single device that is also highly robust in terms of environmental and storage conditions. Moreover, such devices are inherently portable. However, their applicability is generally limited to analyses where "yes/no" results are sufficient or where semi-qualitative results provide meaningful information. Notable examples include pregnancy tests, SARS-CoV-2 tests, and blood typing tests, all of which are now commonly used, even for self-diagnosis.

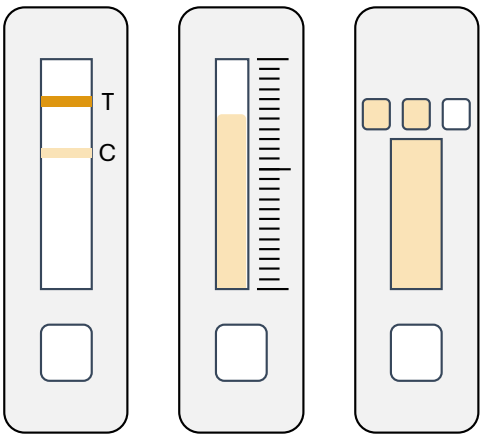

Figure 45. Some conceptual examples of readout methods for LFAs and PADs. From left to right: colorimetric/test line method, distance-based readout, counting-based readout.

In most cases, qualitative results are insufficient, particularly in situations where precise measurements are required, such as determining the concentration of an analyte or the viral load in a sample. The limitations of current "pure paper" diagnostics become insurmountable in these scenarios, especially considering the limited sensitivity and specificity of visual assessments, which can be influenced by lighting conditions, operator perception, humidity, and other factors [105,239,244].

Quantitative results can be obtained from LFAs and PADs by incorporating electronics to read the signal and calculate the result using a calibration curve. In this case, manufacturers may choose to compromise the Affordability and Equipment-free criteria in exchange for significant improvements in accuracy, Robustness, and User-friendliness [44]. Several studies have explored the use of commercial technologies, such as smartphones or scanners, as reflectance or color detectors, yielding promising results and growing acceptance [245–247]. However, concerns remain regarding repeatability and reliability, primarily due to the strong operator dependency introduced by these solutions. Variables such as changes in illumination intensity, distance between the sample and detector, the focal plane of lenses, and proprietary post-processing algorithms can result in inconsistent performance. Additionally, regulatory challenges surrounding the use of consumer

technologies as medical devices are still under debate and will likely take several years to be fully regulated and authorized [248–250].

For these reasons, the optimal choice for manufacturers often lies in developing dedicated, purpose-built external readers. By designing a solution from the ground up, the electronics and components can be carefully selected to achieve the desired features. While this may appear to increase complexity for the manufacturer, it is often more efficient than adapting existing, more complex, and non-specialized technologies like smartphones. In the simplest cases, an external reader may consist of a light source, a detector, a small display for reporting results, and a battery for power [19,251]. Furthermore, external readers allow for the detection and measurement of signals beyond colorimetric ones, which are typically the limit of smartphones and scanners. Recent literature highlights examples of electrochemical [252], chemiluminescent [253], and fluorescent [254] readouts.

Another advantage of incorporating electronics, even if not overly simple, is the ability to ensure the traceability of each measurement, as well as the storage and transmission of results to another device, such as a computer or smartphone. While this feature may initially seem non-essential for extreme POC applications, it represents a significant improvement in usability for the user and reduces post-analytic errors, such as patient mismatching, which benefits the patient [21].

In conclusion, manufacturers should focus on developing diagnostics by first understanding the environment and the intended user, whether that user is the patient or a healthcare worker with a certain level of skills and experience. The A.S.S.U.R.E.D. criteria provide a valuable benchmark for evaluating the design or prototype of a device. Their broad and high-level nature should be viewed not as a limitation but as an opportunity for flexibility and creative freedom in design. The key to interpreting these criteria lies in the context of the specific health issue being addressed, with the goal of maximizing all aspects while assigning the appropriate

priority to each. For instance, while affordability is a headline criterion, it may be compromised to achieve adequate performance or robustness. Similarly, perfect analytical performance may not be the primary objective if ensuring ease of delivery and minimal reliance on additional equipment is more critical. With these premises, the A.S.S.U.R.E.D. paradigm enables more than just technological guidance and induces the manufacturer to evaluate a clinical condition, with its complexities, and elaborate a technological solution to address it, rather than starting from technology and subsequently force it to adapt to a certain environment. On the other side, from the perspective of distributors, donors, and health systems, an A.S.S.U.R.E.D. compliant device could be perceived as a more optimal solution and may be favored in its diffusion, whether they directly care about A.S.S.U.R.E.D. or not. Ultimately, the focus on affordability from the manufacturer and the improved palatability for the other stakeholders together can transform a health condition from "non-profitable" to financially viable and interesting, ultimately leading to a benefit for the population and for healthcare systems that can be supplied with effective and usable diagnostic solutions.

4.4. The role of donors, suppliers, and NRAs: ensuring the quality of diagnostics

4.4.1. Protecting health systems and patients from substandard and falsified products

The role of donors and NGOs in ensuring the availability of medical products, including diagnostics, is crucial in developing and lower-income countries. As discussed in previous sections, their contributions are often irreplaceable, as governments frequently lack the structural and financial capacity to effectively manage the importation and oversight of medical equipment. The complexities of the supply chain, combined with the numerous actors involved in the distribution

process, create opportunities for a shadow economy of dangerous and unregulated products. According to the WHO, substandard medical products are "authorized medical products that fail to meet either quality standards or their specification, or both," while unregistered medical products are "products that have not undergone evaluation and/or approval by the national or regional regulatory authority for the market in which they are marketed or used". Falsified medical products are defined as "products that deliberately or fraudulently misrepresent their identity, composition, or source" [255]. As these definitions suggest, not including falsified products, products can fall into these categories either through intentional malpractice or through negligence. Although substandard products are often the result of malicious intent, they can also arise from negligence or an inability to undergo proper quality assurance [256].

Substandard and falsified products affect virtually every country, regardless of income level, due to the vast trade in health and health-related goods. In fact, both the European and Americas regions are tied for second place in terms of the percentage of reports from quality surveillance networks, with the African region ranking first (Figure 46).

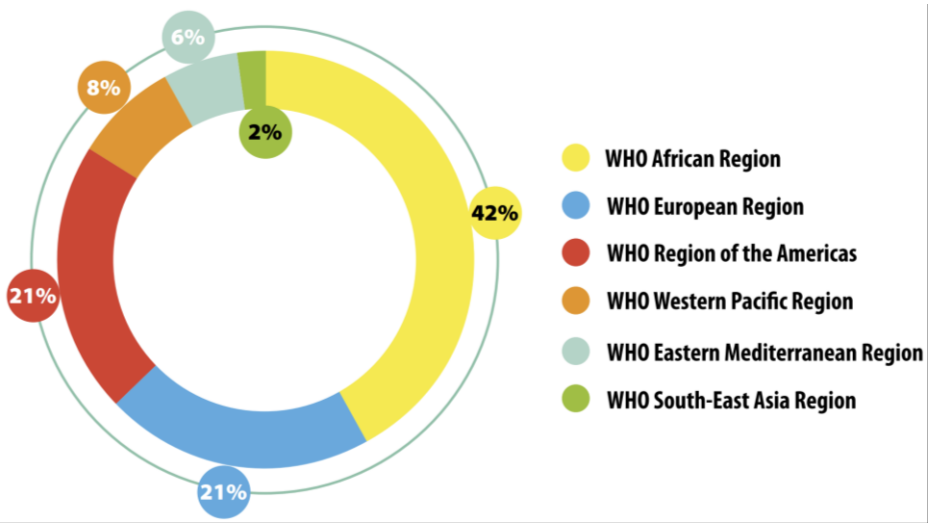

Figure 46. The percentage of reports from each WHO region, data collected from 2013 to 2017. Adapted from [255].

It is important to note that while the number of reports provides an estimate of the prevalence of substandard and falsified products, this figure also depends on the strength and efficiency of surveillance bodies in each region. As the saying goes, "the more one looks, the more one finds", making it likely that the real burden falls disproportionately on developing countries, which have fewer resources to detect and address these products. Substandard and falsified products are most commonly found where: i) access to quality and safe medical products is limited, ii) governance is weak and corruption is higher, and iii) the tools and technical capacity to enforce good practices are lacking.

In summary, limiting the trade and use of substandard and falsified products requires preventing their manufacture, implementing systems and procedures to detect and remove them from the supply chain, and responding swiftly and proportionately to any incidents that arise. Each of these actions presents significant challenges and involves multiple stakeholders—from manufacturers to end-users—at every step of the supply chain. Within the scope of this thesis, the discussion will focus on the role of manufacturers, the WHO's Pre-Qualification program, and the NRAs of developing countries.

4.4.2. NRAs maturity in LMICs and registration of medical devices

NRAs are responsible for overseeing the entry and use of medical products within their respective territories. Mature and well-structured NRAs in developed countries, such as the U.S. Food and Drug Administration (FDA), have established stringent procedures and requirements that manufacturers must meet to gain authorization for product sales. These agencies also implement extensive post-market surveillance and quality assurance programs to ensure that medical products continue to meet safety and performance standards over time. Together, these

processes contribute to what is increasingly referred to as the "governance" of medical devices.

In contrast, NRAs in LMICs are less developed, and their governance over health systems often lacks essential components. The two technology-related challenges discussed earlier—incompatible or outdated donated equipment and substandard and falsified products—are closely linked to the absence or inefficiency of regulatory and oversight bodies [201]. By 2012, 7% of African countries had a NRA in place, while 63% had limited or minimal regulation, and 30% had no regulation at all [257]. As of 2017, most African countries did not have NRAs listed in the WHO Global Atlas of Medical Devices, and only minimal improvements were noted in the subsequent 2022 edition (Figure 47) [258].

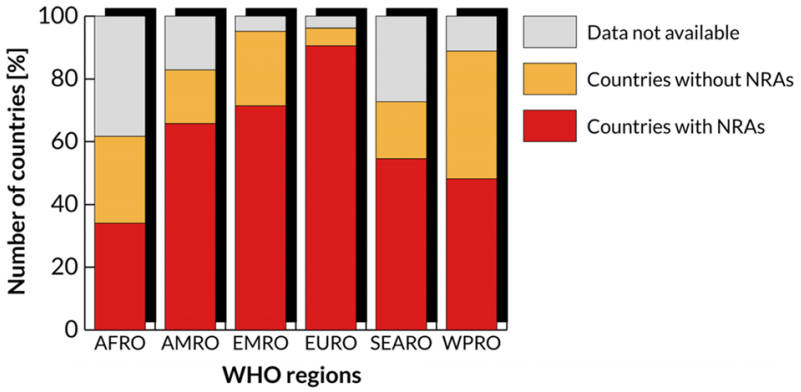

Figure 47. Existence of NRAs by WHO region. Adapted from [259].

Additionally, LMICs with some regulatory capability tend to focus more on overseeing medicines and vaccines than on medical devices and diagnostics [259]. Promising initiatives have been established over the past two decades, particularly in Africa, aimed at developing and harmonizing medical regulatory bodies across countries. These efforts not only strengthen governance but also promote market growth through streamlined and standardized procedures. Notable examples include the African Organization for Standardization (ARSO), the African Network for Drugs and Diagnostic Innovation (ANDI), the African Union (AU), and the United

Nations Economic Commission for Africa (UNECA) [257]. Recent progress has been made in the harmonization of medical device classification, a key principle of a mature NRA. Many African countries with established NRAs now use a risk-based classification system for medical devices, aligning with the systems used by the US FDA or the European MDR and IVDR [201]. However, significant gaps remain in procedural aspects. Most African NRAs either lack pre-market assessment procedures for diagnostics and medical devices or implement them in a limited capacity. Even in countries where such procedures exist, the requirements are often unique and inconsistent [260]. Similarly, post-market surveillance and device traceability are addressed in only a few countries and are frequently limited or inefficient in gathering information from the market or manufacturers [261]. This data confirms that, while harmonization with North American and European regulations is a positive step, it may not be sufficient for overall improvement. Developed countries' stringent regulatory authorities are capable of implementing comprehensive governance, covering both pre-market and post-market activities. In contrast, NRAs in developing countries face challenges such as insufficient and unstable funding, as well as inadequate personnel, knowledge, and technical expertise [259]. These constraints indicate that attempting to replicate the stringent regulations of Western countries may be overly complex and costly, both financially and in terms of time, even with support from organizations like the WHO or the Global Harmonization Task Force (GHTF).

From the manufacturers' perspective, the fragmentation in regulatory processes and requirements presents a significant obstacle in terms of cost and time-to-market, thereby reducing their incentive to invest in solutions for developing markets. Since diagnostics, like other medical products, must be registered in each country where they are to be sold, manufacturers must navigate each country's regulatory process by preparing separate dossiers, collecting different data, and complying with distinct laws.

Beyond the regulatory process itself, a significant obstacle is the time required to obtain authorization. Various, and sometimes conflicting, estimates are found in the literature, likely due to the absence of a standardized method for calculating approval times. One study reported an average of two years for Central and East African NRAs, while Western African NRAs showed shorter timelines of six to twelve months, provided prior approval was obtained in the EU [262]. Another study found similar timelines but noted that approval times were reduced to under a year after implementing a regulatory harmonization program for medicines [263]. In Southern African countries, approval times ranged from six months to nearly two and a half years, depending on the specific country, even after the launch of a similar harmonization initiative [264]. It is important to note that data specifically on diagnostics approval is limited, as these estimates primarily concern medicines and vaccines, which typically have longer timelines. Additionally, due to the complexity of how approval times are calculated by NRAs, these figures may not account for "queuing" time—the period between the application submission and the receipt of a first response—which could extend for several months [264].

Another significant factor is the cost of obtaining multiple approvals. As with timelines, estimating registration costs is challenging due to the limited availability of data from individual NRAs. It is likely that registration costs in LMICs are lower than in developed countries, with some estimates suggesting fees as low as a few thousand US dollars, and some NRAs not charging for this process at all [265,266]. Despite the scarcity of such data, it is plausible that cost is not the primary deterrent for manufacturers, or at least less so than the time required for approval.

In conclusion, the fragmented landscape of regulatory agencies—characterized by uncertainty in time requirements and diverse pathways and regulations—serves as a significant deterrent for manufacturers. A promising solution, though still in its early stages, is the WHO's Pre-Qualification program (WHO-PQ). Covering various

categories of medical products, including diagnostics, this program facilitates the broader diffusion of health products, offering a triple-sided benefit: improved health outcomes for patients, a smoother marketing process for manufacturers, and reassurance for donors that their contributions are safe, of high quality, and not falsified or substandard. It also provides substantial support for under-resourced NRAs in LMICs.

4.5. The role of WHO: PQ as a framework to meet the needs of all stakeholders

4.5.1. Evolution and impact

The Pre-Qualification program was initially established in 1987 to assist UNICEF and other UN procurement agencies in ensuring the quality, safety, and efficacy of vaccines purchased for national immunization programs in developing countries. It was later expanded to include medicines in 2001, IVDs in 2008, and, most recently, vector control products in 2017 (Figure 48) [267]. According to WHO, the program's aim is to "ensure that key health products meet global standards of quality, safety, and efficacy, in order to optimize the use of health resources and improve health outcomes".

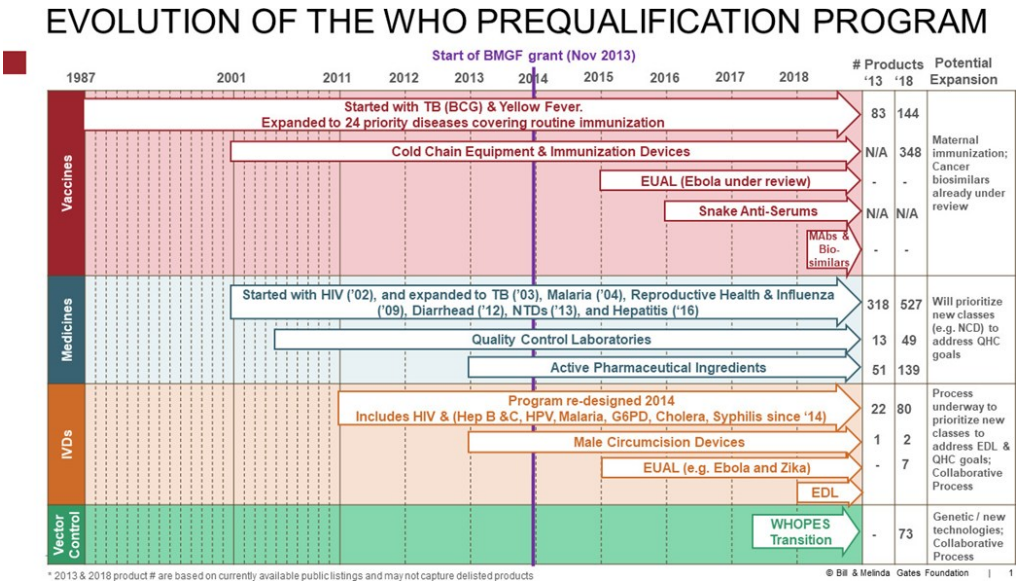

Figure 48. The evolution of WHO-PQ over time. Adapted from [267].

With regard to diagnostics, WHO initially launched a precursor program, the "Test Kit Evaluation Programme", to assess the performance of HIV diagnostics in African populations. This program was expanded in 2010 to cover diagnostics for other priority diseases and restructured in 2012 to include hepatitis, malaria, G6PD deficiency, cholera, and syphilis [268]. Today, WHO-PQ oversees more than 1,700 products across four categories: IVDs and male circumcision devices, medicines, vaccines and immunization devices, and vector control (Figure 49) [269].

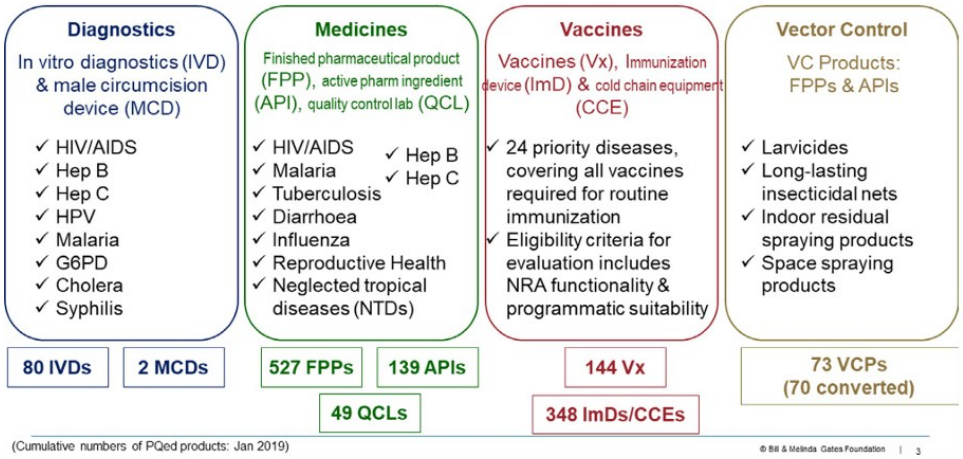

Figure 49. the scope of product streams prequalified by WHO. Adapted from [267].

A global impact assessment of WHO-PQ conducted in 2019 [269] reported encouraging statistics. The program enabled the allocation of approximately $3.5 billion in donor funds to procure safe equipment and medicines, benefiting around 400 million additional patients annually. Furthermore, a cost-benefit analysis revealed that WHO-PQ generates savings through increased market competition, with a return of 30 to 40 times the investment. For certain products, such as first-line antiretroviral therapy, the cost-benefit ratio was even more impressive, reaching 170x. Additionally, the program has played a significant role in raising manufacturing standards in LMICs, which now account for more than 40% of all manufacturers with prequalified medicines and over 50% of those with prequalified vaccines. Prequalified diagnostics available on the market tripled from 25 to 70 between 2013 and 2019, though less than 20% of diagnostic manufacturers are based in LMICs. Another notable contribution of the program is its role in strengthening health and regulatory systems in LMICs and harmonizing regulations among NRAs, which was also enabled by the training of more than 8000 regulators between 1997 and 2017 across all regions.

4.5.2. Overview of the prequalification process

At a high level, the four streams share a common prequalification process, with variations depending on the product type. The process for diagnostics will be described in more detail. It consists of five steps, as outlined in Figure 50.

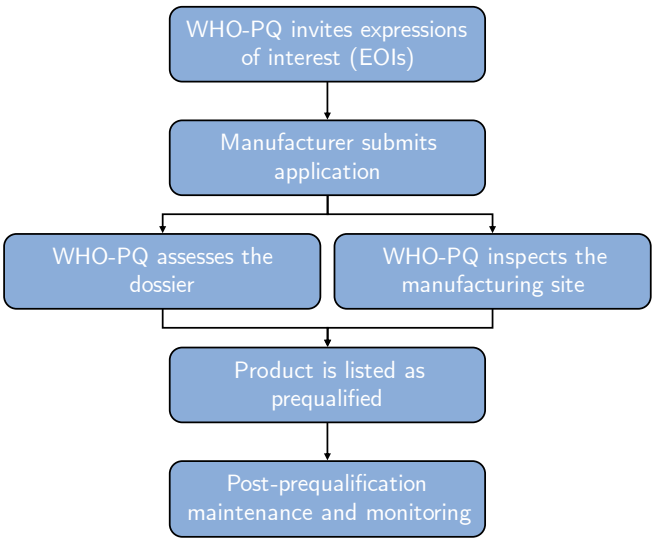

Figure 50. An overview of the prequalification process, valid for all product streams.

Expression of interest (EOIs)

First, WHO publishes an invitation for manufacturers to submit an expression of interest (EOI) for product evaluation. Each product stream has its own EOIs, listing specific products with defined characteristics. It is important to note that any manufacturer can respond to an EOI, but they cannot submit products not covered by the EOI. Therefore, the responsibility of defining which diagnostics are considered "essential" and outlining their performance characteristics rests solely with WHO. Additionally, WHO is committed to informing manufacturers of a product's eligibility after receiving an initial pre-submission form. EOIs are typically open and accessible for extended periods, often years, depending on the product stream.

Application submission

WHO informs the manufacturer of the type of assessment applicable to the specific submission. Products that have already been approved by stringent regulatory authorities, such as those in the USA, EU, Japan, or Australia, may qualify for an "abridged assessment," which requires less documentation, time, and ideally lower costs for the manufacturer. For diagnostics, WHO allows abridged

assessments if key characteristics—such as intended use, test procedure, labeling and instructions for use, design, and manufacturing site—are identical between the previously approved version and the submitted version.

In all other cases, a full assessment is required. The manufacturer must submit a "product dossier," which generally aligns with the product master file or standard technical documentation required by FDA or EU regulations. Essentially, the manufacturer must demonstrate how the diagnostic was developed, designed, validated, and manufactured, and provide information on their quality management system, following the "Essential Principles of Safety and Performance of Medical Devices and IVD Medical Devices" established by the International Medical Device Regulators Forum. If WHO identifies gaps in the submission, the manufacturer must provide the additional information within a specified timeframe.

Dossier assessment and manufacturing site inspection

For a full assessment, the product dossier is reviewed to determine the diagnostic's performance, manufacturing process, and the adequacy of the quality management system. A critical point is that performance and operational characteristics are evaluated either in a WHO collaboration center or an external laboratory designated by the manufacturer, with specific consideration for use in resource-limited settings. This aspect contributes to the uniqueness of the WHO-PQ procedure and has fostered trust among NRAs and procurement agencies over time. Following the dossier review, WHO conducts an on-site inspection of the manufacturing facility indicated by the manufacturer, in relation to the ISO 13485:2017.

For abridged assessments, the manufacturer is not required to submit the full quality management system information, and the on-site inspection is shorter, focusing primarily on key processes at the specific site. In both types of assessments, labeling is also evaluated in parallel.

Product listing

Upon successful completion of the assessment, the product is added to the publicly accessible WHO List of Prequalified IVDs. This list includes details such as the commercial name of the diagnostic, its code and regulatory version, the inspected manufacturing site, the manufacturer's name, product packaging, and the date of prequalification.

However, the product may be delisted or suspended if the manufacturer fails to meet post-market conditions and responsibilities.

Post-prequalification maintenance and monitoring

The manufacturer is responsible for annual reporting on post-market surveillance, notifying WHO of any relevant product changes, preparing the specified manufacturing site for subsequent inspections, and maintaining compliance with WHO-PQ technical specifications. Additionally, WHO may share information related to the prequalification process and outcomes with interested NRAs, ensuring confidentiality, and may conduct joint reviews with NRAs as part of the assessment process.

Times and costs associated with WHO-PQ

As discussed in the previous section, time is a critical factor for manufacturers interested in accessing LMIC markets. To address this, WHO publishes timelines and response times for both WHO and the manufacturer at each stage [270]. For a full assessment, WHO's target timeline is 270 calendar days, or 350 days if an external performance evaluation or WHO-coordinated evaluation is selected. For abridged assessments, timelines are reduced to 100 and 180 days, respectively. Each assessment step has its own timeline. For instance, WHO sets a 30-day timeline to evaluate the pre-submission form from the date of receipt, after which the manufacturer has 30 days to provide any additional information, followed by another 30 days for WHO to respond with the pre-submission outcome. During the

dossier review, WHO has 90 days to provide a response, with parallel timelines set for the performance evaluation and manufacturing site inspection steps.

These detailed timelines, though somewhat complex, offer a significant advantage for manufacturers by enabling them to forecast and schedule each step with notable accuracy—something often unachievable with NRAs, which may have widely variable and unpredictable timelines. Additionally, if a manufacturer causes unjustified delays, WHO states that the application may be canceled, although specific handling procedures and acceptable justifications for extensions are not fully disclosed. On its part, WHO-PQ aims to meet these timelines at least 80% of the time.

Another key factor is the cost of WHO-PQ for manufacturers. According to WHO [271] , the fees cover part of the costs associated with various assessment activities. Most WHO-PQ funding comes from donors like Unitaid and the Bill and Melinda Gates Foundation; however, the specifics regarding donation amounts, the grantmaking mechanism, or whether donations are general or allocated to specific streams, products, or diseases remain unclear [46]. WHO views prequalification as a service for other UN agencies, explaining that the overall financial support is primarily sourced from these organizations, with assessment fees providing additional support.

For diagnostics, WHO charges $5,000 for dossier screening and between $8,000 and $12,000 for full and abridged assessments, respectively. There is also an annual fee of $4,000 for each product listed on the List of Prequalified IVDs. In addition to these fees, manufacturers must often bear significant costs for dossier preparation, device testing, and any clinical trials or field evaluations, which may easily exceed the WHO fees and exclude costs related to the design and development of the diagnostic.

It is difficult to determine whether these fees are ultimately beneficial or detrimental from a manufacturer's perspective [43]. On one hand, while a manufacturer may be willing to pay for prequalification, these costs would likely be passed on to the product price, potentially limiting its affordability for donors and procurers and reducing accessibility for health systems or patients who pay out-of-pocket. Some manufacturers may even opt out of prequalification, choosing instead to pursue alternative regulatory paths, such as direct registration with individual NRAs. On the other hand, eliminating the fees could result in longer timelines, which could again impact the affordability and availability of quality-assured diagnostics on the market.

This overview of the prequalification process, along with the accompanying comments, provides a description of WHO-PQ from WHO's perspective. While the full impact of the program has yet to be thoroughly measured, the prerequisites for its success are in place, with positive outcomes anticipated for those who need them most—namely, the populations of developing countries and their health systems. However, at present, a manufacturer with a prequalified diagnostic is still required to complete the standard assessments by the NRAs of each country where they plan to market the device. This additional step leads to duplicated efforts, significant loss of time and money, and offers no tangible benefit to the manufacturer. Consequently, prequalification remains primarily an additional certification that, according to WHO's own vision, enhances the manufacturer's technical capacity and expands sales and market opportunities [272]. While these assumptions are certainly valid, in practical terms, prequalification alone does not authorize the manufacturer to sell diagnostics in countries with even minimal regulations governing medical equipment and diagnostics distribution.

4.5.3. Collaborative Procedure for Accelerated Registration (CRP)

The term "collaborative procedure for accelerated registration" first appeared in 2013, describing an initiative between WHO and NRAs to streamline the registration of prequalified products. By facilitating regulated and enhanced information sharing, this procedure allowed for faster registration of prequalified products, reducing redundant work for both manufacturers and NRAs [273]. Initially, the program's scope was limited to finished pharmaceutical products, meaning medicines in their final dosage form that have undergone all production stages, including final packaging and labeling. The CRP is based on three core principles: i) voluntary participation, where manufacturers opt to apply for accelerated registration of one or more products in specified countries; ii) confidentiality, ensured through an agreement authorizing WHO to share prequalification assessment reports with designated NRAs; and iii) product consistency, where the product submitted for CRP must be identical to the version that received prequalification or approval from a stringent regulatory authority. When a CRP agreement is signed among WHO, the manufacturer, and the involved NRA(s), the NRA's role is simplified by only needing to confirm the product's consistency with the prequalified version, thereby avoiding a full quality, safety, and performance assessment. This "surveilled sharing" mechanism is highly valuable for manufacturers, saving time, effort, and money. Among the responsibilities of the participating NRA(s) is a 90-day timeline from the receipt of documentation to inform WHO and the manufacturer of their registration decision, followed by an additional 30 days to complete the product registration. While the time needed to obtain WHO-PQ must still be considered, this added CRP period is likely viewed favorably by manufacturers seeking simultaneous registration in multiple countries. Importantly, it remains vastly shorter than the standard timelines required for a "from-scratch" registration.

In 2019, a pilot CRP project for diagnostics was launched, involving five selected African countries and applying the same principles as the original procedure for finished pharmaceutical products [274].

The three primary stakeholders remain the manufacturer, WHO, and the participating NRA(s). The principle of sameness for diagnostics encompasses the product name, regulatory version, product code, manufacturing site, quality management system, design, and data on quality, safety, and performance. WHO encourages the manufacturer to submit the same dossier used for prequalification and, in parallel, advises the NRA(s) to accept this format to reduce additional requests and harmonize requirements across countries. In turn, WHO shares the outcomes of each step of the prequalification process, maintaining confidentiality and usage restrictions (Figure 51).

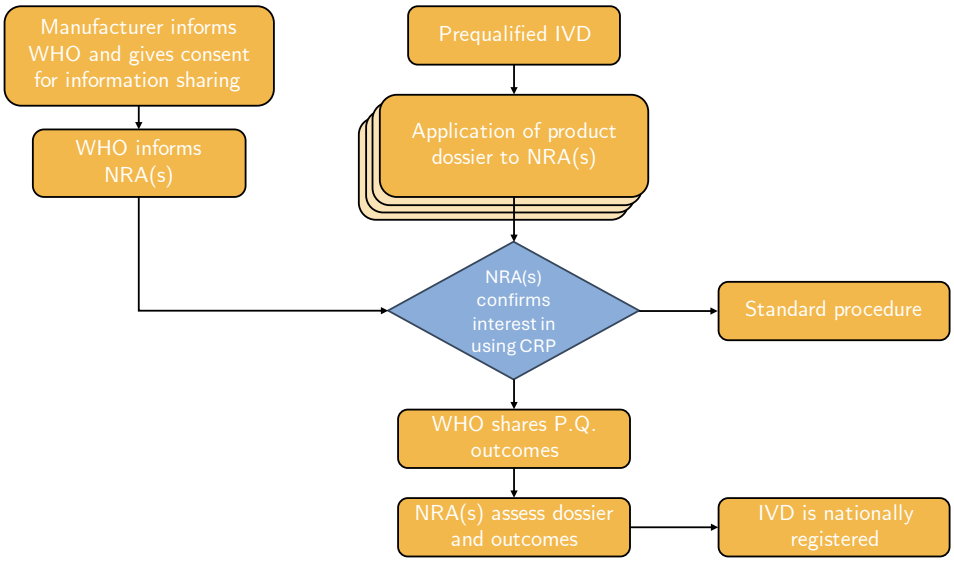

Figure 51. An overview of the steps required to obtain the registration of a diagnostic via CRP.

Currently, NRAs from 31 countries participate in the diagnostics CRP, including 26 from Africa (representing roughly half of all African nations), with the remainder from South Asia and the Middle East.

While no official reports or documents have yet been released by WHO or other trusted sources on the impact of the diagnostics CRP, it is reasonable to speculate that it serves as a highly encouraging tool for advancing diagnostic access in developing countries, benefiting nearly all stakeholders involved in the process.

For manufacturers, WHO Pre-Qualification provides a cost-effective and timely means to assess the quality, safety, and performance of their diagnostics, if these devices are included in the Expression of Interest. By subsequently applying for CRP, manufacturers can avoid the burden of duplicated work, uncertain timelines, and varying requirements, enabling full marketing authorization in participating countries. Although manufacturers are still required to pay individual registration fees, these costs may be outweighed by the advantages of streamlined registration.

Donors and procurement agencies benefit from a broader selection of prequalified diagnostics, supported by market competition, while maintaining the assurance of quality. This advantage is significant, as WHO-PQ functions primarily as a service for donors, who are also the main funders of the program.

For NRAs, WHO's emphasis on harmonized assessment procedures during CRPs offers potential benefits in expertise and knowledge, as NRA staff gain experience through dossier review and inspection outcomes, as reported by WHO [274].

4.6. Conclusions

The first two sections of this chapter presented data and statistics highlighting some of the well-known disparities between wealthier and poorer regions, as well as additional insights not commonly recognized by those in more privileged parts of the world. Addressing health conditions in developing countries and LMICs is an extremely complex challenge, given the multitude of factors involved beyond disease, including the interests and actions of diverse stakeholders. Effective improvement requires leveraging these interests, though they often differ and may

even conflict. Manufacturers, donors and procurement agencies, NRAs, health systems, and patients pursue distinct goals, which encompass both health and economic outcomes.

Diagnostics are of invaluable importance for individual and public health, and several initiatives have been established to ensure effective and safe diagnostics reach resource-constrained settings. Among these, donations have shown significant conceptual limitations and were widely criticized, including by WHO, which published guidelines in 2011 to better define and regulate this practice [220].

Achieving a meaningful impact on diagnostic diffusion requires both technological and regulatory/policy solutions. A purely technology-driven approach often overlooks the specific needs of LMICs, while a purely regulatory or surveillance-focused approach can improve market entry but may not ensure diagnostics are suited to the unique conditions in developing countries. The A.S.S.U.R.E.D. criteria offer manufacturers a valuable, user-oriented guideline, useful from design to evaluation. Despite some criticism regarding its techno-centric approach, which may emphasize cost-effectiveness over inclusivity [45], the criteria show promise when thoughtfully applied. However, even an A.S.S.U.R.E.D.-compliant diagnostic cannot be accessible if time and costs delay delivery by years due to limited or fragmented regulatory pathways.

In this regard, WHO's Prequalification of IVDs offers a promising framework, with an impactful track record in other medical products like vaccines and medicines. Donors and procurement agencies, both suppliers and, to some extent, beneficiaries of WHO-PQ, rely heavily on this certification and look to broaden its scope. Additionally, WHO-PQ reduces the risk of purchasing and distributing substandard and falsified products, a persistent and complex issue.

The Collaborative Registration Procedure (CRP) for IVDs, as a natural extension of WHO-PQ, enables manufacturers and NRAs to significantly expedite the

authorization process while maintaining quality and safety standards. It also reduces duplicated efforts for both parties while enhancing NRA capacities. Together, these tools create a pathway for increasing diagnostic access in LMICs, requiring collaboration across all stakeholders. By promoting affordable, high-performance solutions through Prequalification and facilitating delivery through CRP, WHO enables manufacturers to see potential returns on investment in LMICs while improving access for patients and healthcare providers, ultimately reducing the disparity with developed regions.

Chapter 5. CONCLUSIONS

This thesis presents the studies and experiments conducted to achieve three main objectives: i) the measurement of total serum bilirubin in neonates using a simple, portable device based on two-wavelength diffuse reflectance photometry, with a focus on hemoglobin interference compensation; ii) the estimation of neonatal hematocrit through a novel approach; and iii) a review of the current state of diagnostic diffusion in resource-constrained settings, particularly in developing countries.

For the first objective, an in-depth analysis of the clinical burden of Neonatal Hyperbilirubinemia (NH) revealed significant disparities in diagnosis and management between wealthier and lower-income countries, where the latter experience the vast majority of neonatal and children's deaths and life-long impairments. Following a review of existing bilirubin measurement methods and their feasibility in LMICs, direct spectrophotometry, specifically diffuse reflectance photometry, was selected as a promising approach for these settings. However, it was demonstrated that interference from analytes, primarily hemoglobin, limited the method's accuracy and reliability. To address this limitation, a preliminary study on hemoglobin compensation was conducted using a two-wavelength photometer (465 and 570 nm) without the use of reagents or complex hardware. A novel algorithm was developed, reducing interference errors from 94% to 15.4% in the worst case, thereby demonstrating the feasibility of compensation despite a limited sample panel and moderate accuracy. Nonetheless, using 570 nm as the compensation wavelength was determined to be sub-optimal due to its slight dependency on bilirubin concentration. To overcome this limitation, further investigation was undertaken to identify the optimal compensation wavelength. Three additional wavelengths (575, 590, and 605 nm) were compared to the original

570 nm one under two criteria: independence from bilirubin and sensitivity to hemoglobin concentration. The results demonstrated that 590 nm offered superior independence from bilirubin while maintaining adequate sensitivity to hemoglobin concentration, making it a more suitable choice. Subsequently, the optimized algorithm was tested on a broader sample panel encompassing clinically relevant bilirubin ranges to validate the instrument's improved accuracy and robustness. The findings confirmed enhanced accuracy and the validity of the algorithm across nearly the entire range of clinically significant bilirubin concentrations (4.96 to 28.00 mg/dl). An additional study examining temperature effects on the two original wavelengths revealed notable environmental influences. Specifically, while the 465 nm wavelength exhibited linear temperature dependence, the 570 nm wavelength showed quadratic dependence, with higher temperatures progressively increasing overestimation errors. These findings will support the design and development on a temperature effect compensation algorithm, in coherence with the ultimate aim of ensuring proper accuracy and robustness of diffuse reflectance photometers for point-of-care bilirubin measurement.

For the second objective, the critical need for rapid, accurate, near-patient hematocrit screening was identified, and current hematocrit measurement methods were examined highlighting their limitations relatively to resource-constrained settings. Using the same two-wavelength reflectance photometer, the study tested a panel of whole blood samples at various hematocrit levels, leading to a novel approach for fast, automated neonatal hematocrit screening. Such approach was based on plasma penetration velocity in lateral flow membranes and eliminated the need for any treatment or manipulation of the sample. The results were promising, as this approach covered the full reference range for neonatal hematocrit, namely 30 to 60%. While accuracy was not yet sufficient for diagnostic purposes ($r = 0.87$, $p < 0.001$, and a mean absolute error of 4.29%) the findings demonstrated substantial potential for screening applications. This potential was particularly

evident in terms of very short turnaround times, minimal sample volume required, reduced per-analysis cost, and usability.

Lastly, this thesis investigated the complex challenges and barriers to the diffusion of in-vitro diagnostics (IVDs) in LMICs. Key roles and responsibilities of manufacturers, supranational organizations, and National Regulatory Agencies were examined, and a series of cohesive technological and regulatory solutions was proposed. In particular, the A.S.S.U.R.E.D. guidelines developed by WHO provide a framework to assist manufacturers in designing devices tailored for the developing world in a sustainable manner, considering investments, complexity, and usability. While these guidelines do not address regulatory aspects, the WHO's Prequalification Programme, combined with the Collaborative Registration Procedure, offers a more efficient and comprehensive pathway for manufacturers to achieve regulatory compliance in regions with incomplete or non-harmonized regulations. Additionally, this framework ensures a reliable and trustworthy source of diagnostics for procurement by less structured governments and suppliers. These solutions are intended to facilitate the delivery of safe, high-quality diagnostics to resource-limited settings.

The main findings of this thesis have promising implications for improving NH management in LMICs, where the burden is greatest, by introducing a cost-effective, user-friendly, and accurate method for neonatal bilirubin measurement, specifically designed to be used in such environments. Additionally, the innovative hematocrit screening algorithm offers valuable clinical insight at no additional cost in terms of sample volume, time, or equipment. Finally, the proposed technological and regulatory tools provide a framework that may support more effective diagnostic diffusion, potentially enhancing the overall quality of healthcare services in developing countries.

BIBLIOGRAPHY

(1) Olusanya, B. O.; Kaplan, M.; Hansen, T. W. R. Neonatal Hyperbilirubinaemia: A Global Perspective. *The Lancet Child & Adolescent Health* 2018, *2* (8), 610–620. https://doi.org/10.1016/S2352-4642(18)30139-1.

(2) Greco, C.; Arnolda, G.; Boo, N.-Y.; Iskander, I. F.; Okolo, A. A.; Rohsiswatmo, R.; Shapiro, S. M.; Watchko, J.; Wennberg, R. P.; Tiribelli, C.; Coda Zabetta, C. D. Neonatal Jaundice in Low- and Middle-Income Countries: Lessons and Future Directions from the 2015 Don Ostrow Trieste Yellow Retreat. *Neonatology* 2016, *110* (3), 172–180. https://doi.org/10.1159/000445708.

(3) Olusanya, B. O.; Osibanjo, F. B.; Slusher, T. M. Risk Factors for Severe Neonatal Hyperbilirubinemia in Low and Middle-Income Countries: A Systematic Review and Meta-Analysis. *PLOS ONE* 2015, *10* (2), e0117229. https://doi.org/10.1371/journal.pone.0117229.

(4) Roy-Chowdhury, J.; Roy-Chowdhury, N.; Jansen, P. L. M. Bilirubin Metabolism and Its Disorders. In *Zakim and Boyer's Hepatology*; Elsevier Inc., 2006; pp 1449–1485. https://doi.org/10.1016/B978-1-4160-3258-8.50079-6.

(5) Farouk, Z. L.; Usman, F.; Musa, B. M.; Ezeaka, V. C.; Okolo, A. Societal Awareness on Neonatal Hyperbilirubinemia: A Systematic Review and Meta-Analysis. *Seminars in Perinatology* 2021, *45* (1), 151361. https://doi.org/10.1016/j.semperi.2020.151361.

(6) Iskander, I.; Gamaleldin, R. Acute Bilirubin Encephalopathy: Some Lessons Learned. *Seminars in Perinatology* 2021, *45* (1), 151353. https://doi.org/10.1016/j.semperi.2020.151353.

(7) Amos, R. C.; Jacob, H.; Leith, W. Jaundice in Newborn Babies under 28 Days: NICE Guideline 2016 (CG98). *Archives of Disease in Childhood - Education and Practice* 2017, *102* (4), 207–209. https://doi.org/10.1136/archdischild-2016-311556.

(8) Kemper, A. R.; Newman, T. B.; Slaughter, J. L.; Maisels, M. J.; Watchko, J. F.; Downs, S. M.; Grout, R. W.; Bundy, D. G.; Stark, A. R.; Bogen, D. L.; Holmes, A. V.; Feldman-Winter, L. B.; Bhutani, V. K.; Brown, S. R.; Maradiaga Panayotti, G. M.; Okechukwu, K.; Rappo, P. D.; Russell, T. L. Clinical Practice Guideline Revision: Management of Hyperbilirubinemia in the Newborn Infant 35 or More Weeks of Gestation. *Pediatrics* 2022, *150* (3), e2022058859. https://doi.org/10.1542/peds.2022-058859.

(9) Romagnoli, C.; Barone, G.; Pratesi, S.; Raimondi, F.; Capasso, L.; Zecca, E.; Dani, C. Italian Guidelines for Management and Treatment of Hyperbilirubinaemia of Newborn Infants ≥ 35 Weeks' Gestational Age. *Ital J Pediatr* 2014, *40* (1), 11. https://doi.org/10.1186/1824-7288-40-11.

(10) Sgro, M.; Kandasamy, S.; Shah, V.; Ofner, M.; Campbell, D. Severe Neonatal Hyperbilirubinemia Decreased after the 2007 Canadian Guidelines. *The Journal of Pediatrics* 2016, *171*, 43–47. https://doi.org/10.1016/j.jpeds.2015.12.067.
(11) Satrom, K. M.; Farouk, Z. L.; Slusher, T. M. Management Challenges in the Treatment of Severe Hyperbilirubinemia in Low- and Middle-Income Countries: Encouraging Advancements, Remaining Gaps, and Future Opportunities. *Front. Pediatr.* 2023, *11*. https://doi.org/10.3389/fped.2023.1001141.
(12) Zhang, M.; Tang, J.; He, Y.; Li, W.; Chen, Z.; Xiong, T.; Qu, Y.; Li, Y.; Mu, D. Systematic Review of Global Clinical Practice Guidelines for Neonatal Hyperbilirubinemia. *BMJ Open* 2021, *11* (1), e040182. https://doi.org/10.1136/bmjopen-2020-040182.
(13) Slusher, T. M.; Abdulkadir, I.; Owa, J. A. Relevance of the 2022 American Academy of Pediatrics Hyperbilirubinemia Guidelines for an LMIC. *Pediatrics* 2023, *151* (4), e2022060679. https://doi.org/10.1542/peds.2022-060679.
(14) Riskin, A.; Tamir, A.; Kugelman, A.; Hemo, M.; Bader, D. Is Visual Assessment of Jaundice Reliable as a Screening Tool to Detect Significant Neonatal Hyperbilirubinemia? *The Journal of Pediatrics* 2008, *152* (6), 782-787.e2. https://doi.org/10.1016/j.jpeds.2007.11.003.
(15) Subcommittee on Hyperbilirubinemia. Management of Hyperbilirubinemia in the Newborn Infant 35 or More Weeks of Gestation. *Pediatrics* 2004, *114* (1), 297–316. https://doi.org/10.1542/peds.114.1.297.
(16) Meites, S.; Hogg, C. K. Direct Spectrophotometry of Total Serum Bilirubin in the Newborn. *Clinical Chemistry* 1960, *6* (5), 421–428. https://doi.org/10.1093/clinchem/6.5.421.
(17) Barko, H. A.; Jackson, G. L.; Engle, W. D. Evaluation of a Point-of-Care Direct Spectrophotometric Method for Measurement of Total Serum Bilirubin in Term and near-Term Neonates. *J Perinatol* 2006, *26* (2), 100–105. https://doi.org/10.1038/sj.jp.7211436.
(18) Pierre Ndabakuranye, J.; Li, S.; Burchall, G.; Fox, K.; Piva, T.; Xu, Z.; Kavehei, O.; Prawer, S.; Ahnood, A. 70 Years of Bilirubin Sensing: Towards the Point-of-Care Bilirubin Monitoring in Cirrhosis and Hyperbilirubinemia. *Sensors & Diagnostics* 2022, *1* (5), 932–954. https://doi.org/10.1039/D2SD00033D.
(19) Smith, S.; Land, K.; Joubert, T.-H. Emerging Technology Solutions Towards REASSURED Point-of-Need Diagnostics. In *2021 IEEE 21st International Conference on Nanotechnology (NANO)*; 2021; pp 265–268. https://doi.org/10.1109/NANO51122.2021.9514275.
(20) Lissel, A.; Ottenberg, F.; Bracio, B. R.; Ravizza, A.; De Maria, C.; Ahluwalia, A.; Di Pietro, L.; Trommler, P. Status and Solutions to Medical Device Regulations for Improving the Healthcare Landscape in Africa. In *2016 38th*

Annual International Conference of the IEEE Engineering in Medicine and Biology Society (EMBC); IEEE: Orlando, FL, USA, 2016; pp 4329–4332. https://doi.org/10.1109/EMBC.2016.7591685.

(21) Land, K. J.; Smith, S.; Peeling, R. W. Unmet Diagnostics Needs for the Developing World. In *Paper-based Diagnostics*; Land, K. J., Ed.; Springer International Publishing: Cham, 2019; pp 1–21. https://doi.org/10.1007/978-3-319-96870-4_1.

(22) Pai, N. P.; Vadnais, C.; Denkinger, C.; Engel, N.; Pai, M. Point-of-Care Testing for Infectious Diseases: Diversity, Complexity, and Barriers in Low- And Middle-Income Countries. *PLoS Med* 2012, *9* (9), e1001306. https://doi.org/10.1371/journal.pmed.1001306.

(23) World Health Organization. *WHO Global Model Regulatory Framework for Medical Devices Including in Vitro Diagnostic Medical Devices*; WHO Medical device technical series; World Health Organization: Geneva, 2017.

(24) Mabey, D.; Peeling, R. W.; Ustianowski, A.; Perkins, M. D. Diagnostics for the Developing World. *Nat Rev Microbiol* 2004, *2* (3), 231–240. https://doi.org/10.1038/nrmicro841.

(25) Jiang, J.; Gong, Q.; Zou, D.; Xu, K. Influence of Hemoglobin on Non-Invasive Optical Bilirubin Sensing. *Progress in Biomedical Optics and Imaging - Proceedings of SPIE* 2012, *8222*, 19. https://doi.org/10.1117/12.906509.

(26) Capasso, L.; Parrella, C.; Borrelli, A. C.; Maffucci, R.; Milite, P.; Sodano, A.; Ferrara, T.; Raimondi, F. Is It Worthwhile Using a Transcutaneous Bilirubinometer in the Nursery? *Early Hum Dev* 2012, *88 Suppl 2*, S25-26. https://doi.org/10.1016/S0378-3782(12)70008-7.

(27) Engle, W. D.; Jackson, G. L.; Engle, N. G. Transcutaneous Bilirubinometry. *Seminars in Perinatology* 2014, *38* (7), 438–451. https://doi.org/10.1053/j.semperi.2014.08.007.

(28) Thaler, M.; Luppa, P. B.; Schlebusch, H. Bilirubin Measurement – an Updated Survey1. *LaboratoriumsMedizin* 2008, *32* (1). https://doi.org/10.1515/JLM.2008.005et.

(29) Hulzebos, C. V.; Vitek, L.; Coda Zabetta, C. D.; Dvořák, A.; Schenk, P.; van der Hagen, E. A. E.; Cobbaert, C.; Tiribelli, C. Diagnostic Methods for Neonatal Hyperbilirubinemia: Benefits, Limitations, Requirements, and Novel Developments. *Pediatr Res* 2021, *90* (2), 277–283. https://doi.org/10.1038/s41390-021-01546-y.

(30) Hasan, M. Z.; Yan, J.; Yi, Z.; Korfhage, M. O.; Tong, S.; Zhu, C. Low-Cost Compact Optical Spectroscopy and Novel Spectroscopic Algorithm for Point-of-Care Real-Time Monitoring of Nanoparticle Delivery in Biological Tissue Models. *IEEE Journal of Selected Topics in Quantum Electronics* 2023, *29* (4: Biophotonics), 1–8. https://doi.org/10.1109/JSTQE.2022.3205862.

(31) Chiu, W.-H.; Kong, W.-Y.; Chueh, Y.-H.; Wen, J.-W.; Tsai, C.-M.; Hong, C.; Chen, P.-Y.; Ko, C.-H. Using an Ultra-Compact Optical System to Improve Lateral Flow Immunoassay Results Quantitatively. *Heliyon* 2022, *8* (12). https://doi.org/10.1016/j.heliyon.2022.e12116.

(32) Jopling, J.; Henry, E.; Wiedmeier, S. E.; Christensen, R. D. Reference Ranges for Hematocrit and Blood Hemoglobin Concentration During the Neonatal Period: Data From a Multihospital Health Care System. *Pediatrics* 2009, *123* (2), e333–e337. https://doi.org/10.1542/peds.2008-2654.

(33) Quinn, J. G.; Tansey, E. A.; Johnson, C. D.; Roe, S. M.; Montgomery, L. E. A. Blood: Tests Used to Assess the Physiological and Immunological Properties of Blood. *Advances in Physiology Education* 2016, *40* (2), 165–175. https://doi.org/10.1152/advan.00079.2015.

(34) Scholkmann, F.; Ostojic, D.; Isler, H.; Bassler, D.; Wolf, M.; Karen, T. Reference Ranges for Hemoglobin and Hematocrit Levels in Neonates as a Function of Gestational Age (22–42 Weeks) and Postnatal Age (0–29 Days): Mathematical Modeling. *Children* 2019, *6* (3), 38. https://doi.org/10.3390/children6030038.

(35) Lamola, A. A.; Bhutani, V. K.; Wong, R. J.; Stevenson, D. K.; McDonagh, A. F. The Effect of Hematocrit on the Efficacy of Phototherapy for Neonatal Jaundice. *Pediatr Res* 2013, *74* (1), 54–60. https://doi.org/10.1038/pr.2013.67.

(36) Livshits, L.; Bilu, T.; Peretz, S.; Bogdanova, A.; Gassmann, M.; Eitam, H.; Koren, A.; Levin, C. BACK TO THE "GOLD STANDARD": HOW PRECISE IS HEMATOCRIT DETECTION TODAY? Novel ImageJ-Based Approach for the Precise Hematocrit Measurement. *Mediterr J Hematol Infect Dis* 2022, *14* (1), e2022049–e2022049. https://doi.org/10.4084/MJHID.2022.049.

(37) Gebretsadkan, G.; Ambachew, H. The Comparison between Microhematocrit and Automated Methods for Hematocrit Determination. *International Journal of Blood Research and Disorders* 2015, *2*. https://doi.org/10.23937/2469-5696/1410012.

(38) Mondal, H.; Lotfollahzadeh, S. Hematocrit. In *StatPearls*; StatPearls Publishing: Treasure Island (FL), 2022.

(39) Mashamba-Thompson, T.; Jama, N.; Sartorius, B.; Drain, P.; Thompson, R. Implementation of Point-of-Care Diagnostics in Rural Primary Healthcare Clinics in South Africa: Perspectives of Key Stakeholders. *Diagnostics* 2017, *7* (1), 3. https://doi.org/10.3390/diagnostics7010003.

(40) Olusanya, B. O.; Ogunlesi, T. A.; Slusher, T. M. Why Is Kernicterus Still a Major Cause of Death and Disability in Low-Income and Middle-Income Countries? *Archives of Disease in Childhood* 2014, *99* (12), 1117–1121. https://doi.org/10.1136/archdischild-2013-305506.

(41) Bhutani, V. K.; Zipursky, A.; Blencowe, H.; Khanna, R.; Sgro, M.; Ebbesen, F.; Bell, J.; Mori, R.; Slusher, T. M.; Fahmy, N.; Paul, V. K.; Du, L.; Okolo,

A. A.; de Almeida, M.-F.; Olusanya, B. O.; Kumar, P.; Cousens, S.; Lawn, J. E. Neonatal Hyperbilirubinemia and Rhesus Disease of the Newborn: Incidence and Impairment Estimates for 2010 at Regional and Global Levels. *Pediatr Res* 2013, *74* (1), 86–100. https://doi.org/10.1038/pr.2013.208.

(42) Khadem Broojerdi, A.; Alfonso, C.; Ostad Ali Dehaghi, R.; Refaat, M.; Sillo, H. B. Worldwide Assessment of Low- and Middle-Income Countries' Regulatory Preparedness to Approve Medical Products During Public Health Emergencies. *Front. Med.* 2021, *8*, 722872. https://doi.org/10.3389/fmed.2021.722872.

(43) Morin, S.; Bazarova, N.; Jacon, P.; Vella, S. The Manufacturers' Perspective on World Health Organization Prequalification of In Vitro Diagnostics. *Clinical Infectious Diseases* 2018, *66* (2), 301–305. https://doi.org/10.1093/cid/cix719.

(44) Murray, L. P.; Mace, C. R. Usability as a Guiding Principle for the Design of Paper-Based, Point-of-Care Devices – A Review. *Analytica Chimica Acta* 2020, *1140*, 236–249. https://doi.org/10.1016/j.aca.2020.09.063.

(45) Howard, M. A Market for Diagnostic Devices for Extreme Point-of-Care Testing: Are We ASSURED of an Ethical Outcome? *Developing World Bioethics* 2024, *24* (2), 84–96. https://doi.org/10.1111/dewb.12389.

(46) Leow, A.; Hu, J.; Hird, T. An Overview of WHO Prequalification.

(47) Coyne, P. E. The World Health Organization Prequalification Programme—Playing an Essential Role in Assuring Quality Medical Products. *International Health* 2019, *11* (2), 79–80. https://doi.org/10.1093/inthealth/ihy095.

(48) Bhardwaj, U.; Kohli, V.; Thukral, A. Management of Hyperbilirubinemia in Newborn Infants 35 or More Weeks of Gestation: American Academy of Pediatrics, 2022. *Indian Pediatr* 2023, *60* (1), 63–66. https://doi.org/10.1007/s13312-023-2697-4.

(49) Usman, F.; Diala, U.; Shapiro, S.; Le Pichon, J.-B.; Slusher, T. Acute Bilirubin Encephalopathy and Its Progression to Kernicterus: Current Perspectives. *RRN* 2018, *Volume 8*, 33–44. https://doi.org/10.2147/RRN.S125758.

(50) Slusher, T. M.; Zamora, T. G.; Appiah, D.; Stanke, J. U.; Strand, M. A.; Lee, B. W.; Richardson, S. B.; Keating, E. M.; Siddappa, A. M.; Olusanya, B. O. Burden of Severe Neonatal Jaundice: A Systematic Review and Meta-Analysis. *BMJ Paediatr Open* 2017, *1* (1), e000105. https://doi.org/10.1136/bmjpo-2017-000105.

(51) Wong, R. J.; Stevenson, D. K.; Ahlfors, C. E.; Vreman, H. J. Neonatal Jaundice: Bilirubin Physiology and Clinical Chemistry. *NeoReviews* 2007, *8* (2), e58–e67. https://doi.org/10.1542/neo.8-2-e58.

(52) Fevery, J. Bilirubin in Clinical Practice: A Review: Bilirubin in Clinical Practice. *Liver International* 2008, *28* (5), 592–605. https://doi.org/10.1111/j.1478-3231.2008.01716.x.

(53) Stevenson, D. K.; Vreman, H. J.; Oh, W.; Fanaroff, A. A.; Wright, L. L.; Lemons, J. A.; Verter, J.; Shankaran, S.; Tyson, J. E.; Korones, S. B. Bilirubin Production in Healthy Term Infants as Measured by Carbon Monoxide in Breath. *Clinical Chemistry* 1994, *40* (10), 1934–1939. https://doi.org/10.1093/clinchem/40.10.1934.

(54) Berk, P. D.; Howe, R. B.; Bloomer, J. R.; Berlin, N. I. *Studies of bilirubin kinetics in normal adults.* https://doi.org/10.1172/JCI106184.

(55) Burke, B. L.; Robbins, J. M.; Bird, T. M.; Hobbs, C. A.; Nesmith, C.; Tilford, J. M. Trends in Hospitalizations for Neonatal Jaundice and Kernicterus in the United States, 1988–2005. *Pediatrics* 2009, *123* (2), 524–532. https://doi.org/10.1542/peds.2007-2915.

(56) Clinical Signs That Predict Severe Illness in Children under Age 2 Months: A Multicentre Study. *The Lancet* 2008, *371* (9607), 135–142. https://doi.org/10.1016/S0140-6736(08)60106-3.

(57) Bhutani, V. K.; Stark, A. R.; Lazzeroni, L. C.; Poland, R.; Gourley, G. R.; Kazmierczak, S.; Meloy, L.; Burgos, A. E.; Hall, J. Y.; Stevenson, D. K. Predischarge Screening for Severe Neonatal Hyperbilirubinemia Identifies Infants Who Need Phototherapy. *The Journal of Pediatrics* 2013, *162* (3), 477-482.e1. https://doi.org/10.1016/j.jpeds.2012.08.022.

(58) Global, Regional, and National Age–Sex Specific All-Cause and Cause-Specific Mortality for 240 Causes of Death, 1990–2013: A Systematic Analysis for the Global Burden of Disease Study 2013. *The Lancet* 2015, *385* (9963), 117–171. https://doi.org/10.1016/S0140-6736(14)61682-2.

(59) Olusanya, B. O.; Teeple, S.; Kassebaum, N. J. The Contribution of Neonatal Jaundice to Global Child Mortality: Findings From the GBD 2016 Study. *Pediatrics* 2018, *141* (2), e20171471. https://doi.org/10.1542/peds.2017-1471.

(60) Mitra, S.; Rennie, J. Neonatal Jaundice: Aetiology, Diagnosis and Treatment. *Br J Hosp Med* 2017, *78* (12), 699–704. https://doi.org/10.12968/hmed.2017.78.12.699.

(61) Ogunfowora, O. B.; Daniel, O. J. Neonatal Jaundice and Its Management: Knowledge, Attitude and Practice of Community Health Workers in Nigeria. *BMC Public Health* 2006, *6*, 19. https://doi.org/10.1186/1471-2458-6-19.

(62) Johnson, L.; Bhutani, V. K. Guidelines for Management of the Jaundiced Term and Near-Term Infant. *Clinics in Perinatology* 1998, *25* (3), 555–574. https://doi.org/10.1016/S0095-5108(18)30097-6.

(63) Keahey, P. A.; Simeral, M. L.; Schroder, K. J.; Bond, M. M.; Mtenthaonnga, P. J.; Miros, R. H.; Dube, Q.; Richards-Kortum, R. R. Point-of-Care Device to Diagnose and Monitor Neonatal Jaundice in Low-Resource Settings. *Proceedings of the National Academy of Sciences* 2017, *114* (51), E10965–E10971. https://doi.org/10.1073/pnas.1714020114.

(64) Lain, S. J.; Roberts, C. L.; Bowen, J. R.; Nassar, N. Early Discharge of Infants and Risk of Readmission for Jaundice. *Pediatrics* 2015, *135* (2), 314–321. https://doi.org/10.1542/peds.2014-2388.
(65) Modi, N.; Kirubakaran, C. Reasons for Admission, Causes of Death and Costs of Admission to a Tertiary Referral Neonatal Unit in India. *Journal of Tropical Pediatrics* 1995, *41* (2), 99–102. https://doi.org/10.1093/tropej/41.2.99.
(66) Olusanya, B. O.; Osibanjo, F. B.; Mabogunje, C. A.; Slusher, T. M.; Olowe, S. A. The Burden and Management of Neonatal Jaundice in Nigeria: A Scoping Review of the Literature. *Nigerian Journal of Clinical Practice* 2016, *19* (1), 1–17. https://doi.org/10.4103/1119-3077.173703.
(67) Hay, S. I.; Abajobir, A. A.; Abate, K. H.; Abbafati, C.; Abbas, K. M.; Abd-Allah, F.; Abdulkader, R. S.; Abdulle, A. M.; Abebo, T. A.; Abera, S. F.; Aboyans, V.; Abu-Raddad, L. J.; Ackerman, I. N.; Adedeji, I. A.; Adetokunboh, O.; Afshin, A.; Aggarwal, R.; Agrawal, S.; Agrawal, A.; Ahmed, M. B.; Aichour, M. T. E.; Aichour, A. N.; Aichour, I.; Aiyar, S.; Akinyemiju, T. F.; Akseer, N.; Al Lami, F. H.; Alahdab, F.; Al-Aly, Z.; Alam, K.; Alam, N.; Alam, T.; Alasfoor, D.; Alene, K. A.; Ali, R.; Alizadeh-Navaei, R.; Alkaabi, J. M.; Alkerwi, A.; Alla, F.; Allebeck, P.; Allen, C.; Al-Maskari, F.; AlMazroa, M. A.; Al-Raddadi, R.; Alsharif, U.; Alsowaidi, S.; Althouse, B. M.; Altirkawi, K. A.; Alvis-Guzman, N.; Amare, A. T.; Amini, E.; Ammar, W.; Amoako, Y. A.; Ansha, M. G.; Antonio, C. A. T.; Anwari, P.; Ärnlöv, J.; Arora, M.; Artaman, A.; Aryal, K. K.; Asgedom, S. W.; Atey, T. M.; Atnafu, N. T.; Avila-Burgos, L.; Avokpaho, E. F. G. A.; Awasthi, A.; Awasthi, S.; Azarpazhooh, M. R.; Azzopardi, P.; Babalola, T. K.; Bacha, U.; Badawi, A.; Balakrishnan, K.; Bannick, M. S.; Barac, A.; Barker-Collo, S. L.; Bärnighausen, T.; Barquera, S.; Barrero, L. H.; Basu, S.; Battista, R.; Battle, K. E.; Baune, B. T.; Bazargan-Hejazi, S.; Beardsley, J.; Bedi, N.; Béjot, Y.; Bekele, B. B.; Bell, M. L.; Bennett, D. A.; Bennett, J. R.; Bensenor, I. M.; Benson, J.; Berhane, A.; Berhe, D. F.; Bernabé, E.; Betsu, B. D.; Beuran, M.; Beyene, A. S.; Bhansali, A.; Bhatt, S.; Bhutta, Z. A.; Biadgilign, S.; Bicer, B. K.; Bienhoff, K.; Bikbov, B.; Birungi, C.; Biryukov, S.; Bisanzio, D.; Bizuayehu, H. M.; Blyth, F. M.; Boneya, D. J.; Bose, D.; Bou-Orm, I. R.; Bourne, R. R. A.; Brainin, M.; Brayne, C.; Brazinova, A.; Breitborde, N. J. K.; Briant, P. S.; Britton, G.; Brugha, T. S.; Buchbinder, R.; Bulto, L. N. B.; Bumgarner, B. R.; Butt, Z. A.; Cahuana-Hurtado, L.; Cameron, E.; Campos-Nonato, I. R.; Carabin, H.; Cárdenas, R.; Carpenter, D. O.; Carrero, J. J.; Carter, A.; Carvalho, F.; Casey, D.; Castañeda-Orjuela, C. A.; Castle, C. D.; Catalá-López, F.; Chang, J.-C.; Charlson, F. J.; Chaturvedi, P.; Chen, H.; Chibalabala, M.; Chibueze, C. E.; Chisumpa, V. H.; Chitheer, A. A.; Chowdhury, R.; Christopher, D. J.; Ciobanu, L. G.; Cirillo, M.; Colombara, D.; Cooper, L. T.; Cooper, C.; Cortesi, P. A.; Cortinovis, M.; Criqui, M. H.; Cromwell, E. A.; Cross, M.; Crump, J. A.; Dadi,

A. F.; Dalal, K.; Damasceno, A.; Dandona, L.; Dandona, R.; Das Neves, J.; Davitoiu, D. V.; Davletov, K.; De Courten, B.; De Leo, D.; De Steur, H.; Defo, B. K.; Degenhardt, L.; Deiparine, S.; Dellavalle, R. P.; Deribe, K.; Deribew, A.; Des Jarlais, D. C.; Dey, S.; Dharmaratne, S. D.; Dhillon, P. K.; Dicker, D.; Djalainia, S.; Do, H. P.; Dokova, K.; Doku, D. T.; Dorsey, E. R.; Dos Santos, K. P. B.; Driscoll, T. R.; Dubey, M.; Duncan, B. B.; Ebel, B. E.; Echko, M.; El-Khatib, Z. Z.; Enayati, A.; Endries, A. Y.; Ermakov, S. P.; Erskine, H. E.; Eshetie, S.; Eshrati, B.; Esteghamati, A.; Estep, K.; Fanuel, F. B. B.; Farag, T.; Farinha, C. S. E. S.; Faro, A.; Farzadfar, F.; Fazeli, M. S.; Feigin, V. L.; Feigl, A. B.; Fereshtehnejad, S.-M.; Fernandes, J. C.; Ferrari, A. J.; Feyissa, T. R.; Filip, I.; Fischer, F.; Fitzmaurice, C.; Flaxman, A. D.; Foigt, N.; Foreman, K. J.; Franklin, R. C.; Frostad, J. J.; Fullman, N.; Fürst, T.; Furtado, J. M.; Futran, N. D.; Gakidou, E.; Garcia-Basteiro, A. L.; Gebre, T.; Gebregergs, G. B.; Gebrehiwot, T. T.; Geleijnse, J. M.; Geleto, A.; Gemechu, B. L.; Gesesew, H. A.; Gething, P. W.; Ghajar, A.; Gibney, K. B.; Gillum, R. F.; Ginawi, I. A. M.; Gishu, M. D.; Giussani, G.; Godwin, W. W.; Goel, K.; Goenka, S.; Goldberg, E. M.; Gona, P. N.; Goodridge, A.; Gopalani, S. V.; Gosselin, R. A.; Gotay, C. C.; Goto, A.; Goulart, A. C.; Graetz, N.; Gugnani, H. C.; Gupta, P. C.; Gupta, R.; Gupta, T.; Gupta, V.; Gupta, R.; Gutiérrez, R. A.; Hachinski, V.; Hafezi-Nejad, N.; Hailu, A. D.; Hailu, G. B.; Hamadeh, R. R.; Hamidi, S.; Hammami, M.; Handal, A. J.; Hankey, G. J.; Hao, Y.; Harb, H. L.; Hareri, H. A.; Haro, J. M.; Harun, K. M.; Harvey, J.; Hassanvand, M. S.; Havmoeller, R.; Hay, R. J.; Hedayati, M. T.; Hendrie, D.; Henry, N. J.; Heredia-Pi, I. B.; Heydarpour, P.; Hoek, H. W.; Hoffman, H. J.; Horino, M.; Horita, N.; Hosgood, H. D.; Hostiuc, S.; Hotez, P. J.; Hoy, D. G.; Htet, A. S.; Hu, G.; Huang, J. J.; Huynh, C.; Iburg, K. M.; Igumbor, E. U.; Ikeda, C.; Irvine, C. M. S.; Islam, S. M. S.; Jacobsen, K. H.; Jahanmehr, N.; Jakovljevic, M. B.; James, P.; Jassal, S. K.; Javanbakht, M.; Jayaraman, S. P.; Jeemon, P.; Jensen, P. N.; Jha, V.; Jiang, G.; John, D.; Johnson, C. O.; Johnson, S. C.; Jonas, J. B.; Jürisson, M.; Kabir, Z.; Kadel, R.; Kahsay, A.; Kamal, R.; Kar, C.; Karam, N. E.; Karch, A.; Karema, C. K.; Karimi, S. M.; Karimkhani, C.; Kasaeian, A.; Kassa, G. M.; Kassaw, N. A.; Kassebaum, N. J.; Kastor, A.; Katikireddi, S. V.; Kaul, A.; Kawakami, N.; Keiyoro, P. N.; Kemmer, L.; Kengne, A. P.; Keren, A.; Kesavachandran, C. N.; Khader, Y. S.; Khalil, I. A.; Khan, E. A.; Khang, Y.-H.; Khoja, A. T.; Khosravi, A.; Khubchandani, J.; Kiadaliri, A. A.; Kieling, C.; Kim, Y. J.; Kim, D.; Kimokoti, R. W.; Kinfu, Y.; Kisa, A.; Kissimova-Skarbek, K. A.; Kissoon, N.; Kivimaki, M.; Knudsen, A. K.; Kokubo, Y.; Kolte, D.; Kopec, J. A.; Kosen, S.; Kotsakis, G. A.; Koul, P. A.; Koyanagi, A.; Kravchenko, M.; Krohn, K. J.; Kumar, G. A.; Kumar, P.; Kyu, H. H.; Lager, A. C. J.; Lal, D. K.; Lalloo, R.; Lallukka, T.; Lambert, N.; Lan, Q.; Lansingh, V. C.; Larsson, A.; Leasher, J. L.; Lee, P. H.; Leigh, J.;

Leshargie, C. T.; Leung, J.; Leung, R.; Levi, M.; Li, Y.; Li, Y.; Liang, X.; Liben, M. L.; Lim, S. S.; Linn, S.; Liu, P. Y.; Liu, A.; Liu, S.; Liu, Y.; Lodha, R.; Logroscino, G.; Looker, K. J.; Lopez, A. D.; Lorkowski, S.; Lotufo, P. A.; Lozano, R.; Lucas, T. C. D.; Lunevicius, R.; Lyons, R. A.; Macarayan, E. R. K.; Maddison, E. R.; Magdy Abd El Razek, H. M. A.; Magdy Abd El Razek, M.; Magis-Rodriguez, C.; Mahdavi, M.; Majdan, M.; Majdzadeh, R.; Majeed, A.; Malekzadeh, R.; Malhotra, R.; Malta, D. C.; Mamun, A. A.; Manguerra, H.; Manhertz, T.; Mantovani, L. G.; Mapoma, C. C.; March, L. M.; Marczak, L. B.; Martinez-Raga, J.; Martins, P. H. V.; Martins-Melo, F. R.; Martopullo, I.; März, W.; Mathur, M. R.; Mazidi, M.; McAlinden, C.; McGaughey, M.; McGrath, J. J.; McKee, M.; Mehata, S.; Meier, T.; Meles, K. G.; Memiah, P.; Memish, Z. A.; Mendoza, W.; Mengesha, M. M.; Mengistie, M. A.; Mengistu, D. T.; Mensah, G. A.; Meretoja, T. J.; Meretoja, A.; Mezgebe, H. B.; Micha, R.; Millear, A.; Miller, T. R.; Minnig, S.; Mirarefin, M.; Mirrakhimov, E. M.; Misganaw, A.; Mishra, S. R.; Mitchell, P. B.; Mohammad, K. A.; Mohammadi, A.; Mohammed, M. S. K.; Mohammed, K. E.; Mohammed, S.; Mohan, M. B. V.; Mokdad, A. H.; Mollenkopf, S. K.; Monasta, L.; Montañez Hernandez, J. C.; Montico, M.; Moradi-Lakeh, M.; Moraga, P.; Morawska, L.; Mori, R.; Morrison, S. D.; Moses, M.; Mountjoy-Venning, C.; Mruts, K. B.; Mueller, U. O.; Muller, K.; Murdoch, M. E.; Murthy, G. V. S.; Murthy, S.; Musa, K. I.; Nachega, J. B.; Nagel, G.; Naghavi, M.; Naheed, A.; Naidoo, K. S.; Nangia, V.; Nasher, J. T.; Natarajan, G.; Negasa, D. E.; Negoi, R. I.; Negoi, I.; Newton, C. R.; Ngunjiri, J. W.; Nguyen, C. T.; Nguyen, Q. L.; Nguyen, T. H.; Nguyen, G.; Nguyen, M.; Nichols, E.; Ningrum, D. N. A.; Nong, V. M.; Norheim, O. F.; Norrving, B.; Noubiap, J. J. N.; Nyandwi, A.; Obermeyer, C. M.; O'Donnell, M. J.; Ogbo, F. A.; Oh, I.-H.; Okoro, A.; Oladimeji, O.; Olagunju, A. T.; Olagunju, T. O.; Olsen, H. E.; Olusanya, B. O.; Olusanya, J. O.; Ong, K.; Opio, J. N.; Oren, E.; Ortiz, A.; Osborne, R. H.; Osgood-Zimmerman, A.; Osman, M.; Ota, E.; Owolabi, M. O.; Pa, M.; Pacella, R. E.; Panda, B. K.; Pandian, J. D.; Papachristou, C.; Park, E.-K.; Parry, C. D.; Parsaeian, M.; Patil, S. T.; Patten, S. B.; Patton, G. C.; Paudel, D.; Paulson, K.; Pearce, N.; Pereira, D. M.; Perez, K. M.; Perico, N.; Pesudovs, K.; Peterson, C. B.; Petri, W. A.; Petzold, M.; Phillips, M. R.; Phipps, G.; Pigott, D. M.; Pillay, J. D.; Pinho, C.; Piradov, M. A.; Plass, D.; Pletcher, M. A.; Popova, S.; Poulton, R. G.; Pourmalek, F.; Prabhakaran, D.; Prasad, N.; Purcell, C.; Purwar, M.; Qorbani, M.; Quintanilla, B. P. A.; Rabiee, R. H. S.; Radfar, A.; Rafay, A.; Rahimi, K.; Rahimi-Movaghar, A.; Rahimi-Movaghar, V.; Rahman, M. H. U.; Rahman, M. A.; Rahman, M.; Rai, R. K.; Rajsic, S.; Ram, U.; Ranabhat, C. L.; Rangaswamy, T.; Rankin, Z.; Rao, P. V.; Rao, P. C.; Rawaf, S.; Ray, S. E.; Reiner, R. C.; Reinig, N.; Reitsma, M.; Remuzzi, G.; Renzaho, A. M. N.; Resnikoff, S.; Rezaei, S.; Ribeiro, A. L.; Rivas, J. C.; Roba, H. S.; Robinson, S.

R.; Rojas-Rueda, D.; Rokni, M. B.; Ronfani, L.; Roshandel, G.; Roth, G. A.; Rothenbacher, D.; Roy, A.; Rubagotti, E.; Ruhago, G. M.; Saadat, S.; Safdarian, M.; Safiri, S.; Sagar, R.; Sahathevan, R.; Sahraian, M. A.; Salama, J.; Saleh, M. M.; Salomon, J. A.; Salvi, S. S.; Samy, A. M.; Sanabria, J. R.; Sanchez-Niño, M. D.; Santomauro, D.; Santos, J. V.; Santos, I. S.; Santric Milicevic, M. M.; Sartorius, B.; Satpathy, M.; Sawhney, M.; Saxena, S.; Schelonka, K.; Schmidt, M. I.; Schneider, I. J. C.; Schöttker, B.; Schutte, A. E.; Schwebel, D. C.; Schwendicke, F.; Seedat, S.; Sepanlou, S. G.; Servan-Mori, E. E.; Shaheen, A.; Shaikh, M. A.; Shamsipour, M.; Sharma, R.; Sharma, J.; She, J.; Shi, P.; Shibuya, K.; Shields, C.; Shifa, G. T.; Shiferaw, M. S.; Shigematsu, M.; Shiri, R.; Shirkoohi, R.; Shirude, S.; Shishani, K.; Shoman, H.; Siabani, S.; Sibai, A. M.; Sigfusdottir, I. D.; Silberberg, D. H.; Silva, D. A. S.; Silva, J. P.; Silveira, D. G. A.; Singh, J. A.; Singh, O. P.; Singh, N. P.; Singh, V.; Sinha, D. N.; Skiadaresi, E.; Slepak, E. L.; Smith, D. L.; Smith, M.; Sobaih, B. H. A.; Sobngwi, E.; Soljak, M.; Sorensen, R. J. D.; Sousa, T. C. M.; Sposato, L. A.; Sreeramareddy, C. T.; Srinivasan, V.; Stanaway, J. D.; Stathopoulou, V.; Steel, N.; Stein, D. J.; Steiner, C.; Steinke, S.; Stokes, M. A.; Stovner, L. J.; Strub, B.; Subart, M.; Sufiyan, M. B.; Sunguya, B. F.; Sur, P. J.; Swaminathan, S.; Sykes, B. L.; Sylte, D.; Szoeke, C. E. I.; Tabarés-Seisdedos, R.; Tadakamadla, S. K.; Taffere, G. R.; Takala, J. S.; Tandon, N.; Tanne, D.; Tarekegn, Y. L.; Tavakkoli, M.; Taveira, N.; Taylor, H. R.; Tegegne, T. K.; Tehrani-Banihashemi, A.; Tekelab, T.; Terkawi, A. S.; Tesfaye, D. J.; Tesssema, B.; Thakur, J.; Thamsuwan, O.; Theadom, A. M.; Theis, A. M.; Thomas, K. E.; Thomas, N.; Thompson, R.; Thrift, A. G.; Tobe-Gai, R.; Tobollik, M.; Tonelli, M.; Topor-Madry, R.; Tortajada, M.; Touvier, M.; Traebert, J.; Tran, B. X.; Troeger, C.; Truelsen, T.; Tsoi, D.; Tuzcu, E. M.; Tymeson, H.; Tyrovolas, S.; Ukwaja, K. N.; Undurraga, E. A.; Uneke, C. J.; Updike, R.; Uthman, O. A.; Uzochukwu, B. S. C.; Van Boven, J. F. M.; Varughese, S.; Vasankari, T.; Veerman, L. J.; Venkatesh, S.; Venketasubramanian, N.; Vidavalur, R.; Vijayakumar, L.; Violante, F. S.; Vishnu, A.; Vladimirov, S. K.; Vlassov, V. V.; Vollset, S. E.; Vos, T.; Wadilo, F.; Wakayo, T.; Wallin, M. T.; Wang, Y.-P.; Weichenthal, S.; Weiderpass, E.; Weintraub, R. G.; Weiss, D. J.; Werdecker, A.; Westerman, R.; Whiteford, H. A.; Wijeratne, T.; Williams, H. C.; Wiysonge, C. S.; Woldeyes, B. G.; Wolfe, C. D. A.; Woodbrook, R.; Woolf, A. D.; Workicho, A.; Xavier, D.; Xu, G.; Yadgir, S.; Yaghoubi, M.; Yakob, B.; Yan, L. L.; Yano, Y.; Ye, P.; Yihdego, M. G.; Yimam, H. H.; Yip, P.; Yonemoto, N.; Yoon, S.-J.; Yotebieng, M.; Younis, M. Z.; Yu, C.; Zaidi, Z.; Zaki, M. E. S.; Zegeye, E. A.; Zenebe, Z. M.; Zhang, X.; Zheng, Y.; Zhou, M.; Zipkin, B.; Zodpey, S.; Zoeckler, L.; Zuhlke, L. J.; Murray, C. J. L. Global, Regional, and National Disability-Adjusted Life-Years (DALYs) for 333 Diseases and Injuries and Healthy Life Expectancy

(HALE) for 195 Countries and Territories, 1990–2016: A Systematic Analysis for the Global Burden of Disease Study 2016. *The Lancet* 2017, *390* (10100), 1260–1344. https://doi.org/10.1016/S0140-6736(17)32130-X.

(68) Escobar, G.; Greene, J.; Hulac, P.; Kincannon, E.; Bischoff, K.; Gardner, M.; Armstrong, M.; France, E. Rehospitalisation after Birth Hospitalisation: Patterns among Infants of All Gestations. *Arch Dis Child* 2005, *90* (2), 125–131. https://doi.org/10.1136/adc.2003.039974.

(69) Battersby, C.; Michaelides, S.; Upton, M.; Rennie, J. M. Term Admissions to Neonatal Units in England: A Role for Transitional Care? A Retrospective Cohort Study. *BMJ Open* 2017, *7* (5), e016050. https://doi.org/10.1136/bmjopen-2017-016050.

(70) Bhutani, V. K.; Johnson, L. H.; Keren, R. Diagnosis and Management of Hyperbilirubinemia in the Term Neonate: For a Safer First Week. *Pediatric Clinics of North America* 2004, *51* (4), 843–861. https://doi.org/10.1016/j.pcl.2004.03.011.

(71) Bhutani, V. K.; Johnson, L. H. Newborn Jaundice and Kernicterus--Health and Societal Perspectives. *Indian J Pediatr* 2003, *70* (5), 407–416. https://doi.org/10.1007/BF02723615.

(72) Kirk, J. M. Neonatal Jaundice: A Critical Review of the Role and Practice of Bilirubin Analysis. *Ann Clin Biochem* 2008, *45* (5), 452–462. https://doi.org/10.1258/acb.2008.008076.

(73) Muchowski, K. E. Evaluation and Treatment of Neonatal Hyperbilirubinemia. *American Family Physician* 2014, *89* (11), 873–878.

(74) Shapiro, S.; Le Pichon, J. B.; Riordan, S. M.; Watchkoe, J. The Neurological Sequelae of Neonatal Hyperbilirubinemia: Definitions, Diagnosis and Treatment of the Kernicterus Spectrum Disorders (KSDs). *CPR* 2017, *13*. https://doi.org/10.2174/1573396313666170815100214.

(75) Mir, S. E.; van der Geest, B. A. M.; Been, J. V. Management of Neonatal Jaundice in Low- and Lower-Middle-Income Countries. *BMJ Paediatr Open* 2019, *3* (1), e000408. https://doi.org/10.1136/bmjpo-2018-000408.

(76) Jansen, P. L. M.; Cuypers, H. T.; Peters, W. H. M. Quantitation of Bilirubin Conjugates with High-Performance Liquid Chromatography in Patients with Low Total Serum Bilirubin Levels. *European Journal of Clinical Investigation* 1984, *14* (4), 295–300. https://doi.org/10.1111/j.1365-2362.1984.tb01184.x.

(77) Ngashangva, L.; Bachu, V.; Goswami, P. Development of New Methods for Determination of Bilirubin. *Journal of Pharmaceutical and Biomedical Analysis* 2019, *162*, 272–285. https://doi.org/10.1016/j.jpba.2018.09.034.

(78) Blanckaert, N.; Kabra, P. M.; Farina, F. A.; Stafford, B. E.; Marton, L. J.; Schmid, R. Measurement of Bilirubin and Its Monoconjugates and Diconjugates in Human Serum by Alkaline Methanolysis and High-Performance Liquid Chromatography. *The Journal of Laboratory and Clinical*

Medicine 1980, *96* (2), 198–212. https://doi.org/10.5555/uri:pii:0022214380900232.
(79) Horváth, C. *High-Performance Liquid Chromatography: Advances and Perspectives*; Elsevier, 2013.
(80) Lough, W. J.; Wainer, I. W. *High Performance Liquid Chromatography: Fundamental Principles and Practice*; CRC Press, 1995.
(81) Osawa, S.; Sugo, S.; Yoshida, T.; Yamaoka, T.; Nomura, F. An Assay for Separating and Quantifying Four Bilirubin Fractions in Untreated Human Serum Using Isocratic High-Performance Liquid Chromatography. *Clinica Chimica Acta* 2006, *366* (1), 146–155. https://doi.org/10.1016/j.cca.2005.09.031.
(82) With, T. K. The Direct Diazo Reaction (Hijmans van Den Bergh) and Its Clinical Significance Investigated by Quantitative Measurements. *Acta Medica Scandinavica* 1944, *119* (3), 201–213. https://doi.org/10.1111/j.0954-6820.1944.tb05398.x.
(83) Malloy, H. T.; Evelyn, K. A. THE DETERMINATION OF BILIRUBIN WITH THE PHOTOELECTRIC COLORIMETER. *Journal of Biological Chemistry* 1937, *119* (2), 481–490. https://doi.org/10.1016/S0021-9258(18)74392-5.
(84) Garber, C. C. Jendrassik--Grof Analysis for Total and Direct Bilirubin in Serum with a Centrifugal Analyzer. *Clinical Chemistry* 1981, *27* (8), 1410–1416. https://doi.org/10.1093/clinchem/27.8.1410.
(85) Shull, B. C.; Lees, H.; Li, P. K. Mechanism of Interference by Hemoglobin in the Determination of Total Bilirubin. I. Method of Malloy-Evelyn. *Clinical Chemistry* 1980, *26* (1), 22–25. https://doi.org/10.1093/clinchem/26.1.22.
(86) Shull, B. C.; Lees, H.; Li, P. K. Mechanism of Interference by Hemoglobin in the Determination of Total Bilirubin. II. Method of Jendrassik-Grof. *Clinical Chemistry* 1980, *26* (1), 26–29. https://doi.org/10.1093/clinchem/26.1.26.
(87) Glick, M. R.; Ryder, K. W. Analytical Systems Ranked by Freedom from Interferences. *Clinical Chemistry* 1987, *33* (8), 1453–1458. https://doi.org/10.1093/clinchem/33.8.1453.
(88) Kaumeyer, B. A.; Tjota, M. Y.; Parker, K.; Chan, C. W.; Gant Kanegusuku, A.; Baldwin, A. D.; Yeo, K.-T. J. Use of a Vanadate Oxidation Conjugated Bilirubin Assay to Reduce Test Cancellations Resulting from Hemolyzed Specimens in Pediatric Patients. *American Journal of Clinical Pathology* 2023, *159* (1), 6–9. https://doi.org/10.1093/ajcp/aqac139.
(89) Dhungana, N.; Morris, C.; Krasowski, M. D. Operational Impact of Using a Vanadate Oxidase Method for Direct Bilirubin Measurements at an Academic Medical Center Clinical Laboratory. *Practical Laboratory Medicine* 2017, *8*, 77–85. https://doi.org/10.1016/j.plabm.2017.05.004.
(90) Hertz, H.; Dybkær, R.; Lauritzen, M. Direct Spectrometric Determination of the Concentration of Bilirubins in Serum. *Scandinavian Journal of Clinical and*

Laboratory Investigation 1974, *33* (3), 215–230. https://doi.org/10.1080/00365517409082490.

(91) Kudavelly, S.; Keswarpu, P.; Balakrishnan, S. A Simple and Accurate Method for Estimating Bilirubin from Blood. In *2011 IEEE International Instrumentation and Measurement Technology Conference*; 2011; pp 1–4. https://doi.org/10.1109/IMTC.2011.5944035.

(92) Jackson, S. H. A Direct-Reading Bilirubinometer Incorporating Hemolysis and Turbidity Correction. *Clinical Chemistry* 1965, *11* (12), 1051–1057. https://doi.org/10.1093/clinchem/11.12.1051.

(93) Lo, S. F.; Jendrzejczak, B.; Doumas, B. T. Laboratory Performance in Neonatal Bilirubin Testing Using Commutable Specimens: A Progress Report on a College of American Pathologists Study. *Archives of Pathology & Laboratory Medicine* 2008, *132* (11), 1781–1785. https://doi.org/10.5858/132.11.1781.

(94) Kazmierczak, S. C.; Robertson, A. F.; Catrou, P. G.; Briley, K. P.; Kreamer, B. L.; Gourley, G. R. Direct Spectrophotometric Method for Measurement of Bilirubin in Newborns: Comparison with HPLC and an Automated Diazo Method. *Clinical Chemistry* 2002, *48* (7), 1096–1097. https://doi.org/10.1093/clinchem/48.7.1096.

(95) Jackson, S. H.; Hernandez, A. H. A New "Bilirubinometer" and Its Use in Estimating Total and Conjugated Bilirubin Serum. *Clinical Chemistry* 1970, *16* (6), 462–465. https://doi.org/10.1093/clinchem/16.6.462.

(96) Peake, M.; Mazzachi, B.; Fudge, A.; Bais, R. Bilirubin Measured on a Blood Gas Analyser: A Suitable Alternative for Near-Patient Assessment of Neonatal Jaundice? *Ann Clin Biochem* 2001, *38* (5), 533–540. https://doi.org/10.1177/000456320103800511.

(97) Laterza, O. F.; Smith, C. H.; Wilhite, T. R.; Landt, M. Accurate Direct Spectrophotometric Bilirubin Measurement Combined with Blood Gas Analysis. *Clinica Chimica Acta* 2002, *323* (1–2), 115–120. https://doi.org/10.1016/S0009-8981(02)00178-X.

(98) St John, A.; Price, C. P. Existing and Emerging Technologies for Point-of-Care Testing. *Clin Biochem Rev* 2014, *35* (3), 155–167.

(99) Huang, Y.; Dean, R.; Dubbelman, Y.; Vincent, A.; Khurshid, F. Neonatal Hemoglobin Affects the Accuracy of Whole Blood Bilirubin Measurement on GEM Premier 4000 Blood Gas Analyzers. *Practical Laboratory Medicine* 2021, *25*, e00231. https://doi.org/10.1016/j.plabm.2021.e00231.

(100) Kuang, Z.; Zong, X.; Xing, S.; Zhao, F.; Guo, S.; Li, H.; Wei, D. Analytical Performance Validation and Clinical Application of Blood Gas Analyzer on the Detection of Neonatal Bilirubin. *Transl Pediatr* 2021, *10* (12), 3175–3183. https://doi.org/10.21037/tp-21-541.

(101) Mukerji, S.; Popat, H.; Chung, J. Z. Accuracy of Bilirubin on the Siemens RAPIDPoint 500 Blood Gas Analyser: A Data Mining Study. *Journal of*

Paediatrics and Child Health 2022, *58* (6), 1013–1015. https://doi.org/10.1111/jpc.15890.

(102) Wang, L.; Albert, A. Y. K.; Jung, B.; Hadad, K.; Lyon, M. E.; Basso, M. Limitations and Opportunities of Whole Blood Bilirubin Measurements by GEM Premier 4000®. *BMC Pediatr* 2017, *17* (1), 92. https://doi.org/10.1186/s12887-017-0842-8.

(103) Thomas, N.; McNeil, A.; Collins, C. L. Blood Gas Bilirubin Measurements in Neonates Must Be Adjusted for HbF to Avoid Misleading Results. *Archives of Disease in Childhood - Fetal and Neonatal Edition* 2022, *107* (3), 341–342. https://doi.org/10.1136/archdischild-2021-322071.

(104) Matias, F. A. A.; Vila, M. M. D. C.; Tubino, M. A Simple Device for Quantitative Colorimetric Diffuse Reflectance Measurements. *Sensors and Actuators B: Chemical* 2003, *88* (1), 60–66. https://doi.org/10.1016/S0925-4005(02)00309-X.

(105) Morbioli, G. G.; Mazzu-Nascimento, T.; Stockton, A. M.; Carrilho, E. Technical Aspects and Challenges of Colorimetric Detection with Microfluidic Paper-Based Analytical Devices (μPADs) - A Review. *Analytica Chimica Acta* 2017, *970*, 1–22. https://doi.org/10.1016/j.aca.2017.03.037.

(106) Mirabella, F. M. *Modern Techniques in Applied Molecular Spectroscopy*; Techniques in analytical chemistry series; Wiley: New York, 1998.

(107) Doumas, B. T.; Wu, T. W. The Measurement of Bilirubin Fractions in Serum. *Crit Rev Clin Lab Sci* 1991, *28* (5–6), 415–445. https://doi.org/10.3109/10408369109106872.

(108) McEwen, M.; Reynolds, K. NONINVASIVE DETECTION OF BILIRUBIN USING PULSATILE ABSORPTION.

(109) Zucchini, L.; Ajčević, M.; Accardo, A. A Novel Algorithm for the Compensation of Hemoglobin Interference on Bilirubin Measurement Applied to a Two-Wavelengths Reflectance Photometer. In *19th Nordic-Baltic Conference on Biomedical Engineering and Medical Physics*; Dekhtyar, Y., Saknite, I., Eds.; IFMBE Proceedings; Springer Nature Switzerland: Cham, 2023; pp 18–24. https://doi.org/10.1007/978-3-031-37132-5_3.

(110) Bhutani, V. K.; Johnson, L.; Sivieri, E. M. Predictive Ability of a Predischarge Hour-Specific Serum Bilirubin for Subsequent Significant Hyperbilirubinemia in Healthy Term and Near-Term Newborns. *Pediatrics* 1999, *103* (1), 6–14. https://doi.org/10.1542/peds.103.1.6.

(111) Erdeve, O. Management of Neonatal Jaundice in Low-Income and Middle-Income Countries. *BMJ Paediatr Open* 2020, *4* (1), e000845. https://doi.org/10.1136/bmjpo-2020-000845.

(112) Rolinski, B.; Okorodudu, A. O.; Kost, G.; Roser, M.; Wu, J.; Goerlach-Graw, A.; Kuester, H. Evaluation of Total Bilirubin Determination in Neonatal Whole-Blood Samples by Multiwavelength Photometry on the Roche OMNI S

Point-of-Care Analyzer. *Point of Care* 2005, *4* (1), 3. https://doi.org/10.1097/01.poc.0000157097.59514.62.

(113) Hallemann, H.; Putz, K.; Schweiger, G.; Spitzer, S.; Strohmeier, M. Technical Aspects of Bilirubin Determination in Whole Blood: *Point of Care: The Journal of Near-Patient Testing & Technology* 2005, *4* (1), 9–10. https://doi.org/10.1097/01.poc.0000157101.51422.72.

(114) Inamori, G.; Kamoto, U.; Nakamura, F.; Isoda, Y.; Uozumi, A.; Matsuda, R.; Shimamura, M.; Okubo, Y.; Ito, S.; Ota, H. Neonatal Wearable Device for Colorimetry-Based Real-Time Detection of Jaundice with Simultaneous Sensing of Vitals. *Sci. Adv.* 2021, *7* (10), eabe3793. https://doi.org/10.1126/sciadv.abe3793.

(115) Zucchini, L.; Zabetta, C. D. C.; Ajčević, M.; Accardo, A. Optimization of an Algorithm for Hemoglobin Interference Compensation on a Simple Photometer for Bilirubin Measurement. In *2024 IEEE International Symposium on Medical Measurements and Applications (MeMeA)*; 2024; pp 1–6. https://doi.org/10.1109/MeMeA60663.2024.10596818.

(116) ULLAH, S.; RAHMAN, K.; HEDAYATI, M. Hyperbilirubinemia in Neonates: Types, Causes, Clinical Examinations, Preventive Measures and Treatments: A Narrative Review Article. *Iran J Public Health* 2016, *45* (5), 558–568.

(117) Zabetta, C. D. C.; Iskander, I. F.; Greco, C.; Bellarosa, C.; Demarini, S.; Tiribelli, C.; Wennberg, R. P. Bilistick: A Low-Cost Point-of-Care System to Measure Total Plasma Bilirubin. *NEO* 2013, *103* (3), 177–181. https://doi.org/10.1159/000345425.

(118) Shapiro, A.; Anderson, J.; Mtenthaonga, P.; Kumwenda, W.; Bond, M.; Schwarz, R.; Carns, J.; Johnston, R.; Dube, Q.; Chiume, M.; Richards-Kortum, R. Evaluation of a Point-of-Care Test for Bilirubin in Malawi. *Pediatrics* 2022, *150* (2), e2021053928. https://doi.org/10.1542/peds.2021-053928.

(119) Shapiro, A.; Mtenthaonga, P.; Mjumira, R.; Reuben, M.; Samuel, A.; Bond, M.; Carns, J.; Schwarz, R.; Johnston, R.; Mangwiro, L.; Odedere, O.; Miros, R.; McHugh, S.; Kawaza, K.; Dube, Q.; Ezeaka, C.; Richards-Kortum, R. Design and Field Evaluation of a Lateral Flow Cassette Device for Point-of-Care Bilirubin Measurement. *PLOS Global Public Health* 2023, *3* (8), e0002262. https://doi.org/10.1371/journal.pgph.0002262.

(120) Kazmierczak, S. C. Interferences of Hemolysis, Lipemia and High Bilirubin on Laboratory Tests. In *Accurate Results in the Clinical Laboratory*; Elsevier, 2019; pp 57–67. https://doi.org/10.1016/B978-0-12-813776-5.00005-4.

(121) Meites, S.; Lin, S. S.; Thompson, C. Studies on the Quality of Specimens Obtained by Skin Puncture of Children 1. Tendency to Hemolysis, and Hemoglobin and Tissue Fluid as Contaminants. *Clin Chem* 1981, *27* (6), 875–878.

(122) Algeciras-Schimnich, A.; Cook, W. J.; Milz, T. C.; Saenger, A. K.; Karon, B. S. Evaluation of Hemoglobin Interference in Capillary Heel-Stick Samples Collected for Determination of Neonatal Bilirubin. *Clinical Biochemistry* 2007, *40* (16–17), 1311–1316. https://doi.org/10.1016/j.clinbiochem.2007.08.003.
(123) Tian, G.; Wu, Y.; Jin, X.; Zeng, Z.; Gu, X.; Li, T.; Chen, X.; Li, G.; Liu, J. The Incidence Rate and Influence Factors of Hemolysis, Lipemia, Icterus in Fasting Serum Biochemistry Specimens. *PLoS One* 2022, *17* (1), e0262748. https://doi.org/10.1371/journal.pone.0262748.
(124) Westwood, A. The Analysis of Bilirubin in Serum. *Ann Clin Biochem* 1991, *28* (2), 119–130. https://doi.org/10.1177/000456329102800202.
(125) Zucchini, L.; Coda Zabetta, C. D.; Ajčević, M.; Accardo, A. A Method for Compensating Hemoglobin Interference in Total Serum Bilirubin Measurement Using a Simple Two-Wavelength Reflectance Photometer. *Sensors* 2024, *24* (20), 6749. https://doi.org/10.3390/s24206749.
(126) Naghavi, M.; Abajobir, A. A.; Abbafati, C.; Abbas, K. M.; Abd-Allah, F.; Abera, S. F.; Aboyans, V.; Adetokunboh, O.; Afshin, A.; Agrawal, A.; Ahmadi, A.; Ahmed, M. B.; Aichour, A. N.; Aichour, M. T. E.; Aichour, I.; Aiyar, S.; Alahdab, F.; Al-Aly, Z.; Alam, K.; Alam, N.; Alam, T.; Alene, K. A.; Al-Eyadhy, A.; Ali, S. D.; Alizadeh-Navaei, R.; Alkaabi, J. M.; Alkerwi, A.; Alla, F.; Allebeck, P.; Allen, C.; Al-Raddadi, R.; Alsharif, U.; Altirkawi, K. A.; Alvis-Guzman, N.; Amare, A. T.; Amini, E.; Ammar, W.; Amoako, Y. A.; Anber, N.; Andersen, H. H.; Andrei, C. L.; Androudi, S.; Ansari, H.; Antonio, C. A. T.; Anwari, P.; Ärnlöv, J.; Arora, M.; Artaman, A.; Aryal, K. K.; Asayesh, H.; Asgedom, S. W.; Atey, T. M.; Avila-Burgos, L.; Avokpaho, E. F. G.; Awasthi, A.; Babalola, T. K.; Bacha, U.; Balakrishnan, K.; Barac, A.; Barboza, M. A.; Barker-Collo, S. L.; Barquera, S.; Barregard, L.; Barrero, L. H.; Baune, B. T.; Bedi, N.; Beghi, E.; Béjot, Y.; Bekele, B. B.; Bell, M. L.; Bennett, J. R.; Bensenor, I. M.; Berhane, A.; Bernabé, E.; Betsu, B. D.; Beuran, M.; Bhatt, S.; Biadgilign, S.; Bienhoff, K.; Bikbov, B.; Bisanzio, D.; Bourne, R. R. A.; Breitborde, N. J. K.; Bulto, L. N. B.; Bumgarner, B. R.; Butt, Z. A.; Cahuana-Hurtado, L.; Cameron, E.; Campuzano, J. C.; Car, J.; Cárdenas, R.; Carrero, J. J.; Carter, A.; Casey, D. C.; Castañeda-Orjuela, C. A.; Catalá-López, F.; Charlson, F. J.; Chibueze, C. E.; Chimed-Ochir, O.; Chisumpa, V. H.; Chitheer, A. A.; Christopher, D. J.; Ciobanu, L. G.; Cirillo, M.; Cohen, A. J.; Colombara, D.; Cooper, C.; Cowie, B. C.; Criqui, M. H.; Dandona, L.; Dandona, R.; Dargan, P. I.; Neves, J. das; Davitoiu, D. V.; Davletov, K.; Courten, B. de; Defo, B. K.; Degenhardt, L.; Deiparine, S.; Deribe, K.; Deribew, A.; Dey, S.; Dicker, D.; Ding, E. L.; Djalalinia, S.; Do, H. P.; Doku, D. T.; Douwes-Schultz, D.; Driscoll, T. R.; Dubey, M.; Duncan, B. B.; Echko, M.; El-Khatib, Z. Z.; Ellingsen, C. L.; Enayati, A.; Ermakov, S. P.; Erskine, H. E.; Eskandarieh, S.; Esteghamati, A.; Estep, K.; Farinha, C. S. e S.; Faro, A.; Farzadfar, F.; Feigin,

V. L.; Fereshtehnejad, S.-M.; Fernandes, J. C.; Ferrari, A. J.; Feyissa, T. R.; Filip, I.; Finegold, S.; Fischer, F.; Fitzmaurice, C.; Flaxman, A. D.; Foigt, N.; Frank, T.; Fraser, M.; Fullman, N.; Fürst, T.; Furtado, J. M.; Gakidou, E.; Garcia-Basteiro, A. L.; Gebre, T.; Gebregergs, G. B.; Gebrehiwot, T. T.; Gebremichael, D. Y.; Geleijnse, J. M.; Genova-Maleras, R.; Gesesew, H. A.; Gething, P. W.; Gillum, R. F.; Giref, A. Z.; Giroud, M.; Giussani, G.; Godwin, W. W.; Gold, A. L.; Goldberg, E. M.; Gona, P. N.; Gopalani, S. V.; Gouda, H. N.; Goulart, A. C.; Griswold, M.; Gupta, R.; Gupta, T.; Gupta, V.; Gupta, P. C.; Haagsma, J. A.; Hafezi-Nejad, N.; Hailu, A. D.; Hailu, G. B.; Hamadeh, R. R.; Hambisa, M. T.; Hamidi, S.; Hammami, M.; Hancock, J.; Handal, A. J.; Hankey, G. J.; Hao, Y.; Harb, H. L.; Hareri, H. A.; Hassanvand, M. S.; Havmoeller, R.; Hay, S. I.; He, F.; Hedayati, M. T.; Henry, N. J.; Heredia-Pi, I. B.; Herteliu, C.; Hoek, H. W.; Horino, M.; Horita, N.; Hosgood, H. D.; Hostiuc, S.; Hotez, P. J.; Hoy, D. G.; Huynh, C.; Iburg, K. M.; Ikeda, C.; Ileanu, B. V.; Irenso, A. A.; Irvine, C. M. S.; Islam, S. M. S.; Jacobsen, K. H.; Jahanmehr, N.; Jakovljevic, M. B.; Javanbakht, M.; Jayaraman, S. P.; Jeemon, P.; Jha, V.; John, D.; Johnson, C. O.; Johnson, S. C.; Jonas, J. B.; Jürisson, M.; Kabir, Z.; Kadel, R.; Kahsay, A.; Kamal, R.; Karch, A.; Karimi, S. M.; Karimkhani, C.; Kasaeian, A.; Kassaw, N. A.; Kassebaum, N. J.; Katikireddi, S. V.; Kawakami, N.; Keiyoro, P. N.; Kemmer, L.; Kesavachandran, C. N.; Khader, Y. S.; Khan, E. A.; Khang, Y.-H.; Khoja, A. T. A.; Khosravi, M. H.; Khosravi, A.; Khubchandani, J.; Kiadaliri, A. A.; Kieling, C.; Kievlan, D.; Kim, Y. J.; Kim, D.; Kimokoti, R. W.; Kinfu, Y.; Kissoon, N.; Kivimaki, M.; Knudsen, A. K.; Kopec, J. A.; Kosen, S.; Koul, P. A.; Koyanagi, A.; Kulikoff, X. R.; Kumar, G. A.; Kumar, P.; Kutz, M.; Kyu, H. H.; Lal, D. K.; Lalloo, R.; Lambert, T. L. N.; Lan, Q.; Lansingh, V. C.; Larsson, A.; Lee, P. H.; Leigh, J.; Leung, J.; Levi, M.; Li, Y.; Kappe, D. L.; Liang, X.; Liben, M. L.; Lim, S. S.; Liu, P. Y.; Liu, A.; Liu, Y.; Lodha, R.; Logroscino, G.; Lorkowski, S.; Lotufo, P. A.; Lozano, R.; Lucas, T. C. D.; Ma, S.; Macarayan, E. R. K.; Maddison, E. R.; Razek, M. M. A. E.; Majdan, M.; Majdzadeh, R.; Majeed, A.; Malekzadeh, R.; Malhotra, R.; Malta, D. C.; Manguerra, H.; Manyazewal, T.; Mapoma, C. C.; Marczak, L. B.; Markos, D.; Martinez-Raga, J.; Martins-Melo, F. R.; Martopullo, I.; McAlinden, C.; McGaughey, M.; McGrath, J. J.; Mehata, S.; Meier, T.; Meles, K. G.; Memiah, P.; Memish, Z. A.; Mengesha, M. M.; Mengistu, D. T.; Menota, B. G.; Mensah, G. A.; Meretoja, T. J.; Meretoja, A.; Millear, A.; Miller, T. R.; Minnig, S.; Mirarefin, M.; Mirrakhimov, E. M.; Misganaw, A.; Mishra, S. R.; Mohamed, I. A.; Mohammad, K. A.; Mohammadi, A.; Mohammed, S.; Mokdad, A. H.; Mola, G. L. D.; Mollenkopf, S. K.; Molokhia, M.; Monasta, L.; Montañez, J. C.; Montico, M.; Mooney, M. D.; Moradi-Lakeh, M.; Moraga, P.; Morawska, L.; Morozoff, C.; Morrison, S. D.; Mountjoy-Venning, C.; Mruts, K. B.; Muller, K.; Murthy, G. V. S.; Musa, K.

I.; Nachega, J. B.; Naheed, A.; Naldi, L.; Nangia, V.; Nascimento, B. R.; Nasher, J. T.; Natarajan, G.; Negoi, I.; Ngunjiri, J. W.; Nguyen, C. T.; Nguyen, Q. L.; Nguyen, T. H.; Nguyen, G.; Nguyen, M.; Nichols, E.; Ningrum, D. N. A.; Nong, V. M.; Noubiap, J. J. N.; Ogbo, F. A.; Oh, I.-H.; Okoro, A.; Olagunju, A. T.; Olsen, H. E.; Olusanya, B. O.; Olusanya, J. O.; Ong, K.; Opio, J. N.; Oren, E.; Ortiz, A.; Osman, M.; Ota, E.; Pa, M.; Pacella, R. E.; Pakhale, S.; Pana, A.; Panda, B. K.; Panda-Jonas, S.; Papachristou, C.; Park, E.-K.; Patten, S. B.; Patton, G. C.; Paudel, D.; Paulson, K.; Pereira, D. M.; Perez-Ruiz, F.; Perico, N.; Pervaiz, A.; Petzold, M.; Phillips, M. R.; Pigott, D. M.; Pinho, C.; Plass, D.; Pletcher, M. A.; Polinder, S.; Postma, M. J.; Pourmalek, F.; Purcell, C.; Qorbani, M.; Quintanilla, B. P. A.; Radfar, A.; Rafay, A.; Rahimi-Movaghar, V.; Rahman, M. H. U.; Rahman, M.; Rai, R. K.; Ranabhat, C. L.; Rankin, Z.; Rao, P. C.; Rath, G. K.; Rawaf, S.; Ray, S. E.; Rehm, J.; Reiner, R. C.; Reitsma, M. B.; Remuzzi, G.; Rezaei, S.; Rezai, M. S.; Rokni, M. B.; Ronfani, L.; Roshandel, G.; Roth, G. A.; Rothenbacher, D.; Ruhago, G. M.; Sa, R.; Saadat, S.; Sachdev, P. S.; Sadat, N.; Safdarian, M.; Safi, S.; Safiri, S.; Sagar, R.; Sahathevan, R.; Salama, J.; Salamati, P.; Salomon, J. A.; Samy, A. M.; Sanabria, J. R.; Sanchez-Niño, M. D.; Santomauro, D.; Santos, I. S.; Milicevic, M. M. S.; Sartorius, B.; Satpathy, M.; Schmidt, M. I.; Schneider, I. J. C.; Schulhofer-Wohl, S.; Schutte, A. E.; Schwebel, D. C.; Schwendicke, F.; Sepanlou, S. G.; Servan-Mori, E. E.; Shackelford, K. A.; Shahraz, S.; Shaikh, M. A.; Shamsipour, M.; Shamsizadeh, M.; Sharma, J.; Sharma, R.; She, J.; Sheikhbahaei, S.; Shey, M.; Shi, P.; Shields, C.; Shigematsu, M.; Shiri, R.; Shirude, S.; Shiue, I.; Shoman, H.; Shrime, M. G.; Sigfusdottir, I. D.; Silpakit, N.; Silva, J. P.; Singh, J. A.; Singh, A.; Skiadaresi, E.; Sligar, A.; Smith, D. L.; Smith, A.; Smith, M.; Sobaih, B. H. A.; Soneji, S.; Sorensen, R. J. D.; Soriano, J. B.; Sreeramareddy, C. T.; Srinivasan, V.; Stanaway, J. D.; Stathopoulou, V.; Steel, N.; Stein, D. J.; Steiner, C.; Steinke, S.; Stokes, M. A.; Strong, M.; Strub, B.; Subart, M.; Sufiyan, M. B.; Sunguya, B. F.; Sur, P. J.; Swaminathan, S.; Sykes, B. L.; Tabarés-Seisdedos, R.; Tadakamadla, S. K.; Takahashi, K.; Takala, J. S.; Talongwa, R. T.; Tarawneh, M. R.; Tavakkoli, M.; Taveira, N.; Tegegne, T. K.; Tehrani-Banihashemi, A.; Temsah, M.-H.; Terkawi, A. S.; Thakur, J. S.; Thamsuwan, O.; Thankappan, K. R.; Thomas, K. E.; Thompson, A. H.; Thomson, A. J.; Thrift, A. G.; Tobe-Gai, R.; Topor-Madry, R.; Torre, A.; Tortajada, M.; Towbin, J. A.; Tran, B. X.; Troeger, C.; Truelsen, T.; Tsoi, D.; Tuzcu, E. M.; Tyrovolas, S.; Ukwaja, K. N.; Undurraga, E. A.; Updike, R.; Uthman, O. A.; Uzochukwu, B. S. C.; Boven, J. F. M. van; Vasankari, T.; Venketasubramanian, N.; Violante, F. S.; Vlassov, V. V.; Vollset, S. E.; Vos, T.; Wakayo, T.; Wallin, M. T.; Wang, Y.-P.; Weiderpass, E.; Weintraub, R. G.; Weiss, D. J.; Werdecker, A.; Westerman, R.; Whetter, B.; Whiteford, H. A.; Wijeratne, T.; Wiysonge, C. S.; Woldeyes,

B. G.; Wolfe, C. D. A.; Woodbrook, R.; Workicho, A.; Xavier, D.; Xiao, Q.; Xu, G.; Yaghoubi, M.; Yakob, B.; Yano, Y.; Yaseri, M.; Yimam, H. H.; Yonemoto, N.; Yoon, S.-J.; Yotebieng, M.; Younis, M. Z.; Zaidi, Z.; Zaki, M. E. S.; Zegeye, E. A.; Zenebe, Z. M.; Zerfu, T. A.; Zhang, A. L.; Zhang, X.; Zipkin, B.; Zodpey, S.; Lopez, A. D.; Murray, C. J. L. Global, Regional, and National Age-Sex Specific Mortality for 264 Causes of Death, 1980–2016: A Systematic Analysis for the Global Burden of Disease Study 2016. *The Lancet* 2017, *390* (10100), 1151–1210. https://doi.org/10.1016/S0140-6736(17)32152-9.

(127) Adam C, G.; Ethan M, T.; Hendrik J, V.; Tina M, S. Neonatal Hyperbilirubinemia in Low-Income African Countries. *Int J Pediatr Res* 2021, *7* (1). https://doi.org/10.23937/2469-5769/1510073.

(128) Iskander, I.; Gamaleldin, R.; Kabbani, M. Root Causes for Late Presentation of Severe Neonatal Hyperbilirubinaemia in Egypt. *East Mediterr Health J* 2012, *18* (8), 882–887. https://doi.org/10.26719/2012.18.8.882.

(129) Pace, E. J.; Brown, C. M.; DeGeorge, K. C. Neonatal Hyperbilirubinemia: An Evidence-Based Approach. *J Fam Pract* 2019, *68* (1), E4–E11.

(130) Rennie, J.; Burman-Roy, S.; Murphy, M. S. Neonatal Jaundice: Summary of NICE Guidance. *BMJ* 2010, *340* (may19 3), c2409–c2409. https://doi.org/10.1136/bmj.c2409.

(131) El-Beshbishi, S. N.; Shattuck, K. E.; Mohammad, A. A.; Petersen, J. R. Hyperbilirubinemia and Transcutaneous Bilirubinometry. *Clinical Chemistry* 2009, *55* (7), 1280–1287. https://doi.org/10.1373/clinchem.2008.121889.

(132) De Luca, D.; Jackson, G. L.; Tridente, A.; Carnielli, V. P.; Engle, W. D. Transcutaneous Bilirubin Nomograms: A Systematic Review of Population Differences and Analysis of Bilirubin Kinetics. *Archives of Pediatrics & Adolescent Medicine* 2009, *163* (11), 1054–1059. https://doi.org/10.1001/archpediatrics.2009.187.

(133) Colombo, G.; Szoke, D.; Aloisio, E.; Cavigioli, F.; Dolci, A.; Panteghini, M. Clinicians at Crossroads for a Dangerous Interference in Neonatal Bilirubin Determination at the Point-of-Care. *Clinical Chemistry* 2022, *68* (7), 887–891. https://doi.org/10.1093/clinchem/hvac077.

(134) Alarcón, P. A. de; Werner, E. J.; Christensen, R. D.; Sola-Visner, M. C. *Neonatal Hematology: Pathogenesis, Diagnosis, and Management of Hematologic Problems*; Cambridge University Press, 2021.

(135) Christensen, R. D.; Nussenzveig, R. H.; Yaish, H. M.; Henry, E.; Eggert, L. D.; Agarwal, A. M. Causes of Hemolysis in Neonates with Extreme Hyperbilirubinemia. *J Perinatol* 2014, *34* (8), 616–619. https://doi.org/10.1038/jp.2014.68.

(136) Heireman, L.; Van Geel, P.; Musger, L.; Heylen, E.; Uyttenbroeck, W.; Mahieu, B. Causes, Consequences and Management of Sample Hemolysis in

the Clinical Laboratory. *Clinical Biochemistry* 2017, *50* (18), 1317–1322. https://doi.org/10.1016/j.clinbiochem.2017.09.013.

(137) O'Hara, M.; Wheatley, E. G.; Kazmierczak, S. C. The Impact of Undetected In Vitro Hemolysis or Sample Contamination on Patient Care and Outcomes in Point-of-Care Testing: A Retrospective Study. *The Journal of Applied Laboratory Medicine* 2020, *5* (2), 332–341. https://doi.org/10.1093/jalm/jfz020.

(138) Simundic, A.-M.; Baird, G.; Cadamuro, J.; Costelloe, S. J.; Lippi, G. Managing Hemolyzed Samples in Clinical Laboratories. *Critical Reviews in Clinical Laboratory Sciences* 2020, *57* (1), 1–21. https://doi.org/10.1080/10408363.2019.1664391.

(139) Lee, K.-S.; Gartner, L. M. Spectrophotometric Characteristics of Bilirubin. *Pediatr Res* 1976, *10* (9), 782–788. https://doi.org/10.1203/00006450-197609000-00004.

(140) Tan, W.; Zhang, L.; Doery, J. C. G.; Shen, W. Study of Paper-Based Assaying System for Diagnosis of Total Serum Bilirubin by Colorimetric Diazotization Method. *Sensors and Actuators B: Chemical* 2020, *305*, 127448. https://doi.org/10.1016/j.snb.2019.127448.

(141) Zucchini, L.; Ajčević, M.; Accardo, A. Temperature Influence on Reflectance Photometers for Bilirubin Measurement. In *Eighth National Congress of Bioengineering – Proceedings 2023*; GNB Atti; Patron Editore, 2023; pp 1135–1138.

(142) Penhaker, M.; Kasik, V.; Hrvolova, B. Advanced Bilirubin Measurement by a Photometric Method. *ElAEE* 2013, *19* (3), 47–50. https://doi.org/10.5755/j01.eee.19.3.3696.

(143) Alla, S. K.; Clark, J. F.; Beyette, F. R. Signal Processing System to Extract Serum Bilirubin Concentration from Diffuse Reflectance Spectrum of Human Skin. In *2009 Annual International Conference of the IEEE Engineering in Medicine and Biology Society*; IEEE: Minneapolis, MN, 2009; pp 1290–1293. https://doi.org/10.1109/IEMBS.2009.5333236.

(144) Javid, B.; Fotouhi-Ghazvini, F.; Zakeri, F. Noninvasive Optical Diagnostic Techniques for Mobile Blood Glucose and Bilirubin Monitoring. *J Med Signals Sens* 2018, *8* (3), 125. https://doi.org/10.4103/jmss.JMSS_8_18.

(145) Salim, S. G. R.; Fox, N. P.; Theocharous, E.; Sun, T.; Grattan, K. T. V. Temperature and Nonlinearity Corrections for a Photodiode Array Spectrometer Used in the Field. *Appl. Opt.* 2011, *50* (6), 866. https://doi.org/10.1364/AO.50.000866.

(146) Starks, P. J.; Walter-Shea, E. A.; Schiebe, F. R.; Markham, B. L. Temperature Sensitivity Characterization of a Silicon Diode Array Spectrometer. *Remote Sensing of Environment* 1995, *51* (3), 385–389. https://doi.org/10.1016/0034-4257(94)00109-Z.

(147) Kipp, S.; Mistele, B.; Schmidhalter, U. The Performance of Active Spectral Reflectance Sensors as Influenced by Measuring Distance, Device Temperature and Light Intensity. *Computers and Electronics in Agriculture* 2014, *100*, 24–33. https://doi.org/10.1016/j.compag.2013.10.007.
(148) Wintrobe, M. M. A Simple and Accurate Hematocrit. *The Journal of Laboratory and Clinical Medicine* 1929, *15* (3), 287–289.
(149) Christensen (M.D.), R. D. *Hematologic Problems of the Neonate*; W.B. Saunders Company, 2000.
(150) Greer, J. P. *Wintrobe's Clinical Hematology*; Lippincott Williams & Wilkins, 2009.
(151) Birhaneselassie, M.; Birhanu, A.; Gebremedhin, A.; Tsegaye, A. How Useful Are Complete Blood Count and Reticulocyte Reports to Clinicians in Addis Ababa Hospitals, Ethiopia? *BMC Hematol* 2013, *13* (1), 11. https://doi.org/10.1186/2052-1839-13-11.
(152) Audu I, S.; Ubwa, S.; Igbum, O.; Hati, S.; Alex, N. Analytical Comparison between Microhematocrit and Automated Methods for Packed Cell Volume (PCV). *International Journal of Hematology and Blood Disorders* 2017, *2*, 1–4. https://doi.org/10.15226/2639-7986/2/1/00105.
(153) Bull, B. S.; Rittenbach, J. D. A Proposed Reference Haematocrit Derived from Multiple MCHC Determinations via Haemoglobin Measurements. *Clin Lab Haematol* 1990, *12 Suppl 1*, 43–53.
(154) Furth, F. W. Effect of Spherocytosis on Volume of Trapped Plasma in Red Cell Column of Capillary and Wintrobe Hematocrits. *The Journal of Laboratory and Clinical Medicine* 1956, *48* (3), 421–430. https://doi.org/10.5555/uri:pii:0022214356900105.
(155) Penn, D.; Williams, P. R.; Dutcher, T. F.; Adair, R. M. Comparison of Hematocrit Determinations by Microhematocrit and Electronic Particle Counter. *Am J Clin Pathol* 1979, *72* (1), 71–74. https://doi.org/10.1093/ajcp/72.1.71.
(156) Gotch, F.; Torres, L.; Evans, M.; Keen, M.; Metzner, K.; Westphal, D.; Polaschegc, H. Comparison of Conductivity Measured Hematocrit to Microhematocrit. *ASAIO Journal* 1991, *37* (3), M138.
(157) Pearson, T. C.; Guthrie, D. L. Trapped Plasma in the Microhematocrit. *American Journal of Clinical Pathology* 1982, *78* (5), 770–772. https://doi.org/10.1093/ajcp/78.5.770.
(158) Green, R.; Wachsmann-Hogiu, S. Development, History, and Future of Automated Cell Counters. *Clinics in Laboratory Medicine* 2015, *35* (1), 1–10. https://doi.org/10.1016/j.cll.2014.11.003.
(159) Arneth, B. M.; Menschikowki, M. Technology and New Fluorescence Flow Cytometry Parameters in Hematological Analyzers. *Journal of Clinical*

Laboratory Analysis 2015, *29* (3), 175–183. https://doi.org/10.1002/jcla.21747.

(160) Bosshart, M.; Stover, J. F.; Stocker, R.; Asmis, L. M.; Feige, J.; Neff, T. A.; Schuepbach, R. A.; Cottini, S. R.; Béchir, M. Two Different Hematocrit Detection Methods: Different Methods, Different Results? *BMC Res Notes* 2010, *3* (1), 65. https://doi.org/10.1186/1756-0500-3-65.

(161) Bourner, G.; Dhaliwal, J.; Sumner, J. Performance Evaluation of the Latest Fully Automated Hematology Analyzers in a Large, Commercial Laboratory Setting: A 4-Way, Side-by-Side Study. *Lab Hematol* 2005, *11* (4), 285–297. https://doi.org/10.1532/lh96.05036.

(162) Buttarello, M. Laboratory Diagnosis of Anemia: Are the Old and New Red Cell Parameters Useful in Classification and Treatment, How? *International Journal of Laboratory Hematology* 2016, *38* (S1), 123–132. https://doi.org/10.1111/ijlh.12500.

(163) Watson, P.; Maughan, R. J. Artifacts in Plasma Volume Changes Due to Hematology Analyzer-Derived Hematocrit. *Medicine & Science in Sports & Exercise* 2014, *46* (1), 52–59. https://doi.org/10.1249/MSS.0b013e3182a0537b.

(164) Fleming, K. A.; Naidoo, M.; Wilson, M.; Flanigan, J.; Horton, S.; Kuti, M.; Looi, L. M.; Price, C.; Ru, K.; Ghafur, A.; Wang, J.; Lago, N. An Essential Pathology Package for Low- and Middle-Income Countries. *American Journal of Clinical Pathology* 2017, *147* (1), 15–32. https://doi.org/10.1093/ajcp/aqw143.

(165) Brehm, R.; South, A.; George, E. C. Use of Point-of-Care Haemoglobin Tests to Diagnose Childhood Anaemia in Low- and Middle-Income Countries: A Systematic Review. *Tropical Medicine & International Health* 2024, *29* (2), 73–87. https://doi.org/10.1111/tmi.13957.

(166) Gavala, A.; Myrianthefs, P. Comparison of Point-of-Care versus Central Laboratory Measurement of Hematocrit, Hemoglobin, and Electrolyte Concentrations. *Heart & Lung* 2017, *46* (4), 246–250. https://doi.org/10.1016/j.hrtlng.2017.04.003.

(167) Altunok, İ.; Aksel, G.; Eroğlu, S. E. Correlation between Sodium, Potassium, Hemoglobin, Hematocrit, and Glucose Values as Measured by a Laboratory Autoanalyzer and a Blood Gas Analyzer. *The American Journal of Emergency Medicine* 2019, *37* (6), 1048–1053. https://doi.org/10.1016/j.ajem.2018.08.045.

(168) Bernardes, V. M.; Anderle, F. N.; Anjos, K. D.; Boller, C. Correlation between Hemoglobin and Hematocrit Results Obtained on Full Blood Count and Blood Gas Analysis in Children. *JBPML* 2021, *57*. https://doi.org/10.5935/1676-2444.20210055.

(169) Allardet-Servent, J.; Lebsir, M.; Dubroca, C.; Fabrigoule, M.; Jordana, S.; Signouret, T.; Castanier, M.; Thomas, G.; Soundaravelou, R.; Lepidi, A.;

Delapierre, L.; Penaranda, G.; Halfon, P.; Seghboyan, J.-M. Point-of-Care Versus Central Laboratory Measurements of Hemoglobin, Hematocrit, Glucose, Bicarbonate and Electrolytes: A Prospective Observational Study in Critically Ill Patients. *PLOS ONE* 2017, *12* (1), e0169593. https://doi.org/10.1371/journal.pone.0169593.

(170) Auvet, A.; Espitalier, F.; Grammatico-Guillon, L.; Nay, M.-A.; Elaroussi, D.; Laffon, M.; Andres, C. R.; Legras, A.; Ehrmann, S.; Dequin, P.-F.; Gendrot, C.; Guillon, A. Preanalytical Conditions of Point-of-Care Testing in the Intensive Care Unit Are Decisive for Analysis Reliability. *Ann. Intensive Care* 2016, *6* (1), 57. https://doi.org/10.1186/s13613-016-0152-6.

(171) Hicks, J. M.; Haeckel, R.; Price, C. P.; Lewandrowski, K.; Wu, A. H. B. Recommendations and Opinions for the Use of Point-of-Care Testing for Hospitals and Primary Care: Summary of a 1999 Symposium. *Clinica Chimica Acta* 2001, *303* (1), 1–17. https://doi.org/10.1016/S0009-8981(00)00400-9.

(172) Price, C. P.; Smith, I.; Van den Bruel, A. Improving the Quality of Point-of-Care Testing. *Family Practice* 2018, *35* (4), 358–364. https://doi.org/10.1093/fampra/cmx120.

(173) Heidt, B.; Siqueira, W. F.; Eersels, K.; Diliën, H.; van Grinsven, B.; Fujiwara, R. T.; Cleij, T. J. Point of Care Diagnostics in Resource-Limited Settings: A Review of the Present and Future of PoC in Its Most Needed Environment. *Biosensors* 2020, *10* (10), 133. https://doi.org/10.3390/bios10100133.

(174) Kayiran, S. m.; Özbek, N.; Turan, M.; Gürakan, B. Significant Differences between Capillary and Venous Complete Blood Counts in the Neonatal Period. *Clinical & Laboratory Haematology* 2003, *25* (1), 9–16. https://doi.org/10.1046/j.1365-2257.2003.00484.x.

(175) Oh, W.; Lind, J. Venous and Capillary Hematocrit in Newborn Infants and Placental Transfusion. *Acta Paediatrica* 1966, *55* (1), 38–48. https://doi.org/10.1111/j.1651-2227.1966.tb15207.x.

(176) Henry, E.; Christensen, R. D. Reference Intervals in Neonatal Hematology. *Clinics in Perinatology* 2015, *42* (3), 483–497. https://doi.org/10.1016/j.clp.2015.04.005.

(177) Christensen, R. D. Reference Intervals in Neonatal Hematology. In *Neonatal Hematology*; De Alarcón, P. A., Werner, E. J., Christensen, R. D., Sola-Visner, M. C., Eds.; Cambridge University Press, 2021; pp 440–469. https://doi.org/10.1017/9781108773584.026.

(178) Zucchini, L.; Ajčević, M.; Coda Zabetta, C. D.; Greco, C.; Fernetti, C.; Moretto, C.; Pennini, S.; Accardo, A. Characterization of a Novel Approach for Neonatal Hematocrit Screening Based on Penetration Velocity in Lateral Flow Test Strip. *Sensors* 2023, *23* (5), 2813. https://doi.org/10.3390/s23052813.

(179) Szczerska, M.; Gnyba, M. Optical Investigation of Hematocrit Level in Human Blood. *Acta Physica Polonica Series a* 2011, *4*, 642÷646. https://doi.org/10.12693/APhysPolA.120.642.
(180) Colombatti, R.; Sainati, L.; Trevisanuto, D. Anemia and Transfusion in the Neonate. *Seminars in Fetal and Neonatal Medicine* 2016, *21* (1), 2–9. https://doi.org/10.1016/j.siny.2015.12.001.
(181) Verbrugge, S. E.; Huisman, A. Verification and Standardization of Blood Cell Counters for Routine Clinical Laboratory Tests. *Clinics in Laboratory Medicine* 2015, *35* (1), 183–196. https://doi.org/10.1016/j.cll.2014.10.008.
(182) Woldie, M.; Feyissa, G. T.; Admasu, B.; Hassen, K.; Mitchell, K.; Mayhew, S.; McKee, M.; Balabanova, D. Community Health Volunteers Could Help Improve Access to and Use of Essential Health Services by Communities in LMICs: An Umbrella Review. *Health Policy and Planning* 2018, *33* (10), 1128–1143. https://doi.org/10.1093/heapol/czy094.
(183) Lehmann, U.; Dieleman, M.; Martineau, T. Staffing Remote Rural Areas in Middle- and Low-Income Countries: A Literature Review of Attraction and Retention. *BMC Health Serv Res* 2008, *8*, 19. https://doi.org/10.1186/1472-6963-8-19.
(184) Caldwell, A.; Young, A.; Gomez-Marquez, J.; Olson, K. R. Global Health Technology 2.0. *IEEE Pulse* 2011, *2* (4), 63–67. https://doi.org/10.1109/MPUL.2011.941459.
(185) Li, X.; Cui, K.; Xiu, M.; Zhou, C.; Li, L.; Zhang, J.; Hao, S.; Zhang, L.; Ge, S.; Huang, Y.; Yu, J. *In Situ* Growth of WO_3 /$BiVO_4$ Nanoflowers onto Cellulose Fibers to Construct Photoelectrochemical/Colorimetric Lab-on-Paper Devices for the Ultrasensitive Detection of AFP. *J. Mater. Chem. B* 2022, *10* (21), 4031–4039. https://doi.org/10.1039/D2TB00297C.
(186) Zhou, C.; Cui, K.; Liu, Y.; Li, L.; Zhang, L.; Hao, S.; Ge, S.; Yu, J. Bi_2S_3@MoS_2 Nanoflowers on Cellulose Fibers Combined with Octahedral CeO_2 for Dual-Mode Microfluidic Paper-Based MiRNA-141 Sensors. *ACS Appl. Mater. Interfaces* 2021, *13* (28), 32780–32789. https://doi.org/10.1021/acsami.1c07669.
(187) Waller, A. W.; Toc, M.; Rigsby, D. J.; Gaytán-Martínez, M.; Andrade, J. E. Development of a Paper-Based Sensor Compatible with a Mobile Phone for the Detection of Common Iron Formulas Used in Fortified Foods within Resource-Limited Settings. *Nutrients* 2019, *11* (7), 1673. https://doi.org/10.3390/nu11071673.
(188) Bender, A. T.; Sullivan, B. P.; Zhang, J. Y.; Juergens, D. C.; Lillis, L.; Boyle, D. S.; Posner, J. D. HIV Detection from Human Serum with Paper-Based Isotachophoretic RNA Extraction and Reverse Transcription Recombinase Polymerase Amplification. *Analyst* 2021, *146* (9), 2851–2861. https://doi.org/10.1039/D0AN02483J.

(189) Berry, S. B.; Fernandes, S. C.; Rajaratnam, A.; DeChiara, N. S.; Mace, C. R. Measurement of the Hematocrit Using Paper-Based Microfluidic Devices. *Lab Chip* 2016, *16* (19), 3689–3694. https://doi.org/10.1039/C6LC00895J.

(190) Fernandes, S. C.; Baillargeon, K. R.; Mace, C. R. Reduction of Blood Volume Required to Perform Paper-Based Hematocrit Assays Guided by Device Design. *Anal. Methods* 2019, *11* (15), 2057–2063. https://doi.org/10.1039/C9AY00010K.

(191) Ben, F. D.; Biasizzo, J.; Curcio, F. A Fast, Nondestructive, Low-Cost Method for the Determination of Hematocrit of Dried Blood Spots Using Image Analysis. *Clinical Chemistry and Laboratory Medicine (CCLM)* 2019, *57* (5), e81–e82. https://doi.org/10.1515/cclm-2018-0755.

(192) Miller IV, J. H. An On-Card Approach for Assessment of Hematocrit on Dried Blood Spots Which Allows for Correction of Sample Volume. *J Anal Bioanal Techniques* 2013, *04* (01). https://doi.org/10.4172/2155-9872.1000162.

(193) Punter-Villagrasa, J.; Cid, J.; Páez-Avilés, C.; Rodríguez-Villarreal, I.; Juanola-Feliu, E.; Colomer-Farrarons, J.; Miribel-Català, P. L. An Instantaneous Low-Cost Point-of-Care Anemia Detection Device. *Sensors* 2015, *15* (2), 4564–4577. https://doi.org/10.3390/s150204564.

(194) Cohen, E.; Kramer, M.; Shochat, T.; Goldberg, E.; Krause, I. Relationship between Hematocrit Levels and Intraocular Pressure in Men and Women: A Population-Based Cross-Sectional Study. *Medicine* 2017, *96* (41), e8290. https://doi.org/10.1097/MD.0000000000008290.

(195) Greco, C.; Iskander, I. F.; Houchi, S. Z. E.; Rohsiswatmo, R.; Rundjan, L.; Ogala, W. N.; Ofakunrin, A. O. D.; Moccia, L.; Hoi, N. T. X.; Bedogni, G.; Tiribelli, C.; Zabetta, C. D. C. Diagnostic Performance Analysis of the Point-of-Care Bilistick System in Identifying Severe Neonatal Hyperbilirubinemia by a Multi-Country Approach. *eClinicalMedicine* 2018, *1*, 14–20. https://doi.org/10.1016/j.eclinm.2018.06.003.

(196) Grépin, K. A.; Pinkstaff, C. B.; Shroff, Z. C.; Ghaffar, A. Donor Funding Health Policy and Systems Research in Low- and Middle-Income Countries: How Much, from Where and to Whom. *Health Res Policy Sys* 2017, *15* (1), 1–8. https://doi.org/10.1186/s12961-017-0224-6.

(197) Schneider, M. T.; Chang, A. Y.; Crosby, S. W.; Gloyd, S.; Harle, A. C.; Lim, S.; Lozano, R.; Micah, A. E.; Tsakalos, G.; Su, Y.; Murray, C. J. L.; Dieleman, J. L. Trends and Outcomes in Primary Health Care Expenditures in Low-Income and Middle-Income Countries, 2000–2017. *BMJ Global Health* 2021, *6* (8), e005798. https://doi.org/10.1136/bmjgh-2021-005798.

(198) De Maria, C.; Díaz Lantada, A.; Jämsä, T.; Pecchia, L.; Ahluwalia, A. Biomedical Engineering in Low- and Middle-Income Settings: Analysis of

Current State, Challenges and Best Practices. *Health Technol.* 2022, *12* (3), 643–653. https://doi.org/10.1007/s12553-022-00657-8.
(199) World Health Organization. *Local Production and Technology Transfer to Increase Access to Medical Devices: Addressing the Barriers and Challenges in Low- and Middle-Income Countries*; World Health Organization: Geneva, 2012.
(200) Diaconu, K.-D. Methods for Medical Device and Equipment Procurement in Low and Middle-Income Countries. d_ph, University of Birmingham, 2017. https://etheses.bham.ac.uk/id/eprint/7063/ (accessed 2024-10-10).
(201) Nasir, N.; Molyneux, S.; Were, F.; Aderoba, A.; Fuller, S. S. Medical Device Regulation and Oversight in African Countries: A Scoping Review of Literature and Development of a Conceptual Framework. *BMJ Glob Health* 2023, *8* (8), e012308. https://doi.org/10.1136/bmjgh-2023-012308.
(202) *World Bank country classifications by income level for 2024-2025*. World Bank Blogs. https://blogs.worldbank.org/en/opendata/world-bank-country-classifications-by-income-level-for-2024-2025 (accessed 2024-10-14).
(203) *Population by income level*. Our World in Data. https://ourworldindata.org/grapher/population-by-income-level (accessed 2024-10-14).
(204) Hasell, J.; Arriagada, P.; Ortiz-Ospina, E.; Roser, M. Economic Inequality. *Our World in Data* 2024.
(205) Lustig, N. The "Missing Rich" in Household Surveys: Causes and Correction Approaches. March 9, 2020. https://doi.org/10.31235/osf.io/j23pn.
(206) Hooley, B.; Afriyie, D. O.; Fink, G.; Tediosi, F. Health Insurance Coverage in Low-Income and Middle-Income Countries: Progress Made to Date and Related Changes in Private and Public Health Expenditure. *BMJ Glob Health* 2022, *7* (5), e008722. https://doi.org/10.1136/bmjgh-2022-008722.
(207) Ortiz-Ospina, E.; Roser, M. Healthcare Spending. *Our World in Data* 2024.
(208) World Health Organization. *World Health Statistics 2024: Monitoring Health for the SDGs, Sustainable Development Goals*; World Health Statistics; World Health Organization: Geneva, 2024.
(209) Sangar, S.; Dutt, V.; Thakur, R. Comparative Assessment of Economic Burden of Disease in Relation to Out of Pocket Expenditure. *Front. Public Health* 2019, *7*. https://doi.org/10.3389/fpubh.2019.00009.
(210) *The top 10 causes of death*. https://www.who.int/news-room/fact-sheets/detail/the-top-10-causes-of-death (accessed 2024-10-15).
(211) Islam, S. M. S.; Purnat, T. D.; Phuong, N. T. A.; Mwingira, U.; Schacht, K.; Fröschl, G. Non-Communicable Diseases (NCDs) in Developing Countries: A Symposium Report. *Global Health* 2014, *10* (1), 81. https://doi.org/10.1186/s12992-014-0081-9.

(212) Asogwa, O. A.; Boateng, D.; Marzà-Florensa, A.; Peters, S.; Levitt, N.; Van Olmen, J.; Klipstein-Grobusch, K. Multimorbidity of Non-Communicable Diseases in Low-Income and Middle-Income Countries: A Systematic Review and Meta-Analysis. *BMJ Open* 2022, *12* (1), e049133. https://doi.org/10.1136/bmjopen-2021-049133.

(213) OECD; Organization, W. H. Neonatal Mortality, 2020. https://www.oecd-ilibrary.org/content/component/b1125911-en.

(214) Houweling, T. A. J.; Kunst, A. E. Socio-Economic Inequalities in Childhood Mortality in Low- and Middle-Income Countries: A Review of the International Evidence. *British Medical Bulletin* 2010, *93* (1), 7–26. https://doi.org/10.1093/bmb/ldp048.

(215) Lawn, J. E.; Blencowe, H.; Oza, S.; You, D.; Lee, A. C.; Waiswa, P.; Lalli, M.; Bhutta, Z.; Barros, A. J.; Christian, P.; Mathers, C.; Cousens, S. N. Every Newborn: Progress, Priorities, and Potential beyond Survival. *The Lancet* 2014, *384* (9938), 189–205. https://doi.org/10.1016/S0140-6736(14)60496-7.

(216) Sharrow, D.; Hug, L.; You, D.; Alkema, L.; Black, R.; Cousens, S.; Croft, T.; Gaigbe-Togbe, V.; Gerland, P.; Guillot, M.; Hill, K.; Masquelier, B.; Mathers, C.; Pedersen, J.; Strong, K. L.; Suzuki, E.; Wakefield, J.; Walker, N. Global, Regional, and National Trends in under-5 Mortality between 1990 and 2019 with Scenario-Based Projections until 2030: A Systematic Analysis by the UN Inter-Agency Group for Child Mortality Estimation. *The Lancet Global Health* 2022, *10* (2), e195–e206. https://doi.org/10.1016/S2214-109X(21)00515-5.

(217) United Nations Inter-agency Group for Child Mortality Estimation (UN; IGME). Levels & Trends in Child Mortality: Report 2023, 2024.

(218) Mashamba-Thompson, T. P.; Morgan, R. L.; Sartorius, B.; Dennis, B.; Drain, P. K.; Thabane, L. Effect of Point-of-Care Diagnostics on Maternal Outcomes in Human Immunodeficiency Virus–Infected Women: Systematic Review and Meta-Analysis. *Point of Care* 2017, *16* (2), 67. https://doi.org/10.1097/POC.0000000000000135.

(219) Tucker, J. D.; Bien, C. H.; Peeling, R. W. Point-of-Care Testing for Sexually Transmitted Infections: Recent Advances and Implications for Disease Control. *Current Opinion in Infectious Diseases* 2013, *26* (1), 73. https://doi.org/10.1097/QCO.0b013e32835c21b0.

(220) World Health Organization. *Medical Device Donations: Considerations for Solicitation and Provision*; WHO Medical device technical series; World Health Organization: Geneva, 2011; Vol. 1.

(221) Howie, S. Beyond Good Intentions: Lessons on Equipment Donation from an African Hospital. *Bull World Health Organ* 2008, *86* (1), 52–56. https://doi.org/10.2471/BLT.07.042994.

(222) Marks, I. H.; Thomas, H.; Bakhet, M.; Fitzgerald, E. Medical Equipment Donation in Low-Resource Settings: A Review of the Literature and Guidelines

for Surgery and Anaesthesia in Low-Income and Middle-Income Countries. *BMJ Global Health* 2019, *4* (5), e001785. https://doi.org/10.1136/bmjgh-2019-001785.

(223) Gatrad, A. R.; Gatrad, S.; Gatrad, A. Equipment Donation to Developing Countries. *Anaesthesia* 2007, *62* (s1), 90–95. https://doi.org/10.1111/j.1365-2044.2007.05309.x.

(224) Mullally, S.; Frize, M. Survey of Clinical Engineering Effectiveness in Developing World Hospitals: Equipment Resources, Procurement and Donations. In *2008 30th Annual International Conference of the IEEE Engineering in Medicine and Biology Society*; 2008; pp 4499–4502. https://doi.org/10.1109/IEMBS.2008.4650212.

(225) Perry, L.; Malkin, R. Effectiveness of Medical Equipment Donations to Improve Health Systems: How Much Medical Equipment Is Broken in the Developing World? *Med Biol Eng Comput* 2011, *49* (7), 719–722. https://doi.org/10.1007/s11517-011-0786-3.

(226) Krueger, R.; Telliel, Y.; Soboyejo, W. *Science, Engineering, and Sustainable Development: Cases in Planning, Health, Agriculture, and the Environment*; Walter de Gruyter GmbH & Co KG, 2023.

(227) von Schoen-Angerer, T.; Love, J. P. Equitable Access to Medicines, Vaccines, and Medical Devices. In *Global Health Essentials*; Raviglione, M. C. B., Tediosi, F., Villa, S., Casamitjana, N., Plasència, A., Eds.; Springer International Publishing: Cham, 2023; pp 327–332. https://doi.org/10.1007/978-3-031-33851-9_50.

(228) Schneider, C. B. Global Public Health and Innovation in Governance: The Emergence of Public—Private Partnerships. In *Health for Some: The Political Economy of global Health Governance*; MacLean, S. J., Brown, S. A., Fourie, P., Eds.; Palgrave Macmillan UK: London, 2009; pp 105–117. https://doi.org/10.1057/9780230244399_7.

(229) Rohr, U.-P.; Binder, C.; Dieterle, T.; Giusti, F.; Messina, C. G. M.; Toerien, E.; Moch, H.; Schäfer, H. H. The Value of In Vitro Diagnostic Testing in Medical Practice: A Status Report. *PLoS ONE* 2016, *11* (3), e0149856. https://doi.org/10.1371/journal.pone.0149856.

(230) Malkin, R. A. Design of Health Care Technologies for the Developing World. *Annu. Rev. Biomed. Eng.* 2007, *9* (1), 567–587. https://doi.org/10.1146/annurev.bioeng.9.060906.151913.

(231) Urdea, M.; Penny, L. A.; Olmsted, S. S.; Giovanni, M. Y.; Kaspar, P.; Shepherd, A.; Wilson, P.; Dahl, C. A.; Buchsbaum, S.; Moeller, G.; Hay Burgess, D. C. Requirements for High Impact Diagnostics in the Developing World. *Nature* 2006, *444* (1), 73–79. https://doi.org/10.1038/nature05448.

(232) Gubala, V.; Harris, L. F.; Ricco, A. J.; Tan, M. X.; Williams, D. E. Point of Care Diagnostics: Status and Future. *Anal. Chem.* 2012, *84* (2), 487–515. https://doi.org/10.1021/ac2030199.

(233) Lu, Z.; Rey, E.; Vemulapati, S.; Srinivasan, B.; Mehta, S.; Erickson, D. High-Yield Paper-Based Quantitative Blood Separation System. *Lab on a chip* 2018, *18* (24), 3865. https://doi.org/10.1039/c8lc00717a.

(234) Songjaroen, T.; Dungchai, W.; Chailapakul, O.; Henry, C. S.; Laiwattanapaisal, W. Blood Separation on Microfluidic Paper-Based Analytical Devices. *Lab Chip* 2012, *12* (18), 3392–3398. https://doi.org/10.1039/c2lc21299d.

(235) Nyirimanzi, J. D.; Ngenzi, J.; Kagisha, V.; Bizimana, T.; Kayitare, E. Assessment of Medicines Cold Chain Storage Conformity with the Requirements of the World Health Organization in Health Facilities of the Eastern Province of Rwanda. *J of Pharm Policy and Pract* 2023, *16* (1), 31. https://doi.org/10.1186/s40545-023-00534-3.

(236) Casas-Hernández, A. M.; Aguilar-Caballos, M. P.; Gómez-Hens, A. Application of Time-Resolved Luminescence to Dry Reagent Chemical Technology. *Analytica Chimica Acta* 2002, *452* (2), 169–175. https://doi.org/10.1016/S0003-2670(01)01457-X.

(237) Lai, W.; Shi, Y.; Zhong, J.; Zhou, X.; Yang, Y.; Chen, Z.; Zhang, C. A Dry Chemistry-Based Electrochemiluminescence Device for Point-of-Care Testing of Alanine Transaminase. *Talanta* 2023, *256*, 124287. https://doi.org/10.1016/j.talanta.2023.124287.

(238) Ozer, T.; McMahon, C.; Henry, C. S. Advances in Paper-Based Analytical Devices. *Annual Rev. Anal. Chem.* 2020, *13* (1), 85–109. https://doi.org/10.1146/annurev-anchem-061318-114845.

(239) Koczula, K. M.; Gallotta, A. Lateral Flow Assays. *Essays in Biochemistry* 2016, *60* (1), 111–120. https://doi.org/10.1042/EBC20150012.

(240) Wei, X.; Tian, T.; Jia, S.; Zhu, Z.; Ma, Y.; Sun, J.; Lin, Z.; Yang, C. J. Microfluidic Distance Readout Sweet Hydrogel Integrated Paper-Based Analytical Device (μDiSH-PAD) for Visual Quantitative Point-of-Care Testing. *Anal Chem* 2016, *88* (4), 2345–2352. https://doi.org/10.1021/acs.analchem.5b04294.

(241) Li, M.; Cao, R.; Nilghaz, A.; Guan, L.; Zhang, X.; Shen, W. "Periodic-Table-Style" Paper Device for Monitoring Heavy Metals in Water. *Anal. Chem.* 2015, *87* (5), 2555–2559. https://doi.org/10.1021/acs.analchem.5b00040.

(242) Cate, D. M.; Noblitt, S. D.; Volckens, J.; Henry, C. S. Multiplexed Paper Analytical Device for Quantification of Metals Using Distance-Based Detection. *Lab on a chip* 2015, *15* (13), 2808. https://doi.org/10.1039/c5lc00364d.

(243) Lewis, G. G.; DiTucci, M. J.; Phillips, S. T. Quantifying Analytes in Paper-Based Microfluidic Devices Without Using External Electronic Readers.

Angewandte Chemie International Edition 2012, *51* (51), 12707–12710. https://doi.org/10.1002/anie.201207239.

(244) Noviana, E.; Ozer, T.; Carrell, C. S.; Link, J. S.; McMahon, C.; Jang, I.; Henry, C. S. Microfluidic Paper-Based Analytical Devices: From Design to Applications. *Chem. Rev.* 2021, *121* (19), 11835–11885. https://doi.org/10.1021/acs.chemrev.0c01335.

(245) Yang, Y.; Noviana, E.; Nguyen, M. P.; Geiss, B. J.; Dandy, D. S.; Henry, C. S. Paper-Based Microfluidic Devices: Emerging Themes and Applications. *Anal. Chem.* 2017, *89* (1), 71–91. https://doi.org/10.1021/acs.analchem.6b04581.

(246) Hampton, T. Recent Advances in Mobile Technology Benefit Global Health, Research, and Care. *JAMA* 2012, *307* (19). https://doi.org/10.1001/jama.2012.4465.

(247) Kayingo, G. Transforming Global Health with Mobile Technologies and Social Enterprises: Global Health and Innovation Conference. *The Yale Journal of Biology and Medicine* 2012, *85* (3), 425.

(248) Erickson, D.; O'Dell, D.; Jiang, L.; Oncescu, V.; Gumus, A.; Lee, S.; Mancuso, M.; Mehta, S. Smartphone Technology Can Be Transformative to the Deployment of Lab-on-Chip Diagnostics. *Lab on a Chip* 2014, *14* (17), 3159–3164. https://doi.org/10.1039/C4LC00142G.

(249) Jiang, N.; Ahmed, R.; Damayantharan, M.; Ünal, B.; Butt, H.; Yetisen, A. K. Lateral and Vertical Flow Assays for Point-of-Care Diagnostics. *Advanced Healthcare Materials* 2019, *8* (14), 1900244. https://doi.org/10.1002/adhm.201900244.

(250) Dillon, M. J.; Campbell, K. Chapter Five - Hyphenating Paper-Based Biosensors with Smartphones. In *Comprehensive Analytical Chemistry*; Nelis, J. L. D., Tsagkaris, A. S., Eds.; Smartphones for Chemical Analysis: From Proof-of-concept to Analytical Applications; Elsevier, 2023; Vol. 101, pp 109–141. https://doi.org/10.1016/bs.coac.2022.11.002.

(251) Ellerbee, A. K.; Phillips, S. T.; Siegel, A. C.; Mirica, K. A.; Martinez, A. W.; Striehl, P.; Jain, N.; Prentiss, M.; Whitesides, G. M. Quantifying Colorimetric Assays in Paper-Based Microfluidic Devices by Measuring the Transmission of Light through Paper. *Anal. Chem.* 2009, *81* (20), 8447–8452. https://doi.org/10.1021/ac901307q.

(252) Nie, Z.; Deiss, F.; Liu, X.; Akbulut, O.; Whitesides, G. M. Integration of Paper-Based Microfluidic Devices with Commercial Electrochemical Readers. *Lab Chip* 2010, *10* (22), 3163. https://doi.org/10.1039/c0lc00237b.

(253) Park, J. Y.; Kricka, L. J. Prospects for the Commercialization of Chemiluminescence-Based Point-of-Care and on-Site Testing Devices. *Anal Bioanal Chem* 2014, *406* (23), 5631–5637. https://doi.org/10.1007/s00216-014-7697-8.

(254) Kozma, P.; Lehmann, A.; Wunderlich, K.; Michel, D.; Schumacher, S.; Ehrentreich-Förster, E.; Bier, F. F. A Novel Handheld Fluorescent Microarray Reader for Point-of-Care Diagnostic. *Biosensors and Bioelectronics* 2013, *47*, 415–420. https://doi.org/10.1016/j.bios.2013.03.043.

(255) World Health Organization. *WHO Global Surveillance and Monitoring System for Substandard and Falsified Medical Products*; World Health Organization: Geneva, 2017.

(256) Gryseels, C.; Kuijpers, L. M. F.; Jacobs, J.; Peeters Grietens, K. When 'Substandard' Is the Standard, Who Decides What Is Appropriate? Exploring Healthcare Provision in Cambodia. *Critical Public Health* 2019, *29* (4), 460–472. https://doi.org/10.1080/09581596.2019.1591614.

(257) Lamph, S. Regulation of Medical Devices Outside the European Union. *J R Soc Med* 2012, *105* (1_suppl), 12–21. https://doi.org/10.1258/jrsm.2012.120037.

(258) *Global Atlas of Medical Devices 2022*, 1st ed.; World Health Organization: Geneva, 2022.

(259) Maccaro, A.; Piaggio, D.; Leesurakarn, S.; Husen, N.; Sekalala, S.; Rai, S.; Pecchia, L. On the Universality of Medical Device Regulations: The Case of Benin. *BMC Health Serv Res* 2022, *22* (1), 1031. https://doi.org/10.1186/s12913-022-08396-2.

(260) Kedwani, M.; Schröttner, J.; Baumgartner, C. Analysis of Regulatory Requirements of Medical Devices and In-Vitro Diagnostics Worldwide for the Development of an Efficient Procedure of Registration for Manufacturers of Medical Products. *Current Directions in Biomedical Engineering* 2019, *5* (1), 609–612. https://doi.org/10.1515/cdbme-2019-0153.

(261) Rugera, S. P.; McNerney, R.; Poon, A. K.; Akimana, G.; Mariki, R. F.; Kajumbula, H.; Kamau, E.; Mpawenimana, S.; Said, S. Y.; Toroitich, A.; Ronoh, W.; Sollis, K. A.; Sonoiya, S.; Peeling, R. W. Regulation of Medical Diagnostics and Medical Devices in the East African Community Partner States. *BMC Health Serv Res* 2014, *14* (1), 524. https://doi.org/10.1186/s12913-014-0524-2.

(262) Dellepiane, N.; Pagliusi, S. Challenges for the Registration of Vaccines in Emerging Countries: Differences in Dossier Requirements, Application and Evaluation Processes. *Vaccine* 2018, *36* (24), 3389–3396. https://doi.org/10.1016/j.vaccine.2018.03.049.

(263) Ngum, N.; Mashingia, J.; Ndomondo-Sigonda, M.; Walker, S.; Salek, S. Evaluation of the Effectiveness and Efficiency of the East African Community Joint Assessment Procedure by Member Countries: The Way Forward. *Front. Pharmacol.* 2022, *13*. https://doi.org/10.3389/fphar.2022.891506.

(264) Sithole, T.; Mahlangu, G.; Salek, S.; Walker, S. Evaluating the Success of ZaZiBoNa, the Southern African Development Community Collaborative

Medicines Registration Initiative. *Ther Innov Regul Sci* 2020, *54* (6), 1319–1329. https://doi.org/10.1007/s43441-020-00154-y.

(265) Patel, M.; Patel, M.; Patel, R. Comparing Key Registration Requirements of Generic Drugs in East Africa, West Africa, USA & Europe with Main Focus on Kenya. 2018.

(266) Ratlabyana, M. B. Transparency in Medicines Registration Decision Making: A Closer Look at National Medicines Regulatory Authorities (NMRAs) within the Southern African Development Community (SADC) Region. 2020.

(267) Blaschke, T. F.; Lumpkin, M.; Hartman, D. The World Health Organization Prequalification Program and Clinical Pharmacology in 2030. *Clinical Pharmacology & Therapeutics* 2020, *107* (1), 68–71. https://doi.org/10.1002/cpt.1680.

(268) *History and Mission of WHO Prequalification | WHO - Prequalification of Medical Products (IVDs, Medicines, Vaccines and Immunization Devices, Vector Control)*. https://perma.cc/D62C-GHXE (accessed 2024-10-24).

(269) World Health Organization. Impact Assessment of WHO Prequalification and Systems Supporting Activities, 2019.

(270) *Timelines | WHO - Prequalification of Medical Products (IVDs, Medicines, Vaccines and Immunization Devices, Vector Control)*. https://extranet.who.int/prequal/vitro-diagnostics/timelines (accessed 2024-10-25).

(271) *Prequalification Procedures and Fees: In Vitro Diagnostics | WHO - Prequalification of Medical Products (IVDs, Medicines, Vaccines and Immunization Devices, Vector Control)*. https://extranet.who.int/prequal/vitro-diagnostics/prequalification-procedures-and-fees-vitro-diagnostics (accessed 2024-10-25).

(272) *Manufacturers | WHO - Prequalification of Medical Products (IVDs, Medicines, Vaccines and Immunization Devices, Vector Control)*. https://extranet.who.int/prequal/vitro-diagnostics/manufacturers (accessed 2024-10-25).

(273) *Collaborative Procedure for Accelerated Registration | WHO - Prequalification of Medical Products (IVDs, Medicines, Vaccines and Immunization Devices, Vector Control)*. https://extranet.who.int/prequal/vitro-diagnostics/collaborative-procedure-accelerated-registration (accessed 2024-10-25).

(274) World Health Organization. Collaborative Procedure between the World Health Organization and National Regulatory Authorities in the Assessment and Accelerated National Registration of WHO-Prequalified in Vitro Diagnostics - Annex 4, 2021.